



ScuDo

Scuola di Dottorato ~ Doctoral School  
WHAT YOU ARE, TAKES YOU FAR



Doctoral Dissertation  
Doctoral Program in Civil and Environmental Engineering (31<sup>st</sup> Cycle)

# Resilience Assessment of Physical Infrastructure and Social Systems of Large-Scale Communities

**Omar Kammouh**

\* \* \* \* \*

**Supervisor**

Prof. Gian Paolo Cimellaro, Supervisor

## **Doctoral Examination Committee:**

Prof. Camilo Nuti , Referee, Università degli studi Roma Tre

Prof. Massimo Fragiacomò, Referee, Università degli studi di L'Aquila

Prof. Michael Faber, Referee, AALBORG UNIVERSITEIT

Prof. Giulio Ventura, Referee, Politecnico di Torino

Prof Alberto Giuseppe Sapore, Referee, Politecnico di Torino

Politecnico di Torino

June 20, 2019

---

This thesis is licensed under a Creative Commons License, Attribution - Noncommercial - NoDerivative Works 4.0 International: see [www.creativecommons.org](http://www.creativecommons.org). The text may be reproduced for non-commercial purposes, provided that credit is given to the original author.

I hereby declare that, the contents and organisation of this dissertation constitute my own original work and does not compromise in any way the rights of third parties, including those relating to the security of personal data.



.....  
Omar Kammouh  
Turin, 20 June 2019

---

# Abstract

Community resilience is becoming a growing concern for authorities and decision makers. Resilience is the ability to withstand stress, survive, adapt, and bounce back from a crisis or a disaster and rapidly move on. Current scientific contributions are aimed at understanding disaster resilience and finding new ways to measure it, quantitatively or qualitatively. This dissertation provides new tools for decision-makers to assess the resilience of their communities. The dissertation is divided into three main parts: resilience assessment at the country level, resilience assessment at the community level, and resilience assessment at the Infrastructure level.

At the country level, a novel approach to assess the resilience of countries is presented. The approach is inspired by the classical risk analysis, in which risk is a function of vulnerability, hazard, and exposure. In the proposed analysis, the resilience-based risk is a function of resilience, hazard, and exposure. The methodology is applied to 37 countries for which the resilience is quantified. At the community level, the resilience of communities is tackled by proposing two indicator-based methodologies. The methodologies combine deterministic and probabilistic approaches within a single framework. The first method requires data on previous disasters as an input and returns a performance function for each indicator and a performance function for the whole community as an output. The second method exploits knowledge-based fuzzy modeling for its implementation. A matrix-based interdependency technique that serves as a weighting scheme for the different indicators is also introduced.

In the dissertation, we go in more details when tackling the resilience at the infrastructure level. Resilience can be defined using two main components, the damage incurred following a disastrous event and the restoration time of the system undergone the damage. Therefore, each of the two components is treated separately. For the damage component, two main lifelines, namely water and transportation

---

networks, are tackled. For the water network, a simulation-oriented approach to evaluate the resilience of large-scale water distribution networks is proposed. The failure of the water system occurs when the water flow and the water pressure go below a certain threshold. The resilience of the network is evaluated using two indexes: (1) the number of users without water, (2) the drop in the total water supply. For the transportation network, a resilience evaluation methodology of large-scale transportation networks is presented. First, the road map of a virtual city is transformed into an undirected graph. Random removal of the roads is applied until the network's failure point is reached. The network resilience is then calculated using the Destruction Spectrum (D-spectrum) approach. Multiple coding algorithms are presented in this chapter to solve several computational challenges. For the other component, restoration time, four main infrastructure systems (water, gas, power, and telecommunication) are considered. A large database that includes damage data for many earthquakes that took place in the last century has been collected from the literature. The database has been used to create restoration curves for the lifelines. The restoration curves have been presented in terms of probability of recovery and time; the longer is the time after the disaster, the higher is the probability of the infrastructure to recover its functions.

Finally, a generic resilience framework to assess the resilience of any engineering systems is presented. The temporal dimension is tackled using the Dynamic Bayesian Network (DBN). DBN extends the classical BN by adding the time dimension. This allows predicting the resilience state of a system given its initial condition. Two case studies are presented in the chapter to illustrate the applicability of the introduced framework. One case study evaluates the resilience of Brazil. The other one evaluates the resilience of a transportation system. The framework can be used to study systems that are not explicitly studied in the dissertation. Although it is probabilistic, the framework is practical and can be used by decision-makers in their day-to-day life.

The results of the dissertation provide valuable insights into the decision-making process regarding the resilience of communities. The solutions proposed by the models are improvements over previous work conducted and could benefit decision makers before, during, and after a disaster. In addition, not only does this research provide benefits to decision makers, but it steps beyond research and offers tools that are readily available for the emergency and infrastructure management communities.

---



# Acknowledgment

During my time at the Politecnico di Torino, one lesson that I learned is that I would not have been able to accomplish what I have if it weren't for the help of others. I would like to thank my advisor, Prof. Gian Paolo Cimellaro, for making this dissertation possible. Your guidance and support were necessary for every step of the way.

I would like to acknowledge Professor Paolo Gardoni too for hosting me for 6 months at the University of Illinois at Urbana Champaign. I really enjoyed my research experience there which exposed me to a whole new research environment.

The research leading to these results has received funding from the European Research Council under the Grant Agreement n° ERC\_IDEAL RESCUE\_637842 of the project IDEAL RESCUE—Integrated Design and Control of Sustainable Communities during Emergencies.

---



*To my wife for her constant love and support, to my family for encouraging me to pursue my dreams despite any challenge, and to my God for everything.*

---

# Table of contents

1. Introduction .....	1
1.1 Background .....	1
1.2 Problem definition .....	2
1.3 Research objectives and methods .....	3
1.4 Overview of the dissertation .....	4
2. State of the art.....	6
2.1 Disaster resilience .....	6
2.2 Resilience Evaluation .....	7
2.3 Uncertainty in resilience .....	10
2.4 Downtime Assessment.....	11
2.5 Infrastructure interdependency .....	12
3. Resilience assessment at the Global level .....	13
3.1 Introduction.....	13
3.2 Vulnerability and Resilience analyses .....	13
3.3 Resilience-based risk analysis .....	17
3.4 The World Risk Report (WRR).....	17
3.5 Hyogo framework for action (HFA).....	18
3.6 The methodology: Resilience-Based Risk assessment of countries	21
3.6.1 Method 1: Dependence Tree Analysis (DTA).....	22
3.6.2 Method 2: Weighted Average Analysis (WAA) .....	23
3.6.3 Method 3: Spider Plot Weighted Area Analysis (SPA) .....	24
3.7 Case study .....	25
3.7.1 Resilience results .....	26
3.7.2 Resilience-Based Risk results.....	29
3.8 Concluding remarks .....	30
4. Resilience evaluation framework for urban communities.....	32
4.1 Introduction.....	32
4.2 PEOPLES framework .....	33

---

4.3	Method 1: deterministic resilience quantification of communities based on the PEOPLES framework .....	34
4.3.1	PEOPLES' dimensions, components, and indicators.....	35
4.3.2	Weighting factors: the interdependency matrix technique .....	35
4.3.3	Final functionality function and computing resilience.....	40
4.4	Case study: 1989 Loma Prieta earthquake, San Francisco .....	42
4.5	Software tools for PEOPLES framework .....	47
4.5.1	PEOPLES Web-App .....	47
4.5.2	Desktop software .....	49
4.5.3	Results .....	51
4.6	Method 2: simplified fuzzy logic resilience framework.....	52
4.6.1	Fuzzy logic .....	52
4.6.2	Two- parameter approach.....	55
4.6.3	Four-parameter approach.....	58
4.6.4	Full PEOPLES.....	58
4.7	Discussion.....	59
4.8	Concluding remarks .....	59
5.	Resilience assessment of large-scale water distribution networks: a simulation approach .....	61
5.1	Introduction.....	61
5.2	The resilience of Water Network Distribution .....	61
5.3	IDEAL CITY: Virtual City for Resilience Analyses.....	63
5.4	Model Description, Assumption and Calibration .....	64
5.5	Seismic Hazard and Earthquake Damage of Pipes .....	66
5.6	Vulnerability Analysis of Water Pipes .....	66
5.7	Definition of the event scenarios .....	68
5.8	Numerical results .....	69
5.9	Concluding remarks .....	69
6.	Resilience assessment lifeline networks: application to a large-scale transportation system.....	71
6.1	Introduction.....	71
6.2	Network reliability and components' importance .....	72
6.2.1	Destruction spectrum.....	72
6.2.2	Network reliability.....	73

---

6.2.3	Components' importance.....	74
6.3	Method: application to large scale networks .....	74
6.3.1	D-spectrum for large networks: A Monte Carlo approach .....	74
6.3.2	Reliability and BIM indexes for large scale networks: Incremental calculation .....	75
6.4	Case study: the transportation network of a medium size city .....	77
6.4.1	Network definition.....	77
6.4.2	Network's failure criterion .....	77
6.4.3	Results .....	78
6.5	Concluding remarks .....	80
7.	Downtime assessment of infrastructure systems following earthquakes .....	81
7.1	Introduction.....	81
7.2	Downtime data analysis and interpretation.....	82
7.2.1	Valdivia 1960, Chile (Edwards et al. 2003) .....	85
7.2.2	El-Asnam 1980, Algeria (Nakamura et al. 1983).....	86
7.2.3	Niigata 1964, Japan (Scawthorn et al. 2006c).....	86
7.3	Methodology .....	86
7.3.1	Parameters estimation.....	87
7.3.2	Fitting analysis.....	87
7.3.3	The distribution with optimal fit.....	88
7.4	Results: the restoration curves .....	91
7.4.1	Category 1: Earthquake magnitude .....	91
7.4.2	Category 2: First world countries vs developing countries .....	93
7.4.3	Category 3: countries with a large database (USA, Japan, and countries in South America) .....	94
7.5	Discussion.....	95
7.6	Concluding remarks .....	96
8.	Probabilistic resilience assessment of engineering.....	98
8.1	Introduction.....	98
8.2	Bayesian and Dynamic Bayesian Networks .....	99
8.2.1	Bayesian Network (BN) .....	99
8.2.2	Dynamic Bayesian Network (DBN).....	100

---

8.3	Quantifying Resilience Using Bayesian Network .....	102
8.3.1	Static resilience model.....	102
8.3.2	Network structure and elements connectivity .....	103
8.3.3	Joint probability distribution .....	104
8.4	Case study 1: resilience evaluation of the state of Brazil .....	104
8.4.1	Model definition: Hyogo Framework for Action .....	104
8.4.2	Network structure and elements connectivity .....	105
8.4.3	Probability tables and inference .....	107
8.4.4	Results .....	109
8.5	Time-dependent resilience analysis using DBN .....	109
8.5.1	Dynamic resilience model .....	110
8.5.2	Network structure and elements connectivity .....	110
8.5.3	Joint probability distribution .....	112
8.6	Case study 2: resilience evaluation of a transportation network ...	113
8.6.1	Model definition: Modeling the physical aspect of a transportation network.....	113
8.6.2	Network structure and elements connectivity .....	115
8.6.3	Probability tables and inference .....	116
8.6.4	Results .....	117
8.6.5	Further considerations .....	121
8.7	Concluding remarks .....	122
9.	Summary and conclusions .....	124
9.1	Summary of the dissertation .....	124
9.2	Concluding remarks .....	125
9.3	Future work.....	126
	References.....	127
	Appendix A.....	140

---

# List of Tables

Table 3.1 Difference between vulnerability and resilience at different levels. Adapted from ( <a href="#">Manyena 2006</a> ).....	15
Table 3.2 Priorities and indicators used in the assessment of the Hyogo Framework for Action. Adapted from ( <a href="#">UNISDR 2011</a> ).....	20
Table 3.3 The questions asked by the UN to assess the first indicator. Adapted from ( <a href="#">UNISDR 2011</a> ).....	21
Table 3.4 Indicators scores for the analyzed countries.....	25
Table 3.5 Importance and weighting factors of the HFA indicators.....	27
Table 3.6 Resilience results obtained from the three methods and the exposure of each country.....	29
Table 4.1 Functionality parameters of the indicators within the Physical Infrastructure dimension for the city of San Francisco after the Loma Prieta earthquake.....	43
Table 4.2 The parameters involved in the resilience evaluation.....	44
Table 4.3 The interdependency matrix between the indicators under the component ‘Lifelines’.....	45
Table 4.4 Fuzzy rule base for resilience.....	57
Table 7.1 Summary of the analyzed earthquakes.....	82
Table 7.2 The number of affected infrastructures and the corresponding downtime for each lifeline.....	85
Table 7.3 Downtime data points and corresponding frequencies for the water and power infrastructures with EM 6-6.9.....	88
Table 7.4 <i>Kolmogorov-Smirnov</i> goodness-of-fit test for the water and power infrastructures for EM=6-6.9.....	89
Table 7.5 <i>Chi-square</i> goodness-of-fit test for the water and power infrastructures for EM=6-6.9.....	90
Table 7.6 The distributional parameters derived for Category 1 restoration curves.....	92
Table 7.7 Classification of the countries based on their level of development.....	93
Table 7.8 The distributional parameters derived for Category 2 restoration curves.....	94

---

Table 7.9 The distributional parameters derived for Category 4 restoration curves .....	95
Table 8.1 List of indicators of the Hyogo Framework for Action grouped by priority ( <a href="#">UNISDR 2011</a> ).....	106
Table 8.2 A CPT of a Son node given the states of the father nodes .....	108
Table 8.3 Variables of the proposed transportation network model with corresponding importance factors (I) and nature (Nat) .....	114
Table 8.4 Values for the different input variables .....	117

# List of Figures

Figure 1.1 Flowchart of the dissertation' logical connections between the topics addressed.....	4
Figure 2.1 A conceptual representation of engineering resilience.....	7
Figure 2.2 Evaluating resilience considering the actual initial functionality .....	8
Figure 3.1 Comparison between the vulnerability and the resilience analysis .....	16
Figure 3.2 Typical restoration models .....	16
Figure 3.3 Resilience-based risk analysis Venn diagram .....	17
Figure 3.4 Exposure analysis in the World Risk Report.....	18
Figure 3.5 The ten most exposed countries according to the WRR .....	18
Figure 3.6 Scheme of the proposed framework .....	22
Figure 3.7 A dependence tree diagram showing the different types of components .....	23
Figure 3.8 Spider plot representation of the HFA indicators scores.....	25
Figure 3.9 The dependence tree of the HFA's indicators .....	26
Figure 3.10 Examples of the spider plot method for two countries (France and Monaco).....	28
Figure 3.11 Resilience results obtained by the three methods.....	29
Figure 3.12 Exposure results of the studied countries obtained from the WRR ...	30
Figure 3.13 Risk results obtained using the results of resilience obtained by the three methods.....	30
Figure 4.1 Interdependency matrix between variables in the same group.....	36
Figure 4.2 Interdependency matrices at different levels.....	37
Figure 4.3 Statistical analysis for the expert responses about the weighting factor of each variable .....	38
Figure 4.4 The variation in the interdependency between the PEOPLES seven dimensions given different types of communities .....	38
Figure 4.5 Temporal variation in the interdependency matrix .....	39
Figure 4.6 a) Event-non-sensitive measure (static) b) event-sensitive measure (dynamic).....	40
Figure 4.7 Deriving the functionality function of the community.....	41
Figure 4.8 The resilience curves of two systems showing the same loss of resilience LOR .....	42

---

Figure 4.9 Example of functionality curves (a) sturdier housing type (dynamic indicator), and (b) Physician access (static indicator) .....	46
Figure 4.10 Functionality curves of the components, Facilities and Lifelines, under the dimension Physical infrastructure .....	47
Figure 4.11 (a) Registration/Login page, (b) New scenario definition/load scenario .....	48
Figure 4.12 User interface and data entry environment.....	49
Figure 4.13 (a) starting a new scenario “New case” or loading a saved scenario “Open case”, (b) saving the scenario if the option “New case” is chosen.	50
Figure 4.14 Data entry for the PEOPLES indicators .....	50
Figure 4.15 Data entry for the indicators .....	51
Figure 4.16 Functionality curves of the components “Facilities” and “Lifelines” and the dimension “Physical Infrastructure” .....	51
Figure 4.17 Functionality curves of the components “Facilities” and “Lifelines” and the dimension “Physical Infrastructure” .....	52
Figure 4.18 Fuzzy inference system .....	53
Figure 4.19 Schematic representation of the <i>two-parameter</i> approach .....	55
Figure 4.20 Membership functions for the functionality variable $q^*$ .....	55
Figure 4.21 Membership functions for the downtime variable $T^*$ .....	56
Figure 4.22 Membership functions for the resilience variable $R$ .....	56
Figure 4.23 Hierarchical scheme of the fuzzy system with the weighing process	58
Figure 4.24 Full PEOPLES approach general hierarchical scheme with the weighing process included in the fuzzy system as a separate variable.....	59
Figure 5.1 Functionality of Water Distribution Network, adapted from (Cimellaro et al. 2016c).....	63
Figure 5.2 IDEAL CITY: 3D representation using “ArcGIS” software.....	63
Figure 5.3 Global view of the water network. ....	65
Figure 5.4 (a) Water demand $q_{i,w}$ within a mesh element $w$ , (b) Water demand at a node $i$ .....	65
Figure 5.5 Calibrated water pressure and velocity in the WDN.....	66
Figure 5.6 Pipe break simulation in EPANET 2.0.....	67
Figure 5.7 Distribution of the simulation results. ( $N_s = 5000$ , $K_I = 0.5$ ).....	68
Figure 5.8 Resilience indexes $R$ and $R_Q$ for three $K_I$ values (pipe material). ....	69
Figure 6.1: A simple network with two critical nodes.....	72
Figure 6.2: The transportation network of the virtual city.....	77
Figure 6.3: (a) The D-spectrum of all components of the case study network; (b) a zoomed view at the distribution peak. ....	78
Figure 6.4: (a) The cumulative D-spectrum of all components the case study network; (b) a zoomed view at the transitional part. ....	79
Figure 6.5: The BIM spectra of the network's components.....	79
Figure 7.1 Location of the earthquakes considered in the study .....	82
Figure 7.2 Distribution of the analyzed earthquakes by location .....	83

---

Figure 7.3 Cumulative frequencies with three theoretical CDF fitting distributions for (a) the water distribution infrastructure, and (b) the power network infrastructure for the data corresponding to EM 6-6.9 .....	89
Figure 7.4 Histograms and PDF fitting distributions for (a) the water distribution infrastructure, and (b) the power network infrastructure for the data corresponding to EM 6-6.9 .....	90
Figure 7.5 Restoration curves of the lifelines based on the earthquake magnitude .....	93
Figure 7.6 Restoration curves of the lifelines based on the level of development of the countries .....	94
Figure 7.7 Restoration curves of the lifelines of the USA, Japan, and countries in South America .....	95
Figure 8.1 (a) The initial network of a DBN (typical Bayesian network), (b) the 2TBN or a second order DBN, (c) the unrolled DBN model for T= 4 slices. ....	102
Figure 8.2 The three resilience pillars .....	103
Figure 8.3 A general resilience function of a system .....	103
Figure 8.4 Bayesian network to compute the resilience index of a static system	104
Figure 8.5 Bayesian Network of the Hyogo framework indicators .....	107
Figure 8.6 BN analysis and resilience results of the country “Brazil” .....	109
Figure 8.7 The four resilience components (4R’s) and their interaction with the resilience curve .....	110
Figure 8.8 Dynamic Bayesian network of an engineering system considering external factors such as the resilience characteristics (4R’s) and the Hazard .....	112
Figure 8.9 An indicator layered-model to systematically describe engineering systems.....	113
Figure 8.10 a) Event-non-sensitive indicator (static) b) event-sensitive indicator (dynamic).....	115
Figure 8.11 DBN connectivity of the transportation network model .....	116
Figure 8.12 System’s performance results for the first scenario of the simulation (high damage, high recoverability).....	119
Figure 8.13 System’s performance results for the second scenario of the simulation (high damage, low recoverability).....	119
Figure 8.14 System’s performance results for the third scenario of the simulation (low damage, low recoverability).....	120
Figure 8.15 System’s performance results for the fourth scenario of the simulation (low damage, high recoverability).....	120
Figure 8.16 System’s performance results for the fifth scenario of the simulation (high damage, medium recoverability).....	121
Figure 8.17 Resilience function with multiple hazards .....	121
Figure 8.18 Bayesian network with additional variables in the first and last slices .....	122

---

# Chapter 1

## 1. Introduction

### 1.1 Background

The world is undergoing rapid urbanizing at an unprecedented speed. The global urban population increased from 29% in 1950 to 50% in 2010 and is expected to further increase to 69% by 2050. Communities and societies have become more reliant on a network of infrastructures and technological systems that provide indispensable services for the citizens. The resilience of interdependent engineered lifeline networks, such as electric grids, water systems, and communication networks, to unprecedented hazards induced extreme changes in their statistical attributes. Infrastructure systems often display a high degree of interconnectedness: functional, geographical, cyber, and logical. Such interdependencies play a role in enhancing the level of services provided to the citizens (e.g. ICT penetration in the electricity sector to develop smart grids), but they might also expose the system to harmful domino effects.

Recent disasters in New Zealand have dramatically highlighted the impact shocks can have on society and its ability to function and grow. The Christchurch Earthquakes of 2010-2011 caused over NZ\$40B of economic losses, 185 fatalities, and 10,000 injuries, but also of note is that the rebuild and recovery of the city are still ongoing, some 6 years following the first earthquake. Issues with the recovery of Christchurch have provided the platform for a dialogue on resilience across various sectors in New Zealand. Many other disasters have occurred in other parts of the world resulting in damage to critical community functions. The Bío-Bío, Nepal earthquakes, Hurricanes Sandy and Katrina, and tornadoes in Joplin all resulted in severe damage to the communities, putting great strain on the infrastructure systems of these regions. Therefore, the continued functionality of critical infrastructure is necessary following major disaster events.

To improve the resilience of communities, decision makers first need a way to quantify their performance during extreme loading from natural and man-made hazards, both predictively and retrospectively. This would permit them to assess the current situation of their communities and plan for potential disturbing events. To do that, however, the following questions need to be answered: What kind of infrastructure damage is expected after a disruptive event? How long would the

system continue to provide service to customers? Which customers are impacted the most? What kind of restoration actions would be helpful? How should restoration actions be prioritized? What can utilities do to prepare for undesired events?

## 1.2 Problem definition

Resilience assessment of complex systems starts with static and dynamic interdependency analyses, incorporates service-oriented models, and involves economic impact assessment in relation to business discontinuities. The big issue with resilience assessment to date is: how can you measure progress in your community if you don't know where you started? It is hard to know if any of the programs that you will implement to improve your resilience have been effective if you don't know your baseline. The challenges faced at the community level is that the assessment tools need to be simple, they need to be able to be replicated over time, they have to be meaningful at the local and national scales, and they have to be based on evidence.

There are lots of tools to quantify resilience out there. Some are incredibly complex and difficult to use and implement, others are too simple, and they cannot give the kind of resolution of information that we need. While communities have the potential to develop their own tools to develop simple measurement systems to cage their own baselines, these tools may not be comparable across communities.

Resilience measurements would certainly help communities in understanding the benefit/cost of implementing resilience actions and in evaluating the effects of these actions by looking at different policies and approaches. Measurement tools are helpful in identifying disaster risk, taking steps toward reducing it, assessing how they are doing, and getting stakeholders to work together. However, we have to understand that a single one-size-fits-all approach may not work on the bottom-up scale. What we can collectively do in terms of measuring resilience across a wide geographic area may give us some ideas on where additional resources need to be spent to improve resilience, but may not be sufficient to help us understand what's going on at the very local community level. The main resilience challenges that we face at the local and global scales are:

- The existence of unavoidable disruptions in an increasingly complex, global, and interconnected world: it is impossible to predict and cost-prohibitive to defend against all possible threats to a system.
- The need for a holistic approach to capture community functioning over time.
- The need for models that interface multiple scales (building, institution, community, etc.).
- The need for effective use of data that is collected over a wide range of time scales (e.g., census, tax assessors, reconnaissance, etc.).
- The need for models that capture the complex interactions of many community institutions.

- The need for simplified, yet accurate approaches to quantify resilience, resulting in tools that can be used by decision-makers in practice.

### **1.3 Research objectives and methods**

The core goal of this research is to develop a targeted, multi-scale rapid resilience assessment tools with application to communities, emergent environments, and complex socio-technical systems. Resilience assessment tools can certainly help show and illustrate a path that the community can take to become safer and stronger and certainly more vibrant in the face of unanticipated events.

The primary area of focus is the development of resilience modeling workflows that will be delivered through decision support tools to enable decision makers to better assess resilience strategies in their day-to-day decisions. To achieve that, the following priorities (or sub-goals) have been identified and tackled in the dissertation:

- New ways for complex network modeling with application to large-scale complex infrastructure networks;
- Identifying critical value systems to help select locally acceptable resilience baselines;
- Establishing baselines for monitoring progress and recognizing success;
- Understanding costs (investments) and benefits (results) for resilience improvement measures;
- Assessing/prioritizing needs and goals for communities;
- Resilience improvement alternatives;
- Tools to prioritize emergency actions following a disaster event;
- Study the interdependency among infrastructure systems.

In this dissertation, we also seek to develop disaster scenarios based on real events. This is necessary to optimize the response actions following a disaster and provide necessary insights to policymakers and stakeholders for building resilience.

To achieve the high goal of this research, several modeling and analysis techniques have been used. For resilience modeling, two main approaches have been adopted: the first is the use of resilience indicators, which is effective in preliminary designs or in the assessment of complex systems, and the second is through the use of simulation techniques, which have been applied to investigate the resilience of infrastructure systems where high-resolution and detailed analysis was required. For the resilience analysis, deterministic and probabilistic methods have interchangeably been employed depending on the analyzed case. Fuzzy and Bayesian methods have also been used to deal with uncertainties caused by data deficiency. Case studies are presented throughout the dissertation to illustrate the applicability of the introduced frameworks and methodologies.

## 1.4 Overview of the dissertation

Figure 1.1 shows the workflow of the topics addressed in the dissertation. The dissertation's body is divided into three main parts: resilience quantification at the country level, resilience quantification at the community level, and resilience quantification at the infrastructure level.

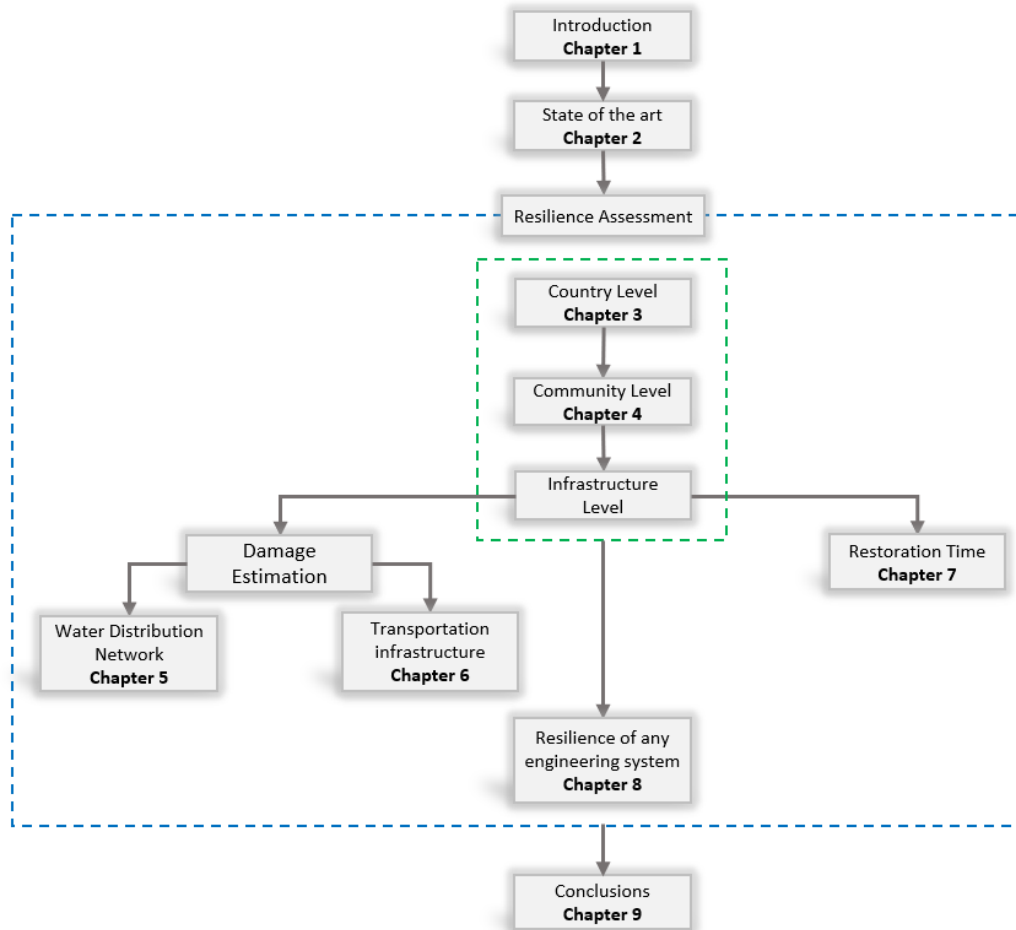


**Figure 1.1** Flowchart of the dissertation's logical connections between the topics addressed

The remainder of the thesis is organized as follows. First, in **Chapter 2**, an overview of relevant literature will be presented. **Chapter 3** presents a quantitative method to assess the resilience and resilience-based risk at the country level. The proposed methodology is applied to a case study composed of 37 countries for which two Resilience indexes are evaluated. **Chapter 4** deals with the resilience of communities. The chapter introduces two indicator-based methods to evaluate the resilience of communities. The first method, introduced in Section 4.3, is a deterministic method, while the second method (Section 4.6) exploits knowledge-based fuzzy modeling for its implementation. **Chapter 5** proposes a simulation-oriented approach to evaluate the resilience of large-scale water distribution networks. The case study used in the research is the water network of a large-scale

virtual city. **Chapter 6** tackles the resilience of large-scale transportation networks. The transportation network of the same virtual city presented in the previous chapter is considered as a case study. **Chapter 7** provides an empirical probabilistic model to estimate the downtime of lifelines following earthquakes. Empirical restoration functions are presented to allow identifying the restoration time of such lifelines given an earthquake of a given magnitude. **Chapter 8** introduces a dynamic Bayesian approach to assess the time-dependent resilience of engineering systems using resilience indicators. The last chapter (**Chapter 9**) presents the summary and conclusions of the dissertation, laying out major research contributions and future research directions.

# Chapter 2

## 2. State of the art

### 2.1 Disaster resilience

Over the years, community resilience has attracted remarkable attention due to the increasing number of natural and man-made disasters. Communities that are able to absorb the impacts and recover quickly after disasters are fairly resilient communities, while communities whose recovery capacity is exceeded need to improve their resilience in order to facilitate a faster recovery. The concept of resilience is multi-dimensional, and therefore involves various subjects of different disciplines ([Bonstrom and Corotis 2014](#); [Chang et al. 2014](#); [Cimellaro et al. 2016a](#); [Cimellaro et al. 2016c](#)). It can be applied to multiple scales and units of analysis, ranging from the individual scale (e.g person, building, etc.) to the global scale (e.g. community, state, etc.). Resilience has been defined differently depending on the field of study ([Manyena 2006](#); [Hosseini et al. 2016](#)). It can be defined as “the ability of social units (e.g. organizations, communities) to mitigate hazards, contain the effects of disasters when they occur, and carry out recovery activities in ways to minimize social disruption and mitigate the effects of further earthquakes” ([Bruneau et al. 2003](#); [Cimellaro et al. 2010](#); [Cimellaro et al. 2016d](#)). [Allenby and Fink \(2005\)](#) defined resilience as “the capability of a system to stay in a functional state and to degrade gracefully in the face of internal and external changes”. In engineering, resilience is the ability to “withstand stress, survive, adapt, and bounce back from a crisis or disaster and rapidly move on” ([Wagner and Breil 2013](#)). Other researchers have also tackled other disciplines linked to resilience and proposed a more inclusive definition in relation to risk and uncertainty. For example, [Ayyub \(2015\)](#) suggested that “the resilience of a system is the persistence of its functions and performances under uncertainty in the face of disturbances”. From the several definitions provided above, it is still difficult to find a generally accepted definition for engineering resilience, mainly because this concept has been applied only recently in the engineering field.

## 2.2 Resilience Evaluation

Measuring resilience has been an exploding field of inquiry in the last decade. [Bruneau et al. \(2003\)](#) stated that the resilience of a system depends on its functionality performance. The functionality of a system is the ability to use it at possibly an impaired level. In this conceptual approach, the performance of any system can range between 0% and 100%, where 100% indicates ‘no drop-in service’ and 0% means ‘no service is available’. The occurrence of a disaster at time  $t_0$  causes damage to the system and this produces an instant drop in the system’s functionality ( $\Delta Q$ ). Afterward, the system is restored to its initial state over the recovery period ( $t_1-t_0$ ). The loss of resilience is considered equivalent to the quality degradation of the system over the recovery period. The conceptual approach described in [Bruneau et al. \(2003\)](#) is illustrated in Figure 2.1. Mathematically, it is defined as follows:

$$LOR = \int_{t_0}^{t_1} [100 - Q(t)] dt \quad (2.1)$$

where  $LOR$  is the loss-in-resilience measure,  $t_0$  is the time at which a disastrous event occurs,  $t_1$  is the time at which the system recovers to 100% of its initial serviceability,  $Q(t)$  is the serviceability of the system at a given time  $t$ .

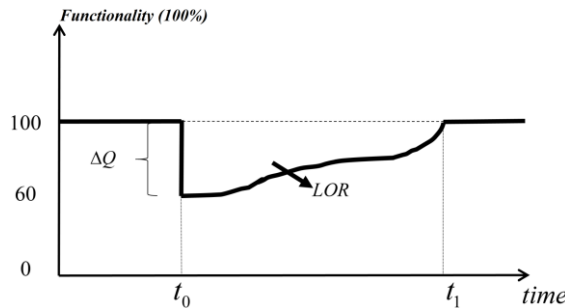


**Figure 2.1** A conceptual representation of engineering resilience

The approach introduced above considers a constant initial functionality ( $Q_0=100\%$ ). This can be problematic if the system recovery includes mitigation and hardening actions that increase the functionality to a level beyond the initial state of the system. Therefore, in this dissertation, the initial functionality is signified by a functionality ( $Q_0$ ) that can take any value between 0% and 100% (Figure 2.2). This means that the functionality function does not necessarily start with 100%. This leaves room for possible improvements in case hardening actions are included in the recovery process. In addition, the  $LOR$  has to be normalized to be time-independent. This is done by dividing over  $T_c$ , which is the control time of the period of interest ([Cimellaro et al. 2010](#)). Thus, Eq. (2.1) can be replaced by Eq. (2.2):

$$LOR = \int_{t_0}^{t_1} \frac{[100 - Q(t)]}{T_c} dt \quad (2.2)$$

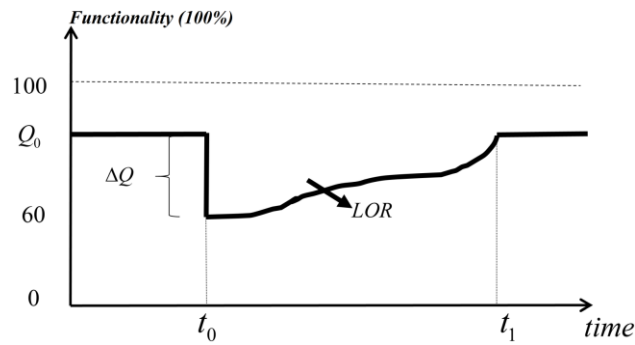


**Figure 2.2** Evaluating resilience considering the actual initial functionality

Many options for measuring resilience are available, ranging from specific measurements to scorecards to indexes. [Liu et al. \(2017\)](#) introduced a method that combines dynamic modeling with resilience analysis. Interdependent critical infrastructures have been analyzed using the framework by performing a numerical analysis of the resilience conditions in terms of design, operation, and control for a given failure scenario. [Cimellaro et al. \(2016c\)](#) proposed a resilience index for water distribution networks that is the product of three indexes. The resilience index has been used to compare different restoration plans in a small town in the South of Italy. [Ayyub \(2015\)](#) proposed other resilience metrics with clear relationships to the most relevant definition of the reliability and risk notions. The framework meets logically consistent requirements drawn from the measure theory considering the recovery phase based on spatial and temporal considerations. [Chang and Shinozuka \(2004\)](#) introduced a measurement framework to quantitatively assess the disaster resilience of communities. They proposed a series of resilience measures in a probabilistic context based on the work by [Bruneau et al. \(2003\)](#). The proposed framework has been implemented in a case study of the Memphis water system under an earthquake event. While these methods did not clearly integrate the social and economic aspects of communities, [Gilbert and Ayyub \(2016\)](#) proposed microeconomic models and metrics to quantify the economic resilience of engineering systems. These metrics provide a sound basis for the development of effective decision-making tools for multi-hazard environments and lead to significant savings through risk reduction and expeditious recovery. [Ouyang et al. \(2012\)](#) proposed a multi-stage framework to analyze infrastructure resilience establishing an expected annual resilience metric by defining a series of resilience-based improvement strategies for each stage. [Kammouh et al. \(2018b\)](#) have introduced a quantitative method to assess the resilience at the state level based on the Hyogo Framework for Action ([ISDR 2005](#)). The approach introduced was an evolution of the risk assessment concept. The resilience of 37 countries has been evaluated and a resilience score between 0 and 100 has been assigned to each of them. [Kwasinski et al. \(2016\)](#) proposed a hierarchical framework for assessing resilience at the community level. The model is represented through community dimensions and their relationships with community services, systems, and resources. Several other works have been carried out to define and quantify the resilience of communities but mostly with a focus on engineering systems

([Hollnagel et al. 2007](#); [Park et al. 2013](#); [Hosseini and Barker 2016](#); [Jovanović et al. 2016](#))

Reviewing the available resilience measurement tools allows distinguishing some features that separate them. Some are related to top-down measurement schemes, others are bottom-up, some measurements schemes are purely qualitative in their approach, and others are quantitative. These measurement tools are also spatially variable, and they differ in their focus and application.

A top-down approach is essentially the decomposing of a system to gain more insight into its compositional sub-systems in a reverse engineering fashion. For example, breaking down the components of a building structure into columns, beams, water system, electrical system, etc. Each of these components is further decomposed; for instance, breaking the beam component into concrete and steel. Each of the lowest level sub-components can then be described and assessed independently. On the other hand, a bottom-up approach is the putting together the systems to produce more complex systems ([Crowder et al. 2015](#)).

Some of the many existing top-down approaches include the PEOPLES framework ([Cimellaro 2016](#)). PEOPLES framework is an example of a top-down approach that starts with the big picture (i.e. resilience) then breaks down into smaller segments. Each subsystem is then refined in yet greater detail, sometimes in many additional subsystem levels, until the entire specification is reduced to base elements ([Cimellaro et al. 2016a](#)). The acronym combines seven dimensions: **P**opulation; **E**nvironment; **O**rganized government services; **P**hysical infrastructure; **L**ifestyle; **E**conomic; and **S**ocial capital. It is classified as a quantitative framework for designing and measuring the resilience of communities. Another top-down measurement tool is the Baseline Resilience Indicator for communities (BRIC) ([Cutter et al. 2014](#)). This measurement tool is also quantitative, but it focuses on the pre-existing resilience of communities. Unlike the PEOPLES framework, BRIC is practically oriented towards the fieldwork. San Francisco Planning and Urban Research Association framework (SPUR) ([SPUR 2009](#)) is a qualitative framework that measures the ability to recover from earthquakes. The framework considers the restoration of buildings, infrastructures, and services. Examples of other top-down approaches are the Hyogo Framework for Action (HFA) ([UNISDR 2005](#)); the UK Department for International Development (DFID) Interagency Group ([Twigg 2009](#)); ResilUS ([Miles and Chang 2011](#)); etc. There are also few bottom-up approaches mainly designed for communities to help them predict and plan for resilience. These bottom-up measurement tools take an all-hazards approach in their assessment. They are generally qualitative types of assessments that the community does itself, or it works with local stakeholders to derive its assessment. Some bottom-up approaches include the Conjoint Community Resiliency Assessment Measure (CCRAM) ([Cohen et al. 2013](#)), the Communities Advancing Resilience Toolkit (CART) ([Pfefferbaum et al. 2011](#)), the Community Resilient System ([White et al. 2015](#)), etc. A more exhaustive list of resilience measurement tools classified according to several characteristics can be found in ([Cutter 2016a](#)).

## 2.3 Uncertainty in resilience

The resilience concept in engineering is recent and therefore it involves uncertainty. Several authors have proposed methodologies to evaluate the resilience of engineering systems; some are deterministic ([Henry and Ramirez-Marquez 2012](#); [Kammouh et al. 2017](#); [Kammouh et al. 2019b](#)) and the others are probabilistic ([Cockburn and Tesfamariam 2012](#); [Shahriar et al. 2012](#); [De Iuliis et al. 2018](#); [Kammouh et al. 2018a](#); [Kammouh et al. 2018c](#)). Nevertheless, developing a standardized methodology to quantify resilience is still challenging due to the presence of uncertainty in the resilience model and its inputs. The interdependency and the weighting factors distribution among the variables are also other issues that cannot be handled in a deterministic way. Therefore, probabilistic methods are usually preferred over deterministic methods. Probabilistic models are more powerful to model uncertainties and interdependencies and they are more appropriate to represent reality. In fact, deterministic models are considered a particular case of probabilistic models ([Pourret et al. 2008](#)).

While probabilistic models solve the gap of modeling capability that deterministic models suffer from, not all probabilistic approaches are suitable to model the behavior of engineering systems, especially in cases where past data is not readily available. One way to properly model the behavior of a system in a probabilistic manner is through the use of Bayesian Networks (BNs). BN is a Directed Acyclic Graph where the nodes represent variables of interest and the links between them indicate causal dependencies. BNs are widely used for knowledge representation and reasoning under uncertainty, especially in the context of partial information. They are effective when different types of variables and knowledge from various sources need to be integrated within a single framework. In addition, BN provides probabilistic relationships among the variables, which allows modeling the interdependencies among them. In the literature, there is a limited number of research contributions that use the BN in resilience analysis. [Johansen and Tien \(2018\)](#) proposed a probabilistic methodology based on the BN approach to model the interdependencies between critical infrastructure systems. Their research aims at understanding the effect of interdependencies on the fragility of the overall system. [Cai et al. \(2017\)](#) developed a universal resilience metric for infrastructure systems. A BN approach was employed to calculate the resilience metric value. The proposed resilience metric can be used to design and/or optimize different types of engineering systems. [Yodo and Wang \(2016\)](#) proposed a framework to model the resilience of engineering systems and the BN was used to quantitatively assess the resilience. The framework permits designers to understand the strength and weakness of their systems against external disruptions and disaster events. The applicability of the framework was demonstrated using two different case studies (supply chain and production process). Moreover, [Hosseini et al. \(2016\)](#) introduced a resilience quantification methodology using BN. In their research, resilience is defined using three parameters: absorptive capacity, adaptive capacity, and restorative capacities. A case study on an inland waterway port, an

essential component in the intermodal transportation network, was used to illustrate the methodology. Rather than the static approaches, [Yodo et al. \(2017\)](#) presented a dynamic resilience analysis method based on the Dynamic Bayesian Network (DBN). The method allows modeling and predicting the resilience of engineering systems in the design and maintenance phases. [Tabandeh et al. \(2018\)](#) developed an indicator-based probabilistic formulation to model the societal impact and estimate the impact considering the immediate consequences and the recovery condition. The methodology uses DBN to integrate the predictive model of the indicators. BNs have also been employed by researchers in fields other than disaster resilience ([Ismail et al. 2011](#); [Cockburn and Tesfamariam 2012](#); [Kabir et al. 2015](#); [Siraj et al. 2015](#); [Kabir et al. 2016](#)). For example, ([Cockburn and Tesfamariam 2012](#)) used BNs to estimate the risk of several cities located in Canada, ([Kabir et al. 2015](#)) evaluated the risk of water mains failure using a BN model, while ([Siraj et al. 2015](#)) employed BNs in the seismic risk assessment of high voltage transformers.

In fact, BN does not capture the behavior of dynamic systems and the interdependencies among the system's components and variables. BN is a snapshot of the system, which implies that the restoration process, which is inherently time-dependent, cannot be modeled. Moreover, a feedback loop is not allowed in a BN model; thus, it cannot be used to model a cyclic relationship. Although there are some research works that use the DBN as an inference tool to express resilience in a dynamic manner, the resilience models adopted in those researches and the transitional model from one step to another in the time-space was not clearly defined.

## 2.4 Downtime Assessment

A key aspect of the resilience assessment process is *downtime*. Downtime is the time required to achieve a recovery state after a disastrous event; therefore, it is strictly linked to the indirect losses of the damaged infrastructure ([Terzic et al. 2014](#)). Estimating the downtime of engineering systems following an earthquake is a subject on which scientists and policymakers have recently focused their attention. Downtime is usually caused by the construction repair of the damaged structure and the arrangements needed to mobilize resources. Comerio (2005) defined downtime as the sum of rational and irrational components ([Comerio 2005](#)). The rational components include construction costs and repair time, while the irrational components consider the time needed to mobilize resources and make decisions.

The downtime is an essential parameter to estimate resilience. One of the first attempts to evaluate the disruption time following a disaster event was done by [Basöz and Mander \(1999\)](#). In their work, they developed downtime fragility curves for the transportation lifeline. The fragility curves were later integrated into the highway transportation lifeline module of HAZUS. Another downtime estimation methodology was developed based on a modified repair-time model ([Beck et al.](#)

1999). This methodology estimates the downtime of only the rational structural components of a system, due to the uncertainty involved in the process. In addition, the Federal Emergency Management Agency (FEMA) has introduced the *Performance Assessment Calculation Tool* (PACT). PACT is an electronic calculation tool, and repository of fragility and consequence data, that calculates and accumulates losses. It includes a series of utilities used to specify building properties and update or modify fragility and consequence information in the referenced databases. PACT is considered the companion to FEMA P-58, a significant 10-year project funded by FEMA to develop a framework for performance-based seismic design and risk assessment of buildings ([Hamburger et al. 2012](#)). Almufti and Willford (2013) have proposed the *Resilience-based Earthquake Design Initiative* (REDi™) based on the results coming from PACT ([Almufti and Willford 2013](#)). The goal was to provide owners and other stakeholders a framework for implementing resilience-based earthquake design and achieving higher performances. Moreover, a performance-based earthquake engineering method to estimate the downtime of infrastructures using fault trees was introduced in ([Porter and Ramer 2012](#)). This method is applicable only when the downtime is mostly controlled by non-structural systems damage. It assumes that the restoration starts immediately after the event and the damaged components are repaired in parallel.

## 2.5 Infrastructure interdependency

Another concern involved in the resilience evaluation is the infrastructure interdependencies. This is a subject on which most of the current research effort is placed, mainly because of its complexity and uncertainty. Critical infrastructure systems are highly interconnected and mutually interdependent where damage to one infrastructure can produce cascading failures on other systems ([Pfefferbaum et al. 2011](#)). For instance, telecommunication and water systems require a continuous supply of energy to maintain their normal functions, while the power infrastructure needs the water and various telecommunication services to generate and deliver electricity. Although the presence of interdependencies can significantly improve the operational efficiency of infrastructure, recent worldwide events have shown that interdependencies can increase systems vulnerability. The level of interdependencies between systems can determine how long a dependent system can stay inoperable. The Lifelines Council of San Francisco completed a study on the interdependencies of the city's infrastructure systems ([CCSF Lifelines Council 2014](#)). They evaluated the infrastructures' performance following a hypothetical major earthquake with a magnitude of 7.9. The study suggests that some of the lifelines were closely coupled and interdependent with the performance and restoration of the other lifelines. The interdependency was responsible for a significant recovery delay when the infrastructures have only experienced moderate damage.

# Chapter 3

## 3. Resilience assessment at the Global level

*Part of the work described in this chapter has been previously published:*

- 1- Kammouh, O., Dervishaj, G., and Cimellaro, G. P. (2017). "A New Resilience Rating System for Countries and States." *Procedia Engineering*, 198 (Supplement C), 985-998. <https://doi.org/10.1016/j.proeng.2017.07.144>.
- 2- Kammouh, O., Dervishaj, G., and Cimellaro, G. P. (2018). "Quantitative Framework to Assess Resilience and Risk at the Country Level." *ASCE-ASME Journal of Risk and Uncertainty in Engineering Systems, Part A: Civil Engineering*, 4(1), 04017033. doi:10.1061/AJRUA6.0000940.

### 3.1 Introduction

The absence of a concise and methodological approach makes resilience extremely difficult to determine. The progress in the Hyogo Framework for Action (HFA) ([UNISDR 2011](#); [UNISDR 2015](#)) — a work developed by the United Nations — has led to the formulation of an international blueprint that is very useful for building the resilience of nations and communities. The methodology adopted by the HFA focuses on implementing detailed measures at the governmental level through policies. The goal is to encourage the countries to implement the HFA in their respective laws. The lifespan for the implementation was from 2005 to 2015, after which each of the participating countries was required to submit a report on their own progress. A score was then given by the UN to each of the submitted reports on the basis of the progress each country had made. Using the results of the Hyogo framework, a quantitative method to assess the resilience and the resilience-based risk of countries is proposed and applied to a case study composed of 37 countries.

### 3.2 Vulnerability and Resilience analyses

One of the many topics discussed when referring to resilience is its relationship with vulnerability and whether they are similar enough to be considered the same. Vulnerability is an elusive concept whose definition varies across disciplines, ranging from engineering to economics to psychology. Despite the range of approaches to measuring vulnerability, several best practices in vulnerability

assessment emerge. For instance, [Peng et al. \(2016\)](#) have developed an engineering-based damage assessment models to assess the vulnerability of low-rise buildings against tornadoes. The models can be implemented in any region regardless of the tornado size and strength. The output of this model is a percentage damage index and the overall building damage ratio. One of the most adopted tools for vulnerability and risk assessment is HAZUS. HAZUS is a standardized risk assessment software developed by the US Federal Emergency Management Agency (FEMA, [fema.gov/Hazus](http://fema.gov/Hazus)) for evaluating potential losses caused by natural hazards ([Nastev and Todorov 2013](#)). HAZUS integrates engineering and science-based knowledge with the geographic information systems (GIS) to determine the loss and damage before or after a disaster occurs. It consists of four main models:

1. The Hazus earthquake model: provides loss estimates of buildings, facilities, transportation, and utility lifelines based on scenario earthquakes to support decision-making process for preparedness and disaster response planning ([Whitman et al. 1997](#)). The model considers debris generation, fire-following, casualties and shelter requirements. Direct losses are estimated based on physical damage to structures, contents, inventory and building interiors. The Hazus earthquake framework consists of six interdependent modules with the output of one module acting as input to another. More information about the framework algorithm and the modules can be found in ([Kircher et al. 2006](#)). In addition, a new extension module “*Advance Engineering Building Module*” (AEBM) has been integrated into the Hazus earthquake model to help seismic engineering experts in the development of building-specific damage and loss functions.
2. The Hazus Hurricane Wind Model: allows estimating hurricane winds and damage to different types of buildings. It also estimates direct economic loss, post-storm shelter needs and building and tree debris quantities and allows assessing the structural changes to buildings to strengthen them for mitigation. This model has been initially developed using principles of wind engineering to allow accurately estimating damage and loss to buildings due to hurricanes ([Vickery et al. 2006a](#)). The approach adopted in this model has been previously calibrated and validated using simulations and field observations of the wind speeds over more than 140 locations ([Vickery et al. 2000a](#); [Vickery et al. 2000b](#)). The HAZUS-MH Hurricane Model comprises five model components (hurricane hazard, terrain, wind Load/debris Modeling, damage, and loss Estimation). The first three components are described in ([Vickery et al. 2006a](#)) while the last two are discussed in a companion paper ([Vickery et al. 2006b](#)).
3. The Hazus Flood Model: evaluates potential damage to buildings, essential facilities, transportation lifelines, utility lifelines, vehicles and agricultural crops caused by riverine and coastal flooding. The model also considers building debris generation and shelter requirements. Direct losses are estimated based on physical damage to structures and to buildings’ contents and interiors. ([Scawthorn et al. 2006a](#)) provide a discussion of the capability

of the software in characterizing riverine and coastal flooding. They also discuss the Flood Information Tool, which allows a quick and convenient analysis of various stream discharge data and topographic mapping to determine flood-frequencies over entire floodplains. In a companion paper, [Scawthorn et al. \(2006b\)](#) tackle the damage and loss estimation capability of the flood model. The model contains over 900 damage curves to estimate the damage of different types of buildings and infrastructures.

4. The Hazus Tsunami Model: represents the most recent disaster module for the Hazus software in the last decade. The model is a joint effort of tsunami experts, engineers, modelers, emergency planners, economists, social scientists, geographic information system (GIS) analysts, and software developers. New features are continuously added to this model in an attempt to increase its capabilities.

Although vulnerability is strongly linked to the concept of risk assessment ([Papadopoulos 2016](#)), it has been pointed out that the concept of vulnerability is associated with resilience under various scientific disciplines ([Richard et al. 1998](#)). Meanwhile, vulnerability has been identified as a lack of capacity ([Cardon et al. 2012](#)). Under this context, the vulnerability of a system is reduced by increasing the system's capacity. Moreover, some literary publications provide the same definitions for resilience and vulnerability ([Klein et al. 2003](#)), while others identified some instances where scholars had different views for the two concepts ([Cutter 2016b](#)), admitting that they may overlap in some areas ([Gallopín 2006](#)). Table 3.1 shows a comparison between vulnerability and resilience on different scales. The comparison suggests that resilience is concerned more with the human capacity to recover from a disaster within a short time and with no outside assistance, while vulnerability is the property of resisting the stress caused by a natural hazard.

**Table 3.1** Difference between vulnerability and resilience at different levels. Adapted from ([Manyena 2006](#))

<b>Vulnerability</b>	<b>Resilience</b>
<b>Resistance</b>	Recovery
<b>Force bound</b>	Time-bound
<b>Safety</b>	Bounce back
<b>Mitigation</b>	Adaptation
<b>Institutional</b>	Community-based
<b>System</b>	Network
<b>Engineering</b>	Culture
<b>Risk assessment</b>	Vulnerability and capacity analysis
<b>Outcome</b>	Process
<b>Standards</b>	Institution

Due to the uncertainty involved in the resilience assessment process, a probabilistic approach similar to the classical vulnerability analysis can be established. Figure 3.1 illustrates the conceptual approaches of both vulnerability and resilience analyses. In the vulnerability analysis, a number of fragility curves are built to interpret the vulnerability of a system. The curves represent the system's probability of exceeding a certain damage state under different hazard intensity levels. In the proposed resilience analysis, the fragility curves describe the probability of a system to be below a predefined resilience threshold under a certain intensity level (see Figure 3.1). Figure 3.1 shows the resilience surface fragility curves when considering more than one intensity measure. Those curves represent the probability of a system having a certain intensity measure IM-1 (e.g., Human resources or man power) and a certain intensity measure IM-2 (e.g., financial resources) to be below a predefined resilience threshold.

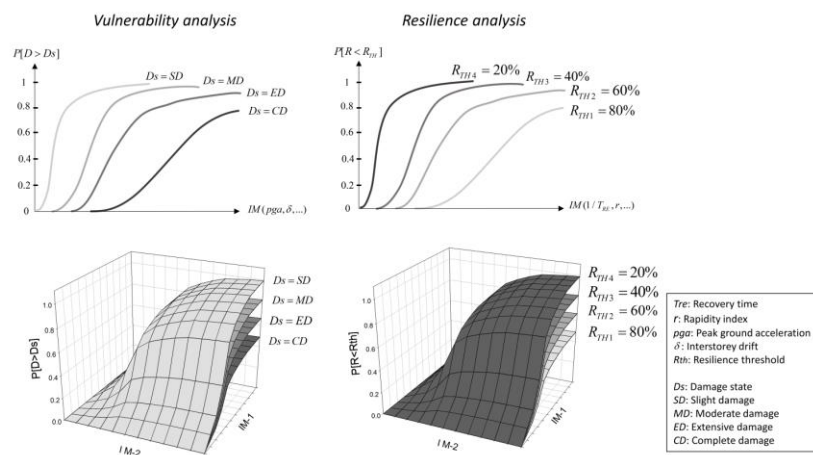


**Figure 3.1** Comparison between the vulnerability and the resilience analysis

The restoration speed (or rapidity) is one of the most important parameters when evaluating resilience. Generally, the rapidity of restoration  $r$  depends on several factors, such as human resources, the restoration plan, the financial resources, etc. Thus, the graphical configuration of the restoration phase can be of infinite shapes. Figure 3.2 shows three types of restoration curves (exponential function, step function, and random function). The rapidity of restoration  $r$  can be considered as the slope of the best-fitting line obtained by applying a linear regression to the restoration curve. In this way,  $r$  can express the rapidity of any restoration curve regardless of its actual configuration.

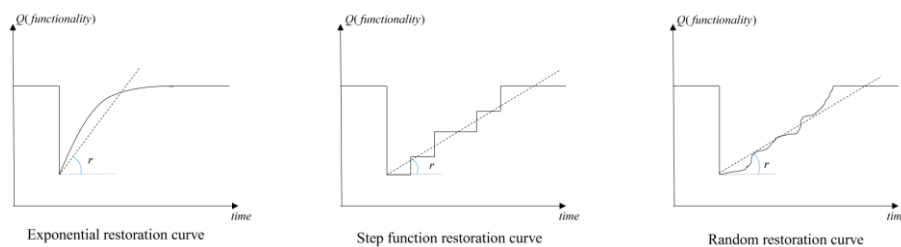
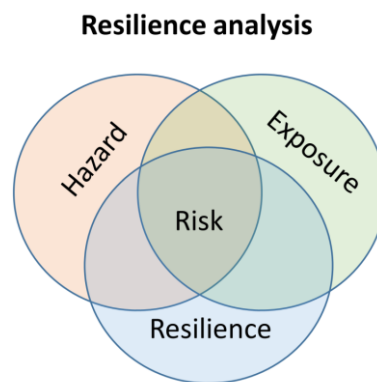


**Figure 3.2** Typical restoration models

### 3.3 Resilience-based risk analysis

In the classical risk assessment methodology, Risk is the combination of Vulnerability, Hazard, and Exposure. Instead, in the proposed formulation, Resilience-Based Risk is a function of Resilience, Hazard, and Exposure (Figure 3.3). While the three parameters can be obtained from various sources, for the specific case study considered in this research, the exposure is obtained from the World Risk Report (WRR), while the effect of hazard is neglected due to the lack of the necessary hazard maps. The third parameter, resilience, is determined using the data provided by the Hyogo Framework for Action (HFA). HFA ranks and scores countries based on a number of equally weighted indicators. However, in order to be used in the resilience assessment, the HFA indicators must be weighted according to their contribution toward resilience. To do that, three weighting methods are introduced. The first two methods are based on the Dependence Tree Analysis (DTA) ([Kammouh et al. 2016](#); [Kammouh et al. 2017](#); [Kammouh et al. 2018b](#)). DTA is a method that determines the correlation between a component and its sub-components (i.e., between resilience and its indicators), assigning different weights to the sub-components accordingly. The third method, Spider Plot Analysis (SPA), is based on a geometrical combination of the indicators using spider plots. In this method, the score of each indicator is plotted on one of the spider plot's axes. Resilience is then quantified as a normalized value of the area inside the enclosed shape made by linking the adjacent indicators' scores. The outputs of the resilience generated by each of the three methods are subsequently used in the evaluation of RBR (by combining them with exposure and hazard). To illustrate the use of the methodology, a case study composed of 37 countries is presented in this chapter, where the resilience and the resilience-based risk indexes of each country are evaluated and compared.



$$Risk = R \times E \times H$$

**Figure 3.3** Resilience-based risk analysis Venn diagram

### 3.4 The World Risk Report (WRR)

The World Risk Report is research performed by the United Nations University for Environment and Human Security (UNU-EHS) and published by the relief

organizations in the Alliance Development Works ([Mucke 2015](#)). The report adopts different measures to rank the countries around the world according to their vulnerability, exposure, and risk levels. In this study, the data on the exposure level of the WRR is used for the resilience-based risk assessment. Exposure is a measure of potential future losses which can be resulted from the occurrence of a hazard event. The strategy adopted by the WRR to evaluate the exposure of the countries is illustrated in Figure 3.4. The exposure is computed as a combination of the people who are exposed to different types of hazards in a country divided over the total population in that country. Figure 3.5 shows the exposure values of the ten most exposed countries according to the WRR.

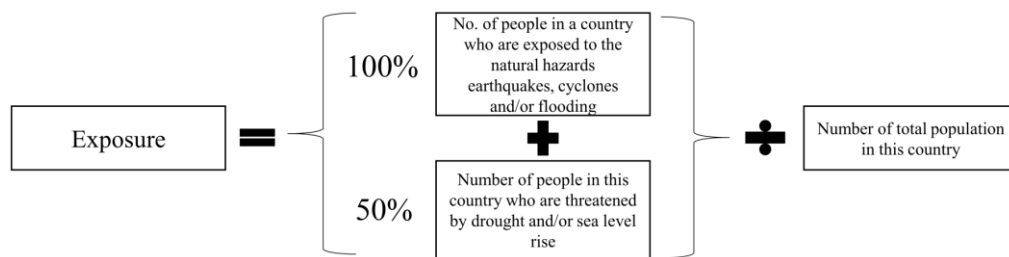


**Figure 3.4** Exposure analysis in the World Risk Report

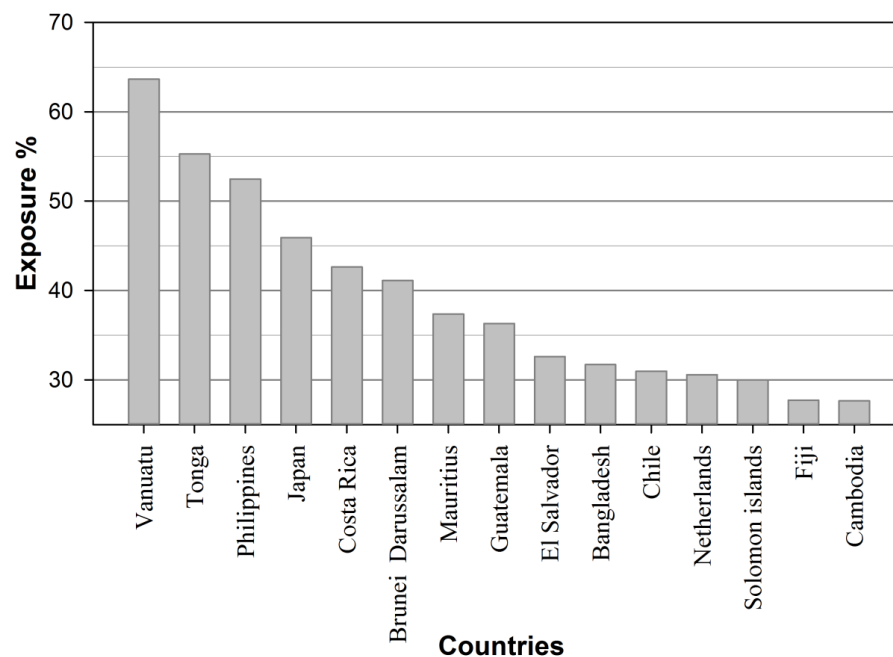


**Figure 3.5** The ten most exposed countries according to the WRR

### 3.5 Hyogo framework for action (HFA)

Hyogo Framework for Action (HFA) was originally conceptualized in Kobe, Japan. It was eventually adopted as a global blueprint for minimizing risk associated with natural hazards by implementing national laws regarding risk management and control ([ISDR 2005](#); [UNISDR 2005](#); [UNISDR 2011](#)). HFA is the product of a long initiative by an affiliate within the United Nations known as the International Strategy of Disaster Reduction (ISDR). The International Strategy of Disaster

Reduction was developed as the result of the experience gained in the International Decade for Natural Disaster Reduction (1990-1999).

The aim of HFA was to boost awareness on disaster risk and to guide committed countries in executing a master plan to avert the loss of lives and the economic impact caused by natural hazards. The HFA consists of five priorities for action. Each priority is satisfied with a number of indicators, with a total of 22 indicators for all five priorities (Table 3.2). The major role of the five priorities of HFA is to identify the specific sectors that every country should focus on to endorse disaster resilience. The indicators are assessed using a detailed survey, which contains a set of questions that aim to provide information about the resilience progress each country has made. The authority of each country is requested to fill the questionnaire and then return it to the UN for further processing. Table 3.3 shows the sort of questions presented in the questionnaire. The answers to the questions can be either 'YES/NO' or 'description text'. The progress recorded by every government is computed on the basis of a five-point scale for each of indicator, where 'one point' indicates weak progress and poor signs of planning and actions, while 'five points' implies a great endeavor and commitment in that specific area ([UNISDR 2008](#)).

The level of accuracy of the data collected by the UN is subjected to the authorized personnel who fills the report. However, the authorities of the countries are aware that providing good quality data allows them to track their resilience progress more accurately.

The expiration of Hyogo and its ten-year plan prompted a new framework known as Sendai Framework. This framework is the evolved version of the HFA and is meant to replace HFA in coming years. The Sendai Framework is a product of the Third World Conference on Disaster Risk Reduction in Sendai, Japan (2015) ([UNISDR 2015](#)). Even though the HFA was widely credited as raising awareness for disaster risk reduction, a significant loss of lives was recorded during the 10-year span of its implementation. Consequently, the Sendai framework stresses the significance of risk assessment and early warning systems. The UN has set a plan to define the risk bases and to embrace new indicators to quantify the resilience improvement made by the participating countries, and this is anticipated to be discussed at another session in 2017([UNISDR 2015](#)). The new framework outlines the following four priorities for action:

1. Understanding disaster risk;
2. Strengthening disaster risk governance to manage disaster risk;
3. Investing in disaster risk reduction for resilience;
4. Enhancing disaster preparedness for effective response and to "Build Back Better" in recovery, rehabilitation, and reconstruction.

**Table 3.2** Priorities and indicators used in the assessment of the Hyogo Framework for Action. Adapted from ([UNISDR 2011](#))

---

<b>PRIORITY 1:</b>	
<b>Ensure that disaster risk reduction (DRR) is a national and a local priority with a strong institutional basis for implementation</b>	
I 1	National policy and legal framework for disaster risk reduction exist with decentralized responsibilities and capacities at all levels.
I 2	Dedicated and adequate resources are available to implement disaster risk reduction plans and activities at all administrative levels
I 3	Community Participation and decentralization is ensured through the delegation of authority and resources to local levels
I 4	A national multi-sectoral platform for disaster risk reduction is functioning.

---

<b>PRIORITY 2:</b>	
<b>Identify, assess and monitor disaster risks and enhance early warning</b>	
I 5	National and local risk assessments based on hazard data and vulnerability information are available and include risk assessments for key sectors.
I 6	Systems are in place to monitor, archive and disseminate data on key hazards and vulnerabilities
I 7	Early warning systems are in place for all major hazards, with outreach to communities.
I 8	National and local risk assessments take account of regional/transboundary risks, with a view to regional cooperation on risk reduction.

---

<b>PRIORITY 3:</b>	
<b>Use knowledge, innovation, and education to build a culture of safety and resilience at all levels</b>	
I 9	Relevant information on disasters is available and accessible at all levels, to all stakeholders (through networks, development of information sharing systems etc.)
I 10	School curricula, education material, and relevant training include disaster risk reduction and recovery concepts and practices.
I 11	Research methods and tools for multi-risk assessments and cost-benefit analysis are developed and strengthened.
I 12	Countrywide public awareness strategy exists to stimulate a culture of disaster resilience, with outreach to urban and rural communities.

---

<b>PRIORITY 4:</b>	
<b>Reduce the underlying risk factors</b>	
I 13	Disaster risk reduction is an integral objective of environment-related policies and plans, including for land use natural resource management and adaptation to climate change.
I 14	Social development policies and plans are being implemented to reduce the vulnerability of populations most at risk.
I 15	Economic and productive sectorial policies and plans have been implemented to reduce the vulnerability of economic activities
I 16	Planning and management of human settlements incorporate disaster risk reduction components, including enforcement of building codes.
I 17	Disaster risk reduction measures are integrated into post-disaster recovery and rehabilitation processes
I 18	Procedures are in place to assess the disaster risk impacts of major development projects, especially infrastructure.

---

<b>PRIORITY 5:</b>	
<b>Strengthen disaster preparedness for effective response at all levels</b>	
I 19	Strong policy, technical and institutional capacities and mechanisms for disaster risk management, with a disaster risk reduction perspective, are in place.
I 20	Disaster preparedness and contingency plans are in place at all administrative levels, and regular training drills and rehearsals are held to test and develop disaster response programs.
I 21	Financial reserves and contingency mechanisms are in place to support effective response and recovery when required.
I 22	Procedures are in place to exchange relevant information during hazard events and disasters, and to undertake post-event reviews

---

**Table 3.3** The questions asked by the UN to assess the first indicator. Adapted from [\(UNISDR 2011\)](#)

Indicator 1	National policy and legal framework for disaster risk reduction exist with decentralized responsibilities and capacities at all levels.	Answer type
	-Is disaster risk taken into account in public investment and planning decisions?	YES/NO
	-National development plan	YES/NO
	-Sector strategies and plans	YES/NO
	-Climate change policy and strategy	YES/NO
	-Poverty reduction strategy papers	YES/NO
Questions	-CCA/ UNDAF (Common Country Assessment/ UN Development Assistance Framework)	YES/NO
	-Civil defense policy, strategy and contingency planning	YES/NO
	-Have legislative and/or regulatory provisions been made for managing disaster risk?	YES/NO
	-Description	Write text
	-Context & Constraints	Write text
Level of progress achieved: (1 to 5)		

### 3.6 The methodology: Resilience-Based Risk assessment of countries

The primary goal of the chapter is to provide an index that enables comparing countries in terms of resilience and its corresponding risk. In this work, risk is the probability of not achieving a certain resilience level and is referred to as resilience-based risk. The RBR is dependent on not only the internal characteristics of a system (resilience) but also on the external factors (exposure and hazard). Figure 3.6 illustrates the proposed framework, where risk is the combination of resilience, exposure, and hazard. The mathematical expression of RBR is given by:

$$RBR = (1 - R) \times E \times H \tag{3.1}$$

where *RBR* is the resilience-based risk index, *R* represents the resilience index, *E* is the exposure to natural hazards, *H* contains information about the hazard. For the purpose of the study, we have chosen public data sources to illustrate the methodology. For example, to compute the resilience parameter, we used the data provided by the Hyogo Framework for Action, which uses a number between 0 and 1 to assess the different resilience indicators of the countries. As already indicated, the 22 indicators in HFA are equally weighted, and this implies that all indicators have the same level of importance. However, it has been found that the indicators vary in importance, and therefore they must be weighted in a specific way in order to be used in the resilience assessment. To do that, three different weighting methods are applied to the HFA indicators, and the corresponding resilience results are compared. In the following, the three weighting methods are explained in detail.

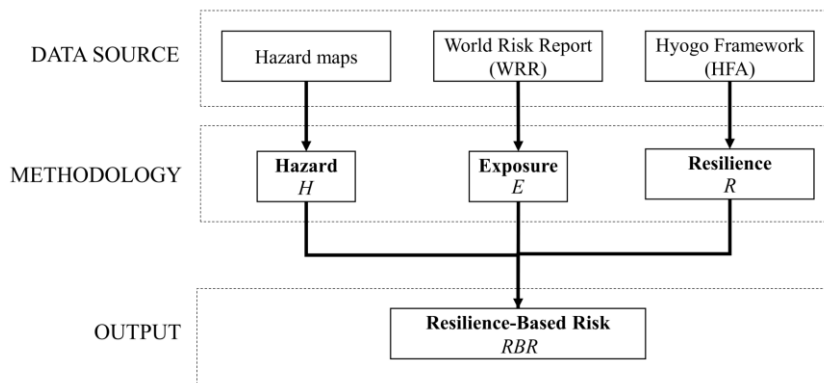


**Figure 3.6** Scheme of the proposed framework

### 3.6.1 Method 1: Dependence Tree Analysis (DTA)

In this section, the Dependence Tree Analysis (DTA) is introduced. The method captures the correlation between a component and its sub-components in a quantitative manner. The DTA is applied to the HFA's indicators in order to combine them according to their contribution towards resilience. Building the dependence tree begins with the identification of all potential components that are capable of influencing the main output. The most common way to do this is by brainstorming or relating to lessons learned. The types of components that exist are: the main component, the intermediate component, and the basic component. The task required to get out of a system is known as the main component, and this component is located on the top of the dependence tree. The essential components required for the successful achievement of the main component are known as the intermediate components, while the basic components refer to those that cannot be split any further into sub-components. Figure 3.7 illustrates how the components are arranged in the dependence tree. The components are presented in the dependence tree according to their logical relationship with one another. The components can show in the dependence tree more than once, and this depends on the importance of that component. In this work, resilience is considered as the main component, while the HFA's indicators are the intermediate and the basic components. Therefore, all sub-components will hereafter be referred to as indicators, while the main component will be referred to as resilience. The results obtained using the DTA are highly dependent on the tree structure which describes the links between the different indicators. Furthermore, another limitation of the method is that only numerical indicators can be combined (e.g. Boolean indicators cannot be used with this methodology).

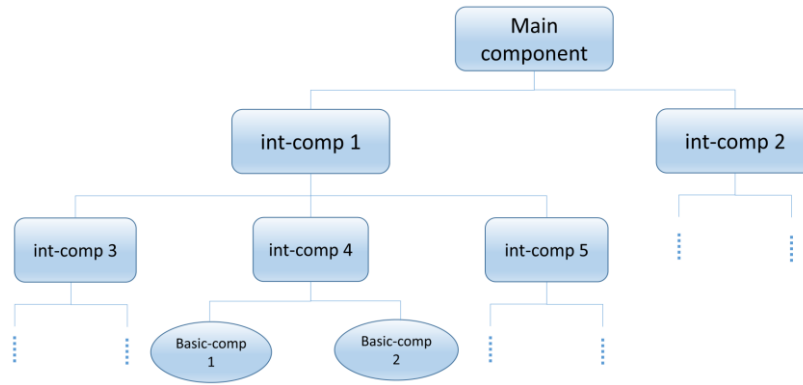


**Figure 3.7** A dependence tree diagram showing the different types of components

The analysis begins with the identification of the indicators and their relationships. The indicators' scores obtained from HFA are normalized with respect to their maximum value ( $I_{\max}=5$ ) using Eq. (3.2). Afterward, resilience is computed using the DTA by combining the indicators' scores in such a way that the indicators that are in series are multiplied, while the weighted average of those in parallel is considered. This leads to obtaining a normalized resilience output that is ranged between 0 and 1.

$$I_{iN} = \frac{I_i}{I_{i,\max}} \quad (3.2)$$

where  $I_{iN}$  is the normalized score of indicator  $i$  ( $0 \leq I_{iN} \leq 1$ ),  $I_i$  is the score of indicator  $i$  obtained from HFA ( $0 \leq I_i \leq 5$ ),  $I_{i,\max}$  is the maximum score that can be achieved by indicator  $i$  ( $I_{\max} = 5$ ).

### 3.6.2 Method 2: Weighted Average Analysis (WAA)

In this method, the dependence tree analysis is used only to find weighting factors for the indicators. Then, the resilience is evaluated as the weighted average of the indicators' weighted scores. The weights are obtained by performing a sensitivity analysis. This is done by setting the score of each indicator to zero once at a time while assigning maximum values to all other indicators. The value of the resilience is computed for each time an indicator is set to zero. A low value of resilience indicates high importance of that indicator. Therefore, the importance factor of the indicator is the opposite of the resilience value when that indicator is set to zero. Eq. (3.3) is used to compute the importance factors.

$$IF_i = 1 - R_i \quad \text{for } I_{iN} = 0; I_{jN} = I_{j,\max,N} = 1 \quad (i=1 \rightarrow k \text{ and } j \neq i) \quad (3.3)$$

where  $IF_i$  is the importance factor of indicator  $i$ ,  $R_i$  is the value of resilience when indicator  $i$  is set to zero while all other indicators are equal to 1,  $k$  is the total number of indicators (i.e.  $k=22$ ).

The execution of the sensitivity analysis enables classifying the indicators starting from the most to the least important. A weighting factor for every indicator

of the HFA is subsequently calculated using Eq. (3.4). In this equation, the weighting factor uses the results of the sensitivity analysis conducted in the previous step.

$$W_i = \frac{1 - IF_i}{\sum_{n=1}^k (1 - IF_n)} \quad (3.4)$$

where  $W_i$  is the weighting factor of indicator  $i$ . The new indicator's score is obtained by multiplying the original indicator's normalized score by its corresponding weighting factor:

$$I_{i,NW} = W_i \cdot I_{i,N} \quad (3.5)$$

where  $I_{i,NW}$  is the normalized weighted score of indicator  $i$ .

Finally, the resilience value  $R$  is the weighted average of the indicators' modified scores. The mathematical equation of resilience is given as follows:

$$R = \sum_{n=1}^k I_{n,NW} \quad (3.6)$$

### 3.6.3 Method 3: Spider Plot Weighted Area Analysis (SPA)

In this last method, the indicators are represented by means of a spider plot (Figure 3.8). Resilience is simply the enclosed area generated by linking the adjacent indicators, normalized with respect to the total area of the polygon. The mathematical expression of resilience is given in Eq. (3.7). One can say that the arrangement of indicators could affect the area in the enclosed shape. To illustrate this, a statistical analysis was performed on the indicators' scores of one country. Different arrangements of the indicators were tried using the permutation command in the software Matlab ([Guide 1998](#)), and the area of each arrangement was computed. It was found that the values of the areas were normally distributed with a standard deviation of 5%. This implies that the value of the area inside the enclosed shape is not very sensitive to the indicators' arrangement order.

$$R = \frac{A}{A_{max}} \quad (3.7)$$

where  $R$  is the resilience index,  $A$  is the area of the geometrical shape obtained by connecting the scores of adjacent indicators,  $A_{max}$  is the total area of the polygon (i.e., maximum area that could be achieved if all indicators are equal to 5).

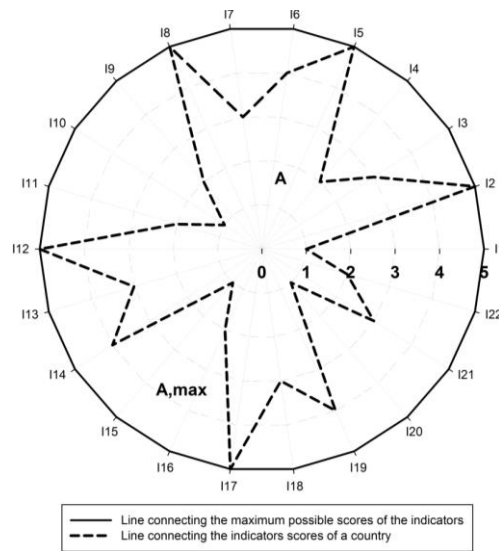


Figure 3.8 Spider plot representation of the HFA indicators scores

### 3.7 Case study

The methodology described in the chapter has been applied to a number of countries that took part in the Hyogo Framework evaluation project. The chosen countries are 37 in total, and they were selected randomly from all five continents. For each country, the resilience index *R* is evaluated, and then the corresponding risk index *RBR* is computed by combining the results of resilience, exposure, and hazard.

In Table 3.4, the indicators' scores of the various countries are listed as presented in the HFA reports. The latest reports to date are used to fill the scores. The indicators' scores of each country are summed up into a single total score (out of 110 points). This score is also presented in percentage form (%), where 100 indicates a maximum score of 5 in all indicators. The final set of total scores act as a data source for the proposed methodology.

Table 3.4 Indicators scores for the analyzed countries

Indicators	1	1	1	1	1	1	1	1	1	1	1	1	1	1	1	1	1	1	1	2	2	2	Total (per 110)	Total (%)
Countries	1	2	3	4	5	6	7	8	9	0	1	2	3	4	5	6	7	8	9	0	1	2		
1-Fiji	5	4	5	5	5	5	5	5	5	5	5	5	5	5	5	5	5	5	5	5	5	5	109	99.1
2-Costa Rica	5	4	4	5	3	4	5	4	4	4	5	4	4	4	3	5	5	5	5	5	5	5	97	88.2
3-Singapore	5	5	5	2	5	5	5	5	5	5	5	5	2	5	5	4	1	1	5	5	4	5	94	85.5
4-Japan	5	4	4	5	4	4	4	4	5	4	3	5	4	4	4	4	4	5	5	4	4	4	93	84.5
5-UAE	5	4	5	4	4	4	3	3	3	4	4	5	5	5	5	5	5	4	4	3	4	93	84.5	
6-Austria	4	5	5	3	4	4	5	5	4	4	3	4	4	4	4	4	4	5	5	4	4	4	92	83.6
7-UK	4	4	5	4	4	4	5	4	4	4	4	4	4	4	4	4	4	4	4	4	4	5	91	82.7
8-Greece	4	4	4	4	4	4	5	4	4	4	4	4	4	4	4	5	4	4	4	4	4	4	90	81.8
9-Australia	4	4	4	4	4	4	5	4	4	4	4	4	4	4	4	4	4	4	4	4	4	4	89	80.9
10-Italy	2	4	4	4	4	4	5	4	5	4	4	4	4	3	3	3	5	4	5	5	4	4	88	80.0
11-Cameroon	4	4	4	5	4	4	4	4	4	4	4	4	4	3	4	4	4	4	4	3	4	4	87	79.1
12-New Zealand	4	4	4	3	4	4	4	4	4	4	4	4	4	4	4	4	4	4	4	4	4	4	87	79.1
13-Germany	5	4	4	4	4	4	4	4	4	3	4	4	4	5	3	4	3	3	4	4	4	4	86	78.2
14-Nigeria	4	4	2	4	4	4	4	4	4	4	4	4	4	4	4	4	4	4	4	4	4	4	86	78.2
15-Canada	4	4	5	4	3	4	4	4	4	3	3	4	3	3	4	4	5	4	5	5	3	3	85	77.3
16-France	4	4	4	4	3	4	5	4	4	3	3	3	4	4	3	4	4	3	4	3	5	5	84	76.4
17-Ecuador	4	4	4	3	4	3	4	4	4	4	4	4	4	4	4	4	4	3	4	4	3	4	84	76.4
18-Ethiopia	4	3	4	4	4	4	4	4	4	4	4	4	4	4	3	3	3	4	4	4	4	4	84	76.4
19-USA	4	4	4	3	4	4	4	4	3	4	4	4	3	3	3	4	4	4	4	4	4	4	83	75.5
20-Chile	4	3	3	4	4	3	4	3	4	4	2	4	3	4	4	4	4	4	4	5	4	82	74.5	

21-Ghana	4	2	2	4	4	4	4	4	5	1	4	4	4	4	3	3	4	4	4	4	4	4	80	72.7
22-Argentina	3	3	4	4	4	3	4	4	3	3	3	4	3	3	3	4	4	4	4	2	4	4	77	70.0
23-South Africa	4	4	4	4	3	3	3	3	3	3	3	3	4	3	3	3	4	4	3	4	4	4	76	69.1
24-Cook Island	4	3	4	4	3	4	4	4	3	3	3	4	4	3	3	3	4	3	4	3	3	3	76	69.1
25-Pakistan	4	4	4	4	3	3	3	4	3	3	3	3	3	3	3	4	3	3	4	4	3	74	67.3	
26-Brazil	4	3	4	3	4	5	1	2	4	2	2	3	3	5	3	4	4	3	3	4	3	4	73	66.4
27-Egypt	4	2	4	4	4	3	3	3	3	3	2	4	4	3	4	3	3	3	4	4	3	3	73	66.4
28-Iran	4	3	4	4	3	3	2	2	3	4	3	3	3	3	3	4	3	3	4	3	4	3	71	64.5
29-Qatar	3	4	3	3	4	3	3	3	3	2	3	3	4	3	3	3	3	3	4	3	3	3	69	62.7
30-Samua	4	3	3	4	4	2	3	4	3	3	3	4	4	3	3	2	2	1	4	3	3	3	68	61.8
31-Thailand	4	2	4	4	2	2	4	3	3	3	2	4	3	4	2	3	2	3	4	4	4	2	68	61.8
32-Madagascar	4	3	4	4	4	2	2	2	4	5	4	2	2	1	2	2	4	2	4	4	2	4	67	60.9
33-Mexico	4	3	3	4	2	3	4	3	3	2	3	2	3	3	3	2	3	3	2	4	3	65	59.1	
34-Morocco	2	3	3	3	3	3	3	3	3	3	3	3	3	3	3	3	3	1	1	3	3	61	55.5	
35-Palestine	3	2	3	4	3	2	4	4	4	3	2	4	3	2	1	2	2	2	3	3	1	2	59	53.6
36-Monaco	3	2	1	3	3	1	3	3	4	4	1	2	3	1	1	1	1	1	3	4	1	1	47	42.7
37-Armenia	2	2	2	2	2	2	2	2	2	2	2	2	2	2	2	2	2	2	2	2	2	2	44	40.0

### 3.7.1 Resilience results

In this section, the resilience indexes of the analyzed countries are computed using the proposed methods and then compared.

#### 3.7.1.1 Method 1: Dependence Tree Analysis (DTA) results

Figure 3.9 shows the final form of the dependence tree, in which all the indicators have been arranged according to their logical relationship with one another. One indicator can take more than one place, and this depends on how significant the indicator is.

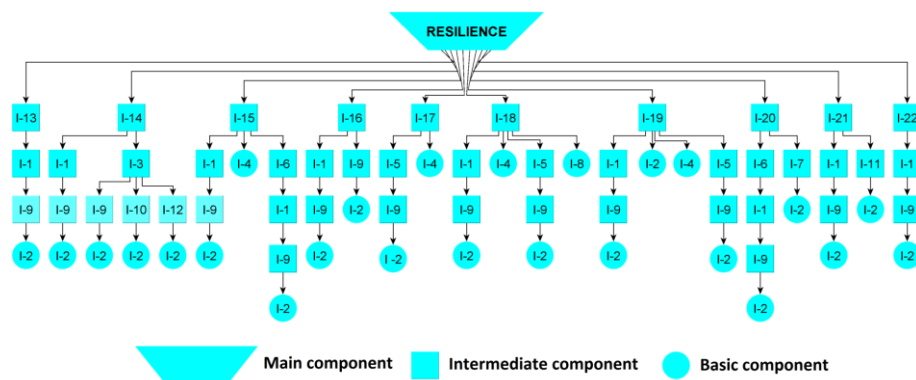


Figure 3.9 The dependence tree of the HFA's indicators

As we mentioned before, the 22 indicators' scores of each country (obtained from HFA) are normalized with respect to their maximum value. The maximum value that can be achieved by an indicator is "5"; therefore, all indicators are divided over five. Once the indicators are normalized, the resilience index of each country is computed by combining the indicators' scores. In the dependence tree, the indicators in series are multiplied by each other, whereas averaging was taken for those indicators in parallel. The resilience index of each country can be obtained by replacing each indicator with its corresponding normalized score value from Eq. (3.2). The general formula to compute the resilience  $R_c$  of a country  $c$  is given by Eq. (3.8). Using the equation, the resilience results of the analyzed countries can be computed.

$$R_c = \frac{1}{10} \left[ \begin{aligned} & I_{13N} I_{1N} I_{9N} I_{2N} + I_{14N} \left( \frac{I_{1N} I_{9N} I_{2N} + I_{3N} \left( \frac{I_{9N} I_{2N} + I_{10N} I_{2N} + I_{12N} I_{2N}}{3} \right)}{2} \right) + I_{15N} \left( \frac{I_{1N} I_{9N} I_{2N} + I_{4N} + I_{6N} I_{1N} I_{9N} I_{2N}}{3} \right) \\ & + I_{16N} \left( \frac{I_{1N} I_{9N} I_{2N} + I_{9N} I_{2N}}{2} \right) + I_{17N} \left( \frac{I_{5N} I_{9N} I_{2N} + I_{4N}}{2} \right) + I_{18N} \left( \frac{I_{1N} I_{9N} I_{2N} + I_{4N} + I_{5N} I_{9N} I_{2N} + I_{8N}}{4} \right) \\ & + I_{19N} \left( \frac{I_{1N} I_{9N} I_{2N} + I_{2N} + I_{4N} + I_{5N} I_{9N} I_{2N}}{4} \right) + I_{20N} \left( \frac{I_{6N} I_{1N} I_{9N} I_{2N} + I_{7N} I_{2N}}{2} \right) + I_{21N} \left( \frac{I_{1N} I_{9N} I_{2N} + I_{11N} I_{2N}}{2} \right) \\ & + I_{22N} I_{1N} I_{9N} I_{2N} \end{aligned} \right] \quad (3.8)$$

### 3.7.1.2 Method 2: Weighted Average Analysis (WAA) results

In this method, the Dependence Tree Analysis (DTA) is used to weight the indicators shown in Table 3.2. A sensitivity analysis is performed to capture the difference in the indicators' contribution to the resilience assessment. This leads to assigning a single weighting factor to each of the 22 indicators. Following the procedure described above, and by using Eqs. (3.3) and (3.4), a list of importance and weighting factors for the 22 indicators is generated (Table 3.5). We can clearly notice the difference in the indicators' weights. For instance, indicator 2 (I-2) recorded the highest weighting factor '0.225'. In fact, this indicator 'Dedicated and adequate resources are available to implement disaster risk reduction plans and activities at all administrative levels' is a financial indicator, and almost all other indicators were dependent on it in the dependence tree (Figure 3.9). Generally, financial indicators are very important because financial resources are necessary for the accomplishment of any task, and this justifies the high weighting factor obtained by that indicator.

**Table 3.5** Importance and weighting factors of the HFA indicators

Indicator	Importance factor $IF$	Weighting factor $W_i$	Indicator	Importance factor $IF$	Weighting factor $W_i$	Indicator	Importance factor $IF$	Weighting factor $W_i$
I-1	0.54	0.154	I-9	0.65	0.187	I-17	0.1	0.028
I-2	0.79	0.225	I-10	0.017	0.005	I-18	0.1	0.028
I-3	0.05	0.014	I-11	0.05	0.014	I-19	0.1	0.028
I-4	0.13	0.038	I-12	0.02	0.006	I-20	0.1	0.028
I-5	0.10	0.028	I-13	0.1	0.028	I-21	0.1	0.028
I-6	0.08	0.024	I-14	0.1	0.028	I-22	0.1	0.028
I-7	0.05	0.014	I-15	0.1	0.028			
I-8	0.025	0.007	I-16	0.1	0.028			

The weighting factors shown in the table above are multiplied by the corresponding indicators' normalized scores using Eq. (3.5). The new 22 indicators' scores are subsequently summed up using Eq. (3.6). The result obtained represents the resilience index  $R_c$  of the country  $c$ .

### 3.7.1.3 Method 3: Spider Plot Weighted Area Analysis (SPA) results

The indicators' spider chart of each country is plotted and the area inside the enclosed shape made by linking the adjacent indicators' scores is obtained. Figure 3.10 shows two examples of the spider plot method corresponding to the countries France and Monaco. Using Eq. (3.7), The resilience index  $R_c$  of a country  $c$  is obtained by normalizing the area inside the enclosed shape  $A_c$  with respect to the

maximum area  $A_{c,max}$  (i.e. the maximum area is obtained when all indicators are maximum ‘5’).

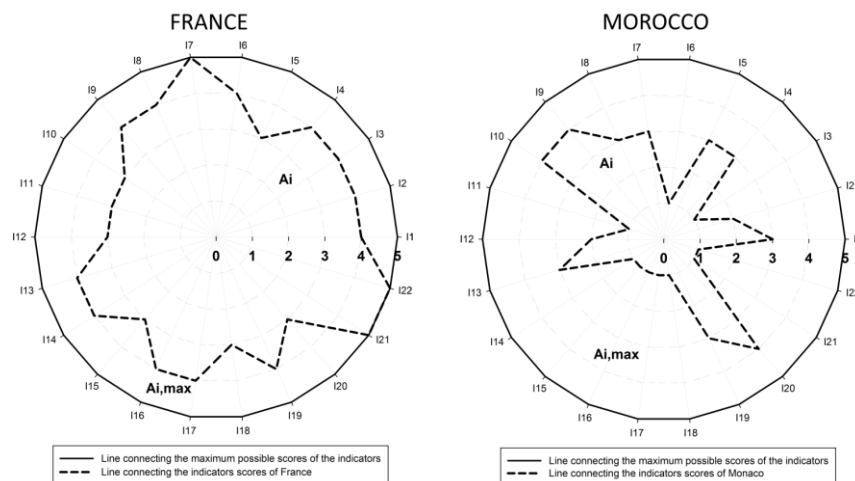


**Figure 3.10** Examples of the spider plot method for two countries (France and Monaco)

Figure 3.11 compares the results of the resilience obtained with the three methods. Interestingly, the results coming from all three methods follow the same trend. The third method (SPA) acts as an average for the first (DTA) and the second (WWA) methods, except for Fiji country, which acquired equal scores in the second and third methods, slightly higher than the score obtained from the first method. Altogether, these results suggest that the resilience outputs are very sensitive to the weighting method. The first method (DTA) provides the highest difference between the largest and the lowest scores, whereas the variability in the results obtained using the second method (WWA) is the lowest, with a difference of 0.58 between the highest value (0.98) and the lowest value (0.4). This can be considered in favor of the first method as it magnifies the range of the resilience results, which allows having a clearer picture of the difference in resilience between countries. In addition, the first method (DTA) does not allow very high values of resilience; for instance, the highest resilience score achieved using the DTA method is that of the Fiji country ( $R=0.84$ ). This assumes that there is no country that is considered fully resilient, and this is a more reasonable result than in the other two methods where the resilience index of Fiji is 0.98, which implies that Fiji can hardly get any better in terms of resilience.

Moreover, the resilience results show that Fiji has always achieved the first position in the resilience ranking, which is rather unexpected. This may be attributed to several reasons, such as the subjectivity in filling the HFA reports in the first place. Fiji has initially achieved a score of 109 out of 110 in the HFA evaluation (Table 3.4), which implies that whatever weighting strategy was adopted, it would still be ineffective in changing the ranking of Fiji. Nevertheless, this does not affect the validity of the Hyogo framework data as there is absolutely no benefit for any country to provide fake data and information. In addition, the results obtained in this study are to give an indication of how well each country is doing in terms of resilience. The results can be used for comparing the countries rather than knowing their actual resilience. The actual resilience of the country may

vary significantly inside the country itself; therefore, we do not intend to provide exact resilience values for the countries, which is absolutely not feasible considering the complexity involved in the process.

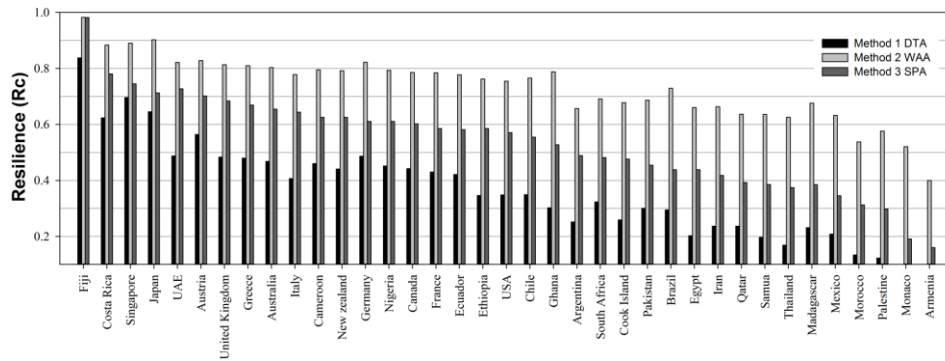


Figure 3.11 Resilience results obtained by the three methods

### 3.7.2 Resilience-Based Risk results

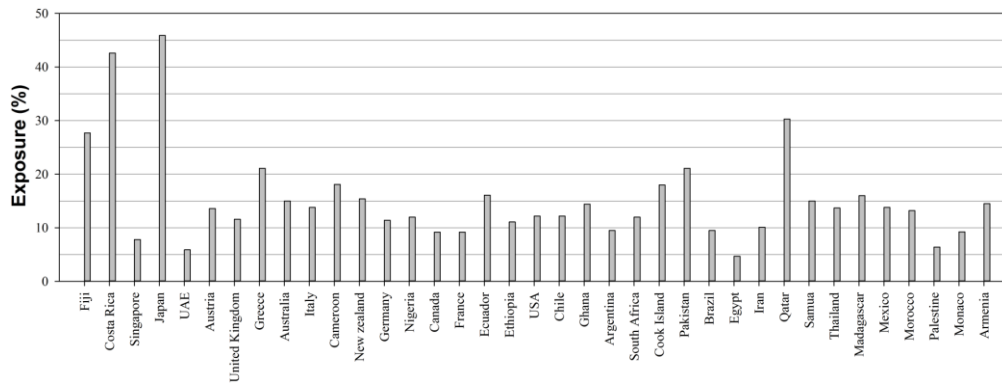
In this framework, the last step is to quantify the resilience-based risk index (RBR). As already indicated, the risk index is a combination of resilience, exposure, and hazard. For the sake of this example, the hazard is assumed to be ‘1’ in an attempt to disregard its effect. Therefore, in this specific case study, the risk index is presented in terms of the hazard parameter, which upon availability it can be combined directly with the results obtained in this study. The table below shows the resilience results derived using the three methods and the exposure of every country obtained from the WRR. The resilience-based risk index of every country is subsequently computed using Eq. (3.1).

Table 3.6 Resilience results obtained from the three methods and the exposure of each country

Country	R <sub>1</sub>	R <sub>2</sub>	R <sub>3</sub>	E (%)	Country	R <sub>1</sub>	R <sub>2</sub>	R <sub>3</sub>	E (%)	Country	R <sub>1</sub>	R <sub>2</sub>	R <sub>3</sub>	E (%)
Fiji	0.84	0.98	0.98	27.7	Germany	0.49	0.82	0.61	11.4	Brazil	0.29	0.73	0.44	9.5
Costa Rica	0.62	0.88	0.78	42.6	Nigeria	0.45	0.79	0.61	12.0	Egypt	0.20	0.66	0.44	4.7
Singapore	0.70	0.89	0.75	7.8	Canada	0.44	0.79	0.60	9.2	Iran	0.24	0.66	0.42	10.1
Japan	0.65	0.90	0.71	45.9	France	0.43	0.78	0.59	9.2	Qatar	0.24	0.64	0.39	30.3
UAE	0.49	0.82	0.73	5.9	Ecuador	0.42	0.78	0.58	16.1	Thailand	0.17	0.63	0.37	13.7
Austria	0.56	0.83	0.70	13.6	Ethiopia	0.35	0.76	0.59	11.1	Madagascar	0.23	0.68	0.39	16.0
United Kingdom	0.48	0.81	0.68	11.6	USA	0.35	0.75	0.57	12.2	Mexico	0.21	0.63	0.35	13.8
Greece	0.48	0.81	0.67	21.1	Chile	0.35	0.77	0.55	12.2	Morocco	0.13	0.54	0.31	13.2
Australia	0.47	0.80	0.65	15.0	Ghana	0.30	0.79	0.53	14.4	Palestine	0.12	0.58	0.30	6.4
Italy	0.41	0.78	0.64	13.8	Argentina	0.25	0.66	0.49	9.5	Monaco	0.08	0.52	0.19	9.25
Cameroon	0.46	0.80	0.63	18.1	South Africa	0.32	0.69	0.48	12.0	Armenia	0.05	0.40	0.16	14.5
New Zealand	0.44	0.79	0.63	15.4	Pakistan	0.30	0.69	0.45	21.1					

The numerical results obtained by combining resilience (Figure 3.11) with exposure (Figure 3.12) using Eq. (3.1) are presented in Figure 3.13. It is clear that the risk and the resilience results are far from proportional, and this supports the notion that the most prepared countries (i.e. having high resilience) do not necessarily have the lowest risk. For instance, Japan is widely known for its high preparedness level against natural disasters. Although it is classified among the ‘best’ countries in the resilience ranking (Figure 3.11), Japan is placed among the

countries with the highest risk (Figure 3.13), and this is because Japan is highly exposed to disasters (Figure 3.12). Therefore, the resilience by itself is not a good indicator of the probability of being under a certain resilience level, because the process depends also on the exposure level.



**Figure 3.12** Exposure results of the studied countries obtained from the WRR

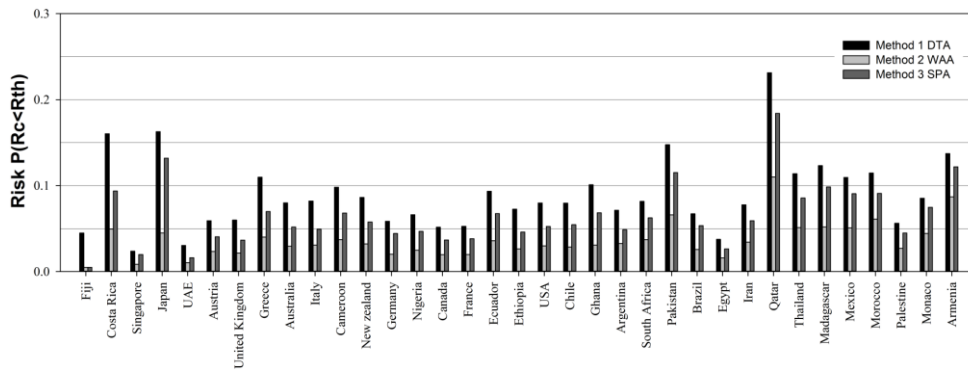


**Figure 3.13** Risk results obtained using the results of resilience obtained by the three methods

### 3.8 Concluding remarks

Resilience measurements are important tools for communities to understand the benefit cost of implementing resilience actions and to evaluate the effects of these actions by looking at different policies and approaches. They can give an idea of where additional resources should be allocated. Although these measurement tools cannot create resilient communities, they can certainly help show and illustrate a path that the community can take to become safer and stronger and more vibrant in the face of unanticipated events.

This chapter presents a new analytical approach for calculating the resilience and the resilience-based risk of countries. The resilience-based risk is defined as the probability of being below a certain resilience threshold and is computed by combining resilience, exposure, and hazard. In this chapter, the resilience parameter is evaluated using the results of the Hyogo Framework for Action, which ranks the countries based on 22 indicators. The indicators of the HFA are combined using three different methods to determine the resilience index. The first two methods are

based on the Dependence Tree Analysis. DTA is a method that identifies the correlation between resilience and its indicators in a quantitative manner, giving weighting factors the indicators accordingly. The third method is a geometrical method in which the indicators' scores are plotted on the spider chart' axes. The resilience is quantified as a normalized value of the area inside the enclosed shape made by linking the adjacent indicators' scores.

The applicability of the proposed methodology has been tested on 37 countries by calculating their respective resilience and risk indexes. Although the results obtained from the three methods are proportional, the sensitivity on the resilience results provided by each method is different. The first method (DTA) is preferred with respect to the other two because it amplifies the score range of the resilience results of the countries. Then, the resilience-based risk index *RBR* for each country is computed. The obtained numerical results show that the risk of being below a certain resilience threshold depends greatly on the exposure level of that country.

In conclusion, in the chapter, a specific data set collected by United Nation has been used to illustrate the methodology. However, the proposed approach is generic, and it can be applied using more reliable data as soon as they are available, such as the data that will be provided in the "Sendai Framework". While this chapter focused on resilience from the global point of view, the next chapter will deal more with resilience at the local level. Multiple methodologies, deterministic and probabilistic, to evaluate the resilience of city-scale communities will be presented.

# Chapter 4

## 4. Resilience evaluation framework for urban communities

*Part of the work described in this chapter has been previously published:*

- 1- Kammouh, O., Noori, A. Z., Cimellaro, G. P., and Mahin, S. A. (2019). "Resilience Assessment of Urban Communities." *ASCE-ASME Journal of Risk and Uncertainty in Engineering Systems, Part A: Civil Engineering*, 5(1), 04019002. doi:10.1061/AJRUA6.0001004.
- 2-Kammouh, O., Noori, A. Z., Taurino, V., Mahin, S. A., and Cimellaro, G. P. (2018). "Deterministic and fuzzy-based methods to evaluate community resilience." *Earthquake Engineering and Engineering Vibration*, 17(2), 261-275. 10.1007/s11803-018-0440-2.

### 4.1 Introduction

Measuring resilience is among the most challenging tasks due to the intricacy involved in the process. Resilience indicators are an effective tool to quantify the resilience of engineering systems because they allow modeling complex systems easily and effectively ([Cutter et al. 2008b](#)). Although the use of indicators is perceived as an important instrument to measure the resilience of a system, developing a standardized set of resilience indicators is clearly challenging for such a dynamic, constantly reshaping and context-dependent concept. ([Cutter et al. 2014](#)) assert that research on quantifying community resilience is still at the preliminary stage. Even though much efforts have already been made to boost research on community resilience indicator ([Norris et al. 2008](#); [Twigg 2009](#); [Cutter et al. 2010](#)), there is still no acceptable method for the evaluation of community resilience and there are still challenges in developing real evaluation strategies ([Abeling et al. 2014](#)).

While the previous chapter focused on state-level resilience, this chapter deals with smaller regions, such as cities. More details are considered here compared to what introduced before. The study presented in this chapter aims at presenting an exhaustive quantitative method for calculating the resilience of urban communities within the context of the PEOPLES framework ([Renschler et al. 2010](#); [Cimellaro et al. 2016a](#)). PEOPLES framework is a hierarchical framework for defining disaster resilience of communities at various scales. It consists of seven dimensions summarized with the acronym PEOPLES: Population; Environment; Organized governmental services; Physical infrastructure; Lifestyle; Economic; and Social capital. Each

of the dimensions is split into several components and indicators. The framework does not identify a clear procedure to quantitatively compute resilience, but rather a qualitative assessment and description of resilience. The goal of this chapter is to use the structure of PEOPLES framework to come up with a quantitative framework that allows evaluation of the resilience of communities. To do so, two different methodologies to analytically quantify the resilience of communities are proposed. The first method is deterministic and requires data on past earthquake events in the form of indicators. The method starts by collecting all community resilience indicators found in the literature. The collected indicators are first filtered to ensure a minimum overlapping between them, then they are allocated to the PEOPLES' components. A single measure is assigned to each indicator allowing it to be quantifiable. Each measure is represented using a performance function, which represents the functionality of the indicator in time. Higher functionality of the indicator leads to higher resilience of the community. These functions can be constructed in a systematic manner using damage and restoration parameters. All measures are weighted according to their contribution to the resilience assessment using a new matrix-based interdependency technique. The performance functions of the indicators are aggregated, passing through the different level of PEOPLES framework, into one function that represents the dynamic performance of the whole community. However, in specific scenarios, some indicators may be difficult to obtain and quantify, as well as the interdependency among them. In order to track and represent such uncertainties, another method based on fuzzy-logic modeling is proposed. This method does not require deterministic data but rather expert knowledge to determine the different parameters involved in the resilience evaluation. It also accounts for the uncertainties involved in the assessment process. This method returns a resilience index for each indicator and a resilience index for the analyzed community. This chapter also introduces an open source tool in which the deterministic resilience method is implemented. A case study illustrating the use of the tool is also presented.

## 4.2 PEOPLES framework

PEOPLES framework is an expansion of the research on resilience, and its attributes were developed at the Multidisciplinary Centre of Earthquake Engineering Research (MCEER) ([Cimellaro et al. 2016a](#)). The framework provides a procedure to measure community resilience at different scales (spatial and temporal) by evaluating the infrastructure's performance considering their interdependency. The method proposed in this study adopts the structure of the PEOPLES framework for its implementation. PEOPLES framework comprises seven dimensions of community summarized with the acronyms PEOPLES. The seven dimensions are:

1. Population and demographics: this dimension identifies the focal community population. The aim of this dimension is to understand the ability and expertise of the society in managing adverse impacts and to recover quickly from disasters;
2. Ecosystem and environmental: signifies the capability of the ecological system to overcome a disturbance and return to its pre-event state;

3. Organized governmental services: specifies the community sectors readiness to respond to an event, and plays a key role in raising community resilience both before (preparedness and mitigation strategies) and after (response and restoration) a disaster;
4. Physical infrastructure: addresses lifelines and facilities that have to be restored to a functional state after the disaster;
5. Lifestyle and community competence: represents both the raw abilities of a community (e.g., skills to find multifaceted solutions to complex problems through the engagement in political networks) and the perceptions of a community (e.g., perception to have the ability to do a positive change through a common effort that relies on PEOPLES' aptitude to resourcefully envision a new future and then move in that direction);
6. Economic development: consists of both the current economy (static state) of a community and its future growth (dynamic development). It represents the capability of the society to keep up in the aftermath of a disaster by means of good substitution, employment, and services redistribution.
7. Social-cultural capital: describes the extent to which the people are willing to stay within their area and help their community to bounce back after the disaster.

Further details on each of the above dimensions can be found in ([Cimellaro et al. 2016a](#)).

### **4.3 Method 1: deterministic resilience quantification of communities based on the PEOPLES framework**

The method introduced in this section can take any indicator-based framework as a conceptual basis. For this study, the PEOPLES framework is considered due to its wide recognition within the disaster resilience community. The structure and organization of PEOPLES framework allow preventing possible overlap among the indicators. Once the framework is fixed, relevant indicators are selected to describe the framework's components in detail. Every indicator found in the literature has been collected and then they are filtered with the purpose of obtaining mutually exclusive indicators. This has necessitated rejecting a number of indicators either because they are not relevant or because they overlapped with other indicators. The interdependency between the variables is tackled by introducing an interdependency matrix technique. The proposed interdependency technique returns as an output a weighting factor for each variable. Once the contribution of the different variables toward the overall resilience is determined, the variables are measured using past data. In the proposed resilience assessment method, the variables are represented by a continuous functionality function rather than a crisp number. Finally, the functionality functions of the different variables are aggregated to obtain a single community functionality function that is used to evaluate the resilience of the community. In the following, the methodology is described in all details.

### 4.3.1 PEOPLES' dimensions, components, and indicators

PEOPLES is a framework for quantifying and defining the disaster resilience of a community at various scales. It is divided into seven dimensions, each of which is further divided into several components. The goal is to convert PEOPLES from its current qualitative version to a quantitative framework. To do so, all resilience indicators found in the literature have been collected and then allocated to the proper components of PEOPLES. Much effort has been done to reduce the overlapping among indicators by removing duplicated ones. This has led to a condensed list of 115 indicators (see Appendix A). Each indicator has a measure assigned to it to make all indicators computable. Each measure is normalized with respect to a fixed quantity, the target value ( $TV$ ). The target value is an essential quantity that provides the baseline to measure the resilience of a system (Cutter et al. 2010). The system's existing functionality at any instance of time is compared with the target value to know how much functionality deficiency is experienced by the system. For instance, if we consider the measure "Red cross volunteers per 10,000 people" (indicator 7.6.1 in Appendix A), the output of this measure would be an absolute number of volunteers that cannot be incorporated with other measures unless it is normalized; therefore, the result is divided over  $TV$ , which in this scenario represents the 'optimum' amount of volunteers per 10,000 people (e.g.  $TV=100$  volunteers /10,000 people). If the *ratio* between the value of the measure and the  $TV$  is less than one, it implies that the indicator could still be enhanced. If the *ratio* is bigger than one, a value of 1 is assigned to that measure. Having all measures normalized empowers the comparison among systems of similar or different natures (e.g. hospitals and water networks).

The measures are classified under two different categories: 'Static measure ( $S$ )', which describes the measures that are not affected by the disastrous event, and 'dynamic measure ( $D$ )' or 'event-sensitive measure', which describes the measures whose values change after the occurrence of the disaster. In addition, each of the PEOPLES' variables (dimensions, components, indicators) contributes to a certain degree towards the resilience output. Therefore, they are classified according to their importance. A weighting factor for each variable is computed using an interdependency matrix technique which considers the interdependency among the PEOPLES' variables. A variable is said to be important if other variables depend on it to deliver their function. A comprehensive list of PEOPLES elements including dimensions, components, and indicators, with their corresponding natures ( $S$  or  $D$ ) is tabulated in Appendix A. For some indicators in which high values correspond to low levels of resilience, a rescaling process involves reversing the order of their contribution to the overall resilience index is presented.

### 4.3.2 Weighting factors: the interdependency matrix technique

Indicators do not contribute equally to the overall resilience output. In this chapter, weighting factors are allocated to the different variables of PEOPLES based on an

interdependency analysis. For the purpose of the analysis, the variables of PEOPLES are classified into three major groups as follows:

1. Indicators that fall within a component are considered as a group;
2. Components classified under a dimension are taken as a group;
3. PEOPLES seven dimensions make a group.

The proposed interdependency technique assumes that the variable’s importance is strictly related to the number of other variables in the same group that depend on it. Variables in the same groups are put together in a  $[n \times n]$  square matrix (Figure 4.1), where  $n$  is the number of variables in the analyzed group. The cells in the matrix can take the values 0 or 1. The value 0 means that the functionality of the variable in the row does not depend on the variable in the column, while the value 1 means that the variable in the row depends on the variable in the column. The importance factor of each variable is obtained by summing up the numbers in each column of the matrix. A high value implies high importance of the corresponding variable. The interdependency analysis is done in a hierarchical manner (Figure 4.2). That is, an interdependency matrix is built for each group of variables so that each variable is analyzed within the group it belongs to. For instance, a single interdependency matrix is constructed for the seven dimensions of PEOPLES. An interdependency matrix is built to each group of components under the dimensions. Finally, every group of indicators under the components are analyzed independently by performing the above-introduced interdependency technique. This results in 37 matrices to perform a full interdependency analysis for the different variables of the framework. The number of matrices depends on the conceptual framework used. That is, frameworks that use fewer variables and simpler structure would require a smaller number of interdependency matrices.

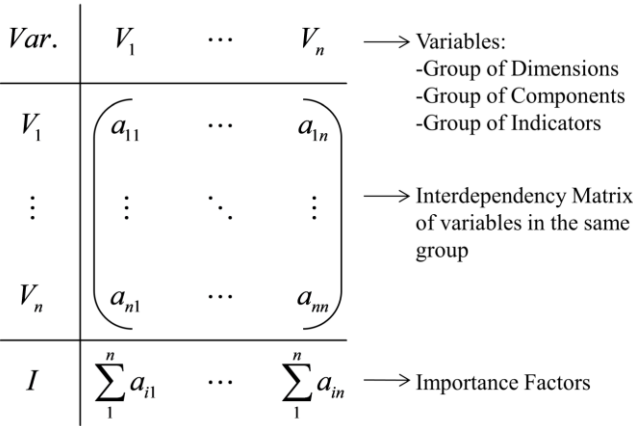


**Figure 4.1** Interdependency matrix between variables in the same group

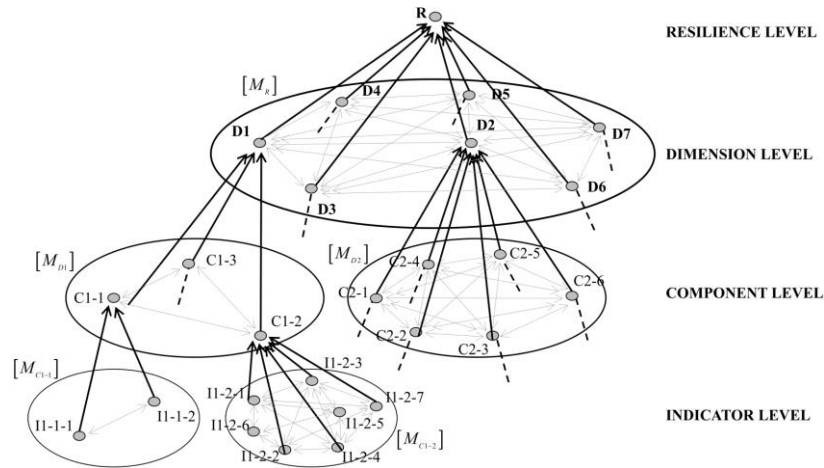


**Figure 4.2** Interdependency matrices at different levels

The matrix can be filled using a walk down survey. The evaluation is performed through an expert and the information is readily provided in a (yes/no) or (1/0) form. Like in any walk down survey, the assessment is denominated by subjectivity and so the evaluation process is prone to vagueness type uncertainty. However, due to the comprehensive structure of PEOPLES framework, the responsible expert will not have difficulties filling the survey and will not have to do arbitrary guessing. The experts will be able to employ their knowledge to decide whether the answer should be yes or no (1 or 0). To reduce possible vagueness and uncertainty, the survey can be filled by a group of experts. That is, the interdependency between any two variables is determined by more than one person. Then, a statistical analysis is performed considering a normal distribution, which is suitable for such statistical problems. Therefore, each variable is represented by a normal probability distribution function (PDF) (Figure 4.3). Three values from each PDF can be used in the consequent analysis: the mean value ( $\mu$ ), the mean value + the standard deviation ( $\mu + \sigma$ ), and the mean value – the standard deviation ( $\mu - \sigma$ ). This results in a final resilience output with the uncertainty bound being considered.

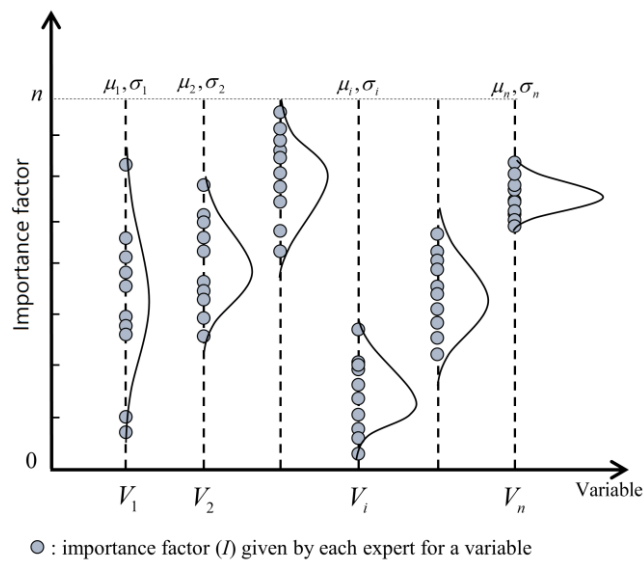


**Figure 4.3** Statistical analysis for the expert responses about the weighting factor of each variable

The interdependency between the variables is greatly related to the community type. Figure 4.4 shows the level of interdependency between the seven dimensions of the PEOPLES framework for three different kinds of communities: urban, rural, and industrial. The area enclosed by the interdependency polygon for the urban community is greater than the others. This indicates a high level of interaction and interdependency for urban communities. Also, the development level of the community plays a role in identifying the interdependency among resilience components because developed communities require more interdependent systems to increase service efficiency. Other factors such as the type of hazard can also affect the interdependency matrix.

Another aspect that is rarely discussed is the temporal alteration of the interdependency. After a perturbation, systems find a new equilibrium, which implies that the relationships between the system's elements change. Therefore, the interdependency matrix does not remain the same after a disaster event takes place (Figure 4.5). Although this is true for every system, in this study the temporal effect is not considered as it would add up unnecessary complexities which do not reflect the priorities of decision makers.

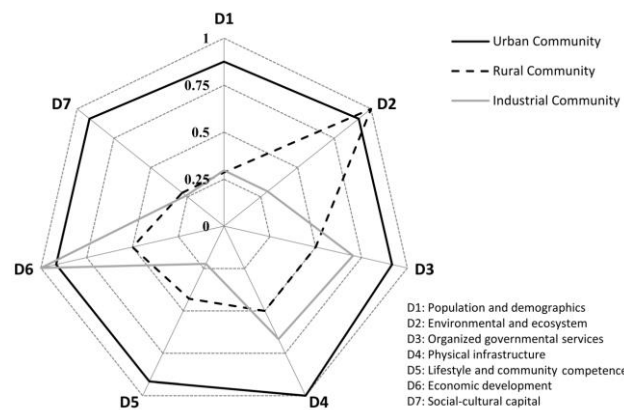


**Figure 4.4** The variation in the interdependency between the PEOPLES seven dimensions given different types of communities

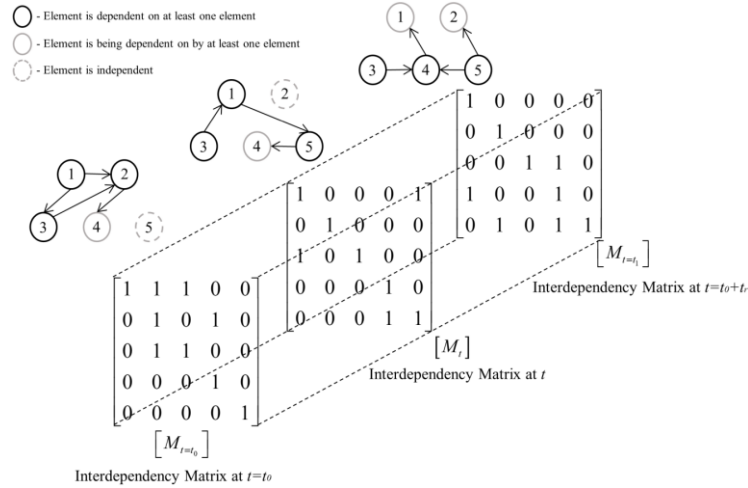


**Figure 4.5** Temporal variation in the interdependency matrix

The importance factors of the variables in the same group can be normalized using a Min-Max rescaling technique to create a set of comparable variables. The Min-Max rescaling technique is a method in which each variable is scaled between zero and one (a score of 0 being the worst rank for a specific variable and a score of 1 being the best) (Cutter et al. 2010). This scaling procedure subtracts the minimum importance factor from the importance factor of the underlying variable and divides it over the range of the importance factors, as shown in Eq. (4.1).

$$w_{v_i} = \frac{\sum_{j=1}^n a_{ji} - \min \left[ \sum_{j=1}^n a_{ji} \text{ for } i = 1, \dots, n \right]}{\max \left[ \sum_{j=1}^n a_{ji} \text{ for } i = 1, \dots, n \right] - \min \left[ \sum_{j=1}^n a_{ji} \text{ for } i = 1, \dots, n \right]} \quad (4.1)$$

where  $w_{v_i}$  is the weighting factor of the  $i^{th}$  variable ( $v_i$ ),  $a_{ji}$  is the interdependency value between variable  $j$  and variable  $i$  (Figure 4.1),  $n$  is the total number of variables in the analyzed group.

The above technique assumes that at least one variable is assigned a weighting factor equal to 0. This implies that the variable with a ‘zero’ weighting factor does not contribute to the overall resilience. In this research, a simpler technique that divides the importance factor over the maximum importance factor, as indicated in Eq. (4.2), is used.

$$w_{v_i} = \frac{\sum_{j=1}^n a_{ji}}{\sum_{i=1}^n \sum_{j=1}^n a_{ji}} \quad (4.2)$$

Eq. (4.2) transforms the importance factor of each variable into a weighting factor ( $w$ ). The equation is applicable to each group apart. Weighting factors are then multiplied by their corresponding functionality functions ( $q$ ), as indicated in Eq. (4.3):

$$q_i^* = w_i \times q_i \quad (4.3)$$

where  $q_i^*$  is the weighted functionality function of variable  $i$ ,  $q_i$  is the functionality function of the variable  $i$  in the analyzed group.

### 4.3.3 Final functionality function and computing resilience

Each variable is represented by a functionality function; a uniform function for event-non-sensitive measures ‘static measures’ and non-uniform function for event-sensitive measures ‘dynamic measures’ (see Figure 4.6). The functionality function can be defined using a set of parameters that mark the outline of the functionality function (e.g. initial functionality  $q_0$ , post-disaster functionality  $q_1$ , restoration time  $T_r$ , recovered functionality  $q_f$ , etc.). These parameters can be obtained from past events and/or by performing hazard analyses specific to each measure. Afterward, all functionality functions are weighted based on their contribution to the resilience assessment, as described in the previous section. The summation of the weighted functionality functions of the variables in the same group is considered to move to an upper layer. That is, to obtain the functionality function of component  $j$ , the summation of the weighted functionality functions of the indicators under component  $j$  is considered. Similarly, to obtain the functionality function of dimension  $i$ , the sum of the weighted functionality functions of the components under dimension  $i$  is considered. Finally, the functionality function of the community is the summation of the weighted functionality functions of the seven dimensions.

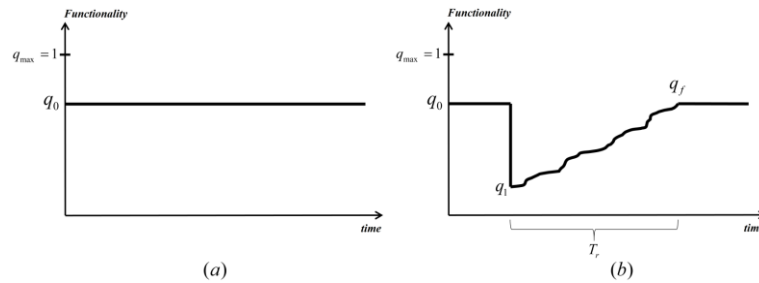


**Figure 4.6** a) Event-non-sensitive measure (static) b) event-sensitive measure (dynamic)

The conceptual approach for the consolidation of functionality functions through the different hierarchical levels of the framework is depicted in a flowchart (see Figure 4.7). The final functionality function represents the functionality of the community over time. It is obtained using the Eq. (4.4):

$$R(t) = \sum_{i=1}^{d=7} w_i(t) \cdot D_i(t) \quad (4.4)$$

where  $R(t)$  is the resilience function of the community,  $w_i(t)$  is the weighting function of dimension  $i$ ,  $D_i(t)$  is the functionality function of dimension  $i$ . In this equation, the weighting factors are written as a function of  $t$  because generally the weight of variable can change after the perturbation. The functionality function of dimension  $i$  is obtained using Eq. (4.5):

$$D_i(t) = \sum_{j=1}^{n_i} (w_{i,j}(t) \cdot C_{i,j}(t)) \quad (4.5)$$

where  $w_{i,j}(t)$  is the weighting function of the component  $j$  under dimension  $i$ ,  $C_{i,j}(t)$  is the functionality function of component  $j$  under dimension  $i$ ,  $n_i$  is the number of components under dimension  $i$ . This function is obtained by aggregation the functionality functions of the indicators in the same group. Eq. (4.6) can be used to do the operation:

$$C_{i,j}(t) = \sum_{k=1}^{n_{i,j}} (w_{i,j,k}(t) \cdot I_{i,j,k}(t)) \quad (4.6)$$

where  $w_{i,j,k}(t)$  is the weighting function of the indicator  $k$  under component  $j$ , which belongs to dimension  $i$ ,  $I_{i,j,k}(t)$  is the functionality function of indicator  $k$  under component  $j$ , which belongs to dimension  $i$ ,  $n_{i,j}$  is the number of indicators under component  $j$ , which belongs to dimension  $i$ . The resilience of the community  $R$  can then be evaluated as the area under the functionality function  $R(t)$  for a defined time following the disaster event, known as the ‘control period’  $t_c$ . Eq. (4.7) expresses the resilience index in its most explicit form using only the known parameters:

$$R = \int_{t=t_0}^{t_c} R(t).dt = \int_{t=t_0}^{t_c} \left\{ \sum_{i=1}^{d=7} w_i(t) \cdot \left[ \sum_{j=1}^{n_i} w_{i,j}(t) \cdot \sum_{k=1}^{n_{i,j}} (w_{i,j,k}(t) \cdot I_{i,j,k}(t)) \right] \right\} .dt \quad (4.7)$$

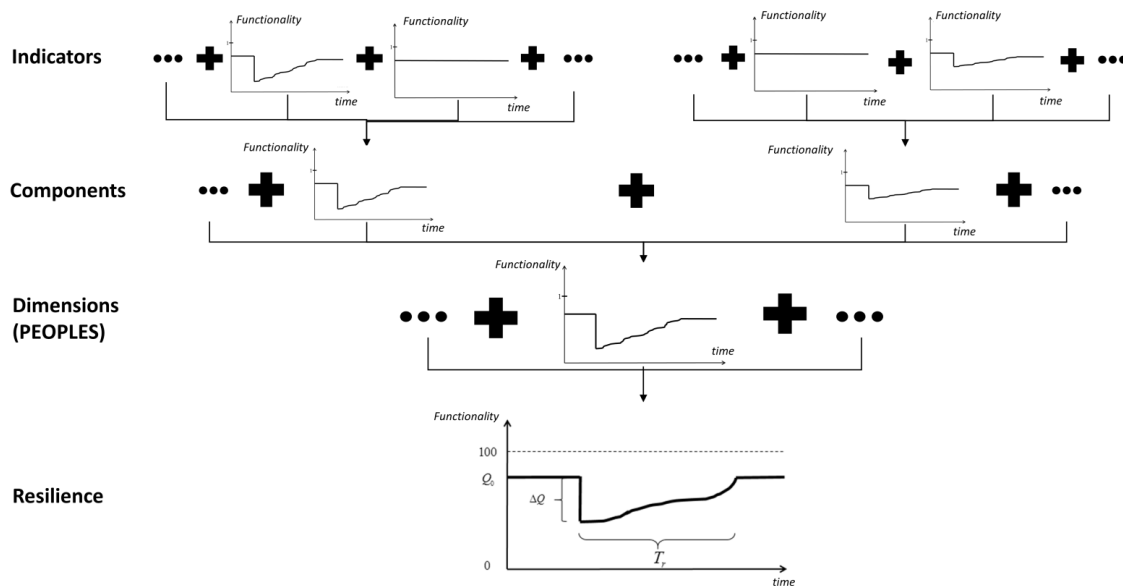


**Figure 4.7** Deriving the functionality function of the community

The introduced method is a decision-making tool, and the usefulness of the final resilience metric is to give an indication whether the community needs to improve in terms of resilience by comparing it to a given acceptable level. Using this metric, the user can identify immediately if the community is experiencing a high functionality deficiency, then the user can decide to

look into specific components and indicators that are found to cause the highest impact on resilience. The significance of the proposed methodology lies in its graphical representation that helps communities take proper actions to improve their resilience. While all previous works generally provide a single index to measure community resilience, the proposed method indicates in detail whether the resilience deficiency is caused by the system’s lack of robustness or by the slow restoration process. For example, it is possible for two communities to have the same resilience deficiency induced by different reasons (e.g. lack of robustness, slow recovery, etc). This is represented in Figure 4.8 where two systems have the same loss of resilience (*LOR*) caused by different reasons. The proposed method recognizes where exactly the resources should be spent to efficiently improve resilience. The final resilience index allows the user to have a broad picture about the resilience of the community, while the functionality curves of single indicators are used for analyses that focus more on specific resilience issues of the community.

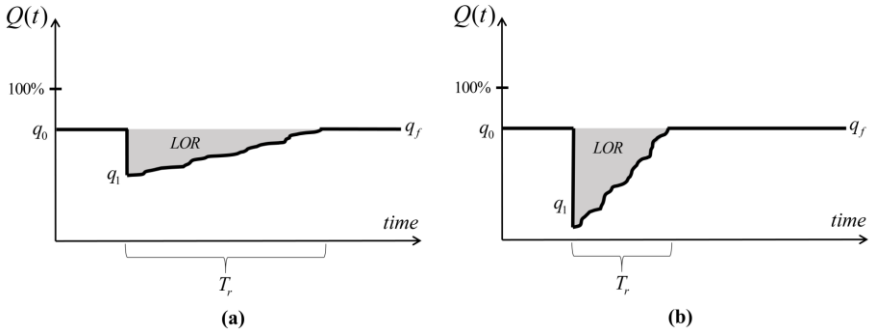


**Figure 4.8** The resilience curves of two systems showing the same loss of resilience *LOR*

### 4.4 Case study: 1989 Loma Prieta earthquake, San Francisco

In this section, the resilience of the city of San Francisco is evaluated using the proposed resilience method. The case study intends to show the applicability of the proposed methodology and not the actual evaluation of the resilience of San Francisco. The 1989 Loma Prieta earthquake, with a moment magnitude of 6.9  $M_w$ , has been considered as the disaster event. For the purpose of this study, only one of the PEOPLES dimensions ‘Physical Infrastructure’ has been considered. Table 4.1 shows the extended list of the components and indicators within the dimension ‘Physical Infrastructure’. Each indicator is linked to a measure that describes the indicator numerically. As shown in Figure 4.6, dynamic measures (*D*) are interpreted graphically using functionality curves, which are determined using a set of parameters (normalized initial functionality  $q_0$ , post-disaster functionality  $q_1$ , restoration time  $T_r$ , and recovered functionality  $q_f$ ), whereas the static measures (*S*) are non-sensitive to the event and remain constant even after the disaster occurrence. In this study, the parameters were determined using open database sources (see notes under Table 4.1), which offer data on all cities across the US.

In Table 4.1,  $q_{0u}$  is the not-normalized initial functionality of the measure. The normalization of this quantity is necessary to combine it with the other measures that fall in the same group. This is done by defining the parameter  $TV$  (target value). This parameter represents the quantity at which the analyzed measure is considered fully resilient, and it can be defined by an expert or a group of experts. Therefore, by dividing the non-normalized functionality  $q_{0u}$  over the target value  $TV$ , one could obtain a normalized functionality  $q_0$  which now can be combined with other indicators in the same group.

Right after the disaster, the functionality function of a dynamic measure drops to  $q_I$  (see Figure 4.6 (b)). Recovery actions are started immediately after the event, trying to bring the service back to an acceptable level. In this example, the recovered functionality  $q_r$  is assumed equal to the initial functionality  $q_0$ . The restoration time  $T_r$  is usually determined using probabilistic or statistical approaches. In this case study, restoration fragility curves recently developed by [Kammouh et al. \(2018a\)](#) have been used to determine the restoration time for the different variables. In their work, they have introduced an empirical probabilistic model to estimate the downtime of lifelines following an earthquake. Different restoration functions were derived for different earthquake magnitudes using a large earthquake database that contains data on the downtime of infrastructures. The functions were presented in terms of probability of recovery versus time. The downtime corresponding to 95% of exceedance probability of recovery has been used as a deterministic downtime for the considered infrastructure. As for the rate of restoration, a linear interpolation is assumed for all measures.

**Table 4.1** Functionality parameters of the indicators within the Physical Infrastructure dimension for the city of San Francisco after the Loma Prieta earthquake

Component /Indicator	Measure	$w$	$Nat$	$q_{0u}$	$TV$	$q_0$	$q_I$	$q_r$	$T_r$ (days)
<b>4.1 Facilities</b>									
4.1.1 Sturdy (robust) housing types	% housing units that are not manufactured homes	0.5	D	1	1	1	0.599	0.998	120
4.1.2 Temporary housing availability	% vacant units that are for rent	0.5	D	2.68	5	0.536	0.050	0.536	620
4.1.3 Housing stock construction quality	100-% housing units built prior to 1970	0.75	D	0.241	1	0.241	0.145	0.241	700
4.1.4 Community services	%Area of community services (recreational facilities, parks, historic sites, libraries, museums) total area ÷ TV	1	D	0.16	0.2	0.800	0.480	0.800	430
4.1.5 Economic infrastructure exposure	% commercial establishments outside of high hazard zones ÷ total commercial establishment	0.75	S	0.85	1	0.850	-	-	-
4.1.6 Distribution commercial facilities	%Commercial infrastructure area per area ÷ TV	0.5	D	0.13	0.15	0.867	0.520	0.867	160
4.1.7 Hotels and accommodations	Number of hotels per total area ÷ TV	0.75	D	102	128	0.797	0.478	0.797	130
4.1.8 Schools	Schools area (primary and secondary education) per population ÷ TV	0.5	D	134	140	0.957	0.574	0.957	90
<b>4.2 Lifelines</b>									
4.2.1 Telecommunication	Average number of Internet, television, radio, telephone, and telecommunications	0.73	D	5	6	0.833	0.500	0.833	90

	broadcasters per household ÷ TV								
4.2.2 Mental health support	number of beds per 100 000 population ÷ TV	0.09	D	69	75	0.920	0.644	0.920	35
4.2.3 Physician access	Number of physicians per population ÷ TV	0.18	S	2.5	3	0.833	-	-	-
4.2.4 Medical care capacity	Number of available hospital beds per 100000 population ÷ TV	0.27	D	544	600	0.907	0.635	0.907	35
4.2.5 Evacuation routes	Major road egress points per building ÷ TV	0.36	S	0.67	1	0.670	-	-	-
4.2.6 Industrial re-supply potential	Rail miles per total area ÷ TV	0.27	D	5412	6000	0.902	0.631	0.902	45
4.2.7 High-speed internet infrastructure	% population with access to broadband internet service	0.18	D	0.9	1	0.900	0.450	0.900	300
4.2.8 Efficient energy use	Ratio of Megawatt power production to demand	1.0	D	0.8	1	0.800	0.160	0.800	25
4.2.9 Efficient Water Use	Ratio of water available to water demand	0.64	D	1	1	1.000	0.240	1.000	60
4.2.10 Gas	Ratio of gas production to gas demand	0.45	D	0.1	1	0.100	0.050	0.100	70
4.2.11 Access and evacuation	Principal arterial miles per total area ÷ TV	0.73	D	17213 8	200000	0.861	0.602	0.861	45
4.2.12 Transportation	Number of rail miles per area ÷ TV	0.82	D	5412	6000	0.902	0.631	0.902	72
4.2.13 Waste water treatment	Number of WWT units per population ÷ TV	0.55	D	3	4	0.750	0.300	0.750	65

-Note:  $q_{0i}$  = the initial functionality;  $TV$  = the target value;  $q_0$  = the initial normalized functionality;  $q_1$  = post-disaster functionality;  $q_r$  = the recovered functionality;  $T_r$  = the restoration time.

-Source: City Data, Census Data, This Study, City Assessor's Data, Dept of Numbers, SF Indicator Project, Data World Bank, Dot Ca, SF Bos, Arcadis, SF Water, Energy Ca.

Table 4.2 lists all the parameters required for the realization of the functionality functions. The weighting factors of the different variables under the analyzed dimension have been determined using the proposed interdependency matrix technique. Table 4.3 shows the interdependency matrix of the indicators under the component 'Lifelines'. The report by the National Institute of Standards (NIST 2015) and Technology and the Lifelines Council (CCSF Lifelines Council 2014) have been used to fill the interdependency matrix. The recommendations of some experts in the field were also critical in concluding the matrix. In the matrix, the number '1' represents a significant interdependency while '0' means limited interaction and interdependency between the indicators. The results of the matrix have been used to find the weighting factor of each indicator (see the last row of Table 4.3). The weighting factors of the different indicators are used in the combination of the different variables to represent the contribution of each of them in the overall resilience evaluation.

**Table 4.2** The parameters involved in the resilience evaluation

Parameter	Definition
Weighting factor ( $w$ )	The weighting factor of a variable using the proposed interdependency matrix technique
Indicator nature ( $Nat$ ):	the indicators are classified according to their nature: "Static ( $S$ )", assigned to the measures that are not affected by the disastrous event, and "Dynamic ( $D$ )" or event-sensitive measures, assigned to the measures whose values change after a hazard takes place

Un-normalized functionality before the event ( $q_{0u}$ )	is the un-normalized initial functionality of the measure?
The target value ( $TV$ )	represents the optimal quantity or the baseline for the indicator in order to be considered as fully resilient
Normalized functionality before the event ( $q_0$ )	is the normalized initial functionality of the measure? It is obtained by dividing the un-normalized functionality $q_{0u}$ over the target value $TV$ ;
Functionality after the event ( $q_t$ )	The normalized residual functionality after the disaster.
Functionality after recovery ( $q_r$ )	it is the recovered functionality, which can be equal, higher, or lower than the initial $q_0$ .
Restoration time ( $T_r$ )	it is the time needed to finish the recovery process. This value is usually determined using probabilistic or statistical approaches.

**Table 4.3** The interdependency matrix between the indicators under the component ‘Lifelines’

Indicator	<i>Telecommunication</i>	<i>Mental health support</i>	<i>Physician access</i>	<i>Medical care capacity</i>	<i>Evacuation routes</i>	<i>Industrial re-supply potential</i>	<i>High-speed internet infrastructure</i>	<i>Efficient energy use</i>	<i>Efficient Water Use</i>	<i>Gas</i>	<i>Access and evacuation</i>	<i>Transportation</i>	<i>Wastewater treatment</i>
<i>Telecommunication</i>	1	0	0	0	0	0	1	1	0	0	1	1	0
<i>Mental health support</i>	0	1	0	1	0	0	0	0	0	0	0	0	0
<i>Physician access</i>	0	0	1	1	0	0	0	0	0	0	0	0	0
<i>Medical care capacity</i>	1	0	1	1	0	0	0	1	1	1	0	1	1
<i>Evacuation routes</i>	0	0	0	0	1	1	0	1	1	1	0	1	1
<i>Industrial re-supply potential</i>	0	0	0	0	1	1	0	1	0	0	1	1	0
<i>High-speed internet infrastructure</i>	1	0	0	0	0	0	1	1	0	0	0	0	0
<i>Efficient energy use</i>	0	0	0	0	0	0	0	1	1	0	1	0	0
<i>Efficient Water Use</i>	1	0	0	0	0	0	0	1	1	0	1	1	1
<i>Gas</i>	1	0	0	0	0	0	0	1	1	1	1	1	1
<i>Access and evacuation</i>	1	0	0	0	1	0	0	1	1	1	1	1	1
<i>Transportation</i>	1	0	0	0	1	1	0	1	0	1	1	1	0
<i>Wastewater treatment</i>	1	0	0	0	0	0	0	1	1	0	1	1	1
<b>Importance factor</b>	<b>8</b>	<b>1</b>	<b>2</b>	<b>3</b>	<b>4</b>	<b>3</b>	<b>2</b>	<b>11</b>	<b>7</b>	<b>5</b>	<b>8</b>	<b>9</b>	<b>6</b>
<b>Weighting Factor</b>	<b>0.12</b>	<b>0.01</b>	<b>0.03</b>	<b>0.04</b>	<b>0.06</b>	<b>0.04</b>	<b>0.03</b>	<b>0.16</b>	<b>0.10</b>	<b>0.07</b>	<b>0.12</b>	<b>0.13</b>	<b>0.09</b>

Note: For the level of interdependency if each indicator on the other read across each row

‘0’: Limited interaction and dependency on this indicator

‘1’: Significant interaction and dependency on this indicator

Figure 4.9 shows graphically the functionality function of two indicators. The first indicator “4.1.1 sturdy housing type” is an event-sensitive indicator (dynamic) for which the functionality level drops after the occurrence of the earthquake (i.e. the functionality decreased from 100 to 59.9 after the disaster). The service is fully restored after 120 days. The second indicator ‘4.2.3 Physician access’, whose measure is “Number of physicians per population”, is an event-non-sensitive measure (static) because even if the number of physicians is decreased after the disaster, the ratio of the number of physicians to the total population remains constant. This implies that the functionality level of the measure retains its original level regardless of the occurrence of the disaster. The functionality curves of all measures whether they are static or dynamic can be obtained using the data in Table 4.1. Several data sources were used to compile

the data for the case study, such as City-Data, Census Data, This Study, City Assessor’s Data etc.

Data collection was a challenging part of the analysis since data about the functionality of community systems is not usually shared with the public. However, this does not imply that data is not available but rather is not accessible. Interested parties, such as decision-makers and authorities, can use the framework with its full potential since data is usually available to them.

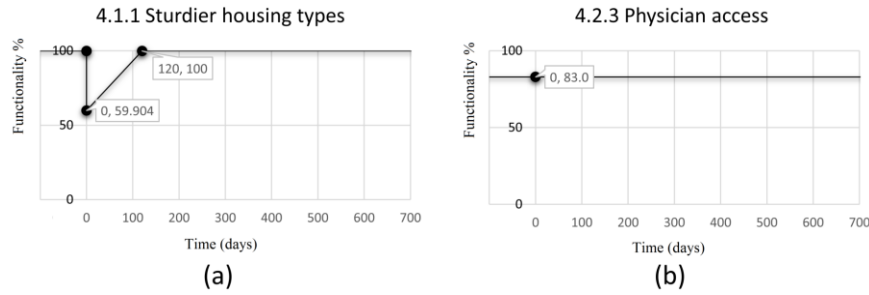


**Figure 4.9** Example of functionality curves (a) sturdier housing type (dynamic indicator), and (b) Physician access (static indicator)

As explained in the previous section, the functionality functions of the measures under a certain component are combined point by point into a single functionality function, taking into account their weighting factors which have been obtained using the interdependency matrix technique explained before. The weighting factors of the analyzed components are presented in Table 4.1. The functionality function of each component (i.e. facilities and lifeline) was obtained by summing the derived functionality functions of all measures that belong to the underlying component. Similarly, the functionality function of the dimension ‘physical infrastructure’ was derived by summing the weighted functionality functions of the corresponding components (i.e. facilities and lifelines).

Figure 4.10 shows the un-weighted functionality functions of the components: facilities and lifelines, and the combined functionality function of the dimension of physical infrastructure. The two components have different weighting factors ( $I_{Lifelines}=1$ ,  $I_{Facilities}=0.5$ ). Thus, the combined curve is closer to the high importance component (i.e. Lifelines).

The loss of resilience of the physical infrastructure was computed using Eq. (2.2). The time interval for calculation of resilience was considered from the time that event occurs ( $t_0=0$ ) until the end of full recovery (i.e. the time corresponding to the instance where the curve reaches its pre-disaster level;  $t_r=700$  days). The control time  $T_c$  can take any value and it is determined based on the period of interest. In this example,  $T_c$  is set equal to two years (730 days). The loss of resilience  $LOR$  in this case study is computed using Eq. (4.8):

$$LOR_{phys.inf.} = \int_{t_0}^{t_r} \frac{[100 - Q(t)]}{T_c} dt = \int_0^{700} \frac{[100 - Q(t)]}{730} dt = 25.63 \quad (4.8)$$

The area above the functionality curve of the ‘physical infrastructure’ for the time interval (0 to 700 days) is evaluated and normalized with respect to  $T_c=730$  days. The  $LOR$  metric is not a percentage but an absolute value that reflects the overall response of the community to

the earthquake event. That is, higher *LOR* signifies a poor response of the community. This number significantly depends on the control period. If the control period approaches to infinity, *LOR* tends to be zero. When the control period is short (e.g., 1 or 2 days), the *LOR* tends to be large.

In this case study, the obtained value of *LOR* corresponds only to the physical infrastructure dimension of the community. In order to have a resilience index for the whole community, the functionality functions of other dimensions have to be similarly evaluated and to be combined in the same way the measures were aggregated. It is also interesting to compare the resilience of the two components facilities and lifelines. From Figure 4.10, it is clear that the city of San Francisco has more problems in facilities (*LOR*=31.29%) than lifelines (*LOR*=21.85%). In this case, it is suggested that the authorities should focus more on enhancing the facilities as the benefit they would get is higher.

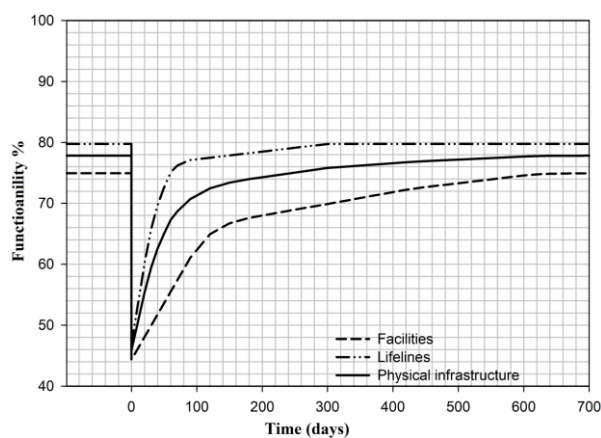


**Figure 4.10** Functionality curves of the components, Facilities and Lifelines, under the dimension Physical infrastructure

## 4.5 Software tools for PEOPLES framework

This section introduces two software tools in which the community resilience approach described above is implemented. The first tool is online software that is accessible at <http://borispio.ddns.net/PEOPLES/login.php>. (*Note: contact the author if the webpage is unreachable*), while the other is portable desktop software. Both tools require the same inputs and return the same outputs. The user is asked to insert information about the specific community resilience indicators before and after a disaster event. The output is presented in the form of a resilience curve of the whole community. In the following, the use of each tool is described in detail.

### 4.5.1 PEOPLES Web-App

The use of the online software tool is illustrated here. A Login/Register window appears when accessing the website link <http://borispio.ddns.net/PEOPLES/login.php> (Figure 4.11(a)). The user must register prior to using the tool. Once registered, the user can start a new scenario for which the resilience is to be evaluated (Figure 4.11 (b)).

## PEOPLES Framework login

Figure 4.11 consists of two screenshots of the PEOPLES Framework web interface. Screenshot (a) shows the login and registration page with fields for 'Username' and 'Password', a green 'Login' button, and a blue 'Register' button. Screenshot (b) shows the 'New scenario definition/load scenario' page. It features the 'PEOPLES Framework' logo, a 'Logged as Test' status with a 'Logout' button, a 'Saved Scenario' list containing a 'test' scenario, and a search bar with 'test' entered. Below the search bar is a '+ Create New Scenario' button.

**Figure 4.11** (a) Registration/Login page, (b) New scenario definition/load scenario

After defining the scenario, a data-entry page that displays the various variables of the PEOPLES framework appears (Figure 4.12). On the left side of the webpage, the seven dimensions of PEOPLES are listed. A separate page for each dimension can be accessed by clicking on the dimension. For each dimension, a list of components and indicators is shown with blank spaces for the user to insert the data for the parameters required for the resilience evaluation. A pop-up description is triggered when hovering the mouse over a parameter in the window. This is to get extra information that helps the user identify what kind of information they should insert. The parameters are:

- Importance factor ( $I$ ): each indicator is associated with an importance factor that represents the weight of the indicator towards the resilience output;
- Indicator nature ( $Nat$ ): the indicators are classified according to their nature: “Static (S)”, assigned to the measures that are not affected by the disastrous event, and “Dynamic (D)” or event-sensitive measures, assigned to the measures whose values change after a hazard takes place;
- Un-normalized functionality before the event ( $q_{0u}$ ): is the unnormalized initial functionality of the measure;
- Standard value ( $SV$ ), previously introduced as  $TV$  (Target value): represents the optimal quantity for the indicator in order to be considered as fully resilient;
- Normalized functionality before the event ( $q_0$ ): is the normalized initial functionality of the measure. It is obtained automatically by the software by dividing the unnormalized functionality  $q_{0u}$  over the standard value  $SV$ ;
- Functionality after the event ( $q_l$ ): The residual functionality after the disaster. This quantity should be normalized by the user with respect to  $SV$ ;
- Functionality after recovery ( $q_r$ ): it is the recovered functionality, which can be equal, higher, or lower than the initial functionality ( $q_0$ ). In this research. The recovered functionality  $q_r$  is assumed equal to the initial functionality  $q_0$ ;
- Restoration time ( $T_r$ ): It is the time needed to finish the recovery process. This value is usually determined using probabilistic or statistical approaches.

A list of importance factors ( $I$ ) has been set as default in the software; however, the user can change the numerical values in the list according to their preference. The importance factors can also be set all to “1” in case the user finds no justification to change the weights of the

indicators; in this case, the indicators will be equally weighted. The nature of the indicator “Nat” can also be changed by the user because this parameter depends on the type of hazard and type of community considered in the analysis. If the indicator is *Static* ‘S’, it is enough for the user to insert data about the initial functionality of the system  $q_{0u}$ , and the standard value  $SV$ . If otherwise the indicator is *Dynamic* ‘D’, the user should proceed and insert data about the post-event damage  $q_1$ , functionality level after restoration  $q_r$ , and restoration time  $T_r$ . The parameter  $q_{0u}$  is inserted as unnormalized value while other functionality parameters  $q_1$  and  $q_r$  have to be normalized by the user with respect to  $SV$  (divide over  $SV$ ). A functionality curve for each component is shown at the bottom of the page when filling all data. The functionality curve of the analyzed dimension, which is the weighted average of all functionality functions of the components, is also shown on the same graph.

After inserting all the required data for all the dimensions, the user will be able to see the functionality curve of the community by clicking on the ‘The community resilience curve’ on the left side of the screen. For each of the functionality curves, the software automatically evaluates the *LOR*, which is an indicator for the functionality loss incurred during the event.

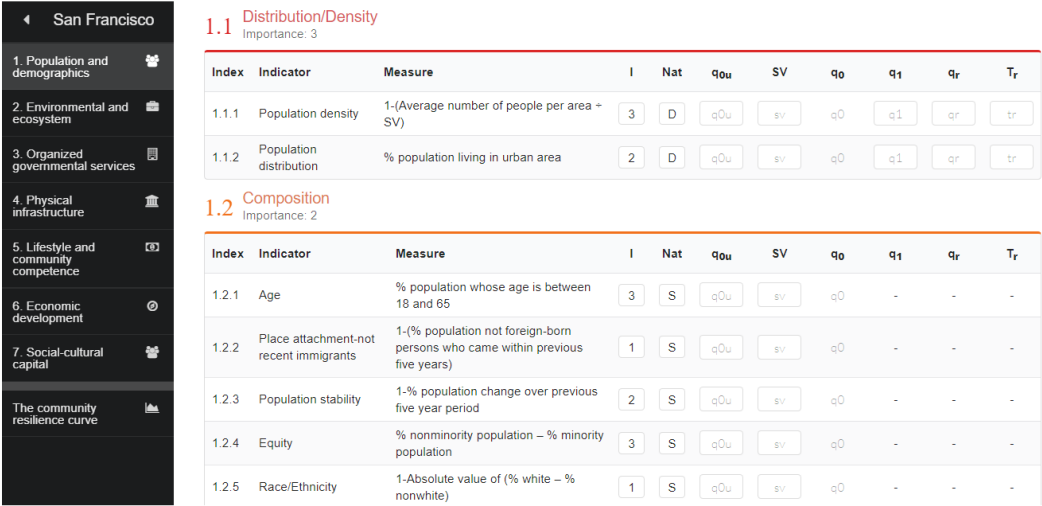
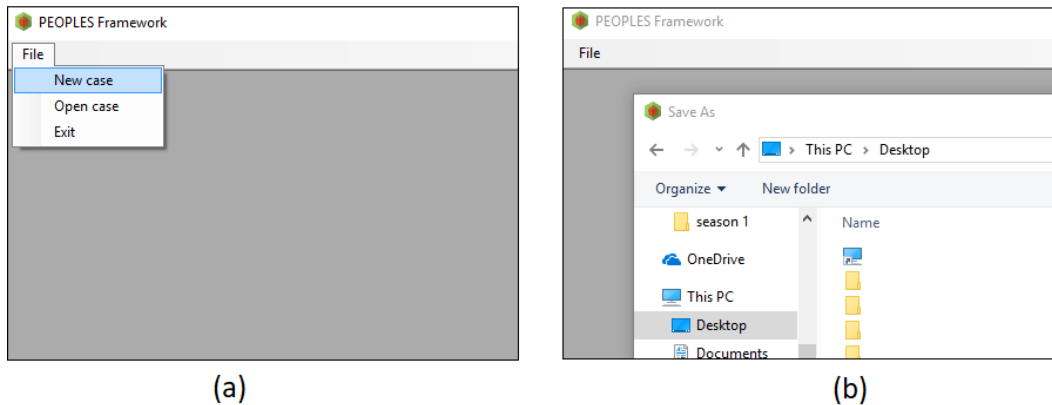


Figure 4.12 User interface and data entry environment

### 4.5.2 Desktop software

The software introduced in this section is a portable version that does not require installation. To run the software, only one file containing the indicators database is required. This file comes preloaded in the software package. The user cannot modify the indicators and the results accumulation hierarchy of the methodology as these are fixed according to the PEOPLES framework. When the software is run, the user will be required to choose whether they want to start a new scenario “New case” or to load a saved one “Open case” (Figure 4.13 (a)). If the user chooses to start a new scenario, a new window, shown in Figure 4.13 (b), asking the user to define the directory to which the scenario is saved will pop up.



**Figure 4.13** (a) starting a new scenario “New case” or loading a saved scenario “Open case”, (b) saving the scenario if the option “New case” is chosen

After saving the new scenario, a new blank page with only three functions “Add”, “Remove”, and “Edit” will display (Figure 4.14(a)). At this stage, the user needs to insert the database specific to the analyzed case study. To do that, the user should click on the “Add” function, which triggers a window containing all the indicators of the PEOPLES framework (Figure 4.14(b)). The user can delete and modify the indicators using the functions “Remove” and “Edit”. Each of the indicators is accessed independently to insert the data required for its evaluation.

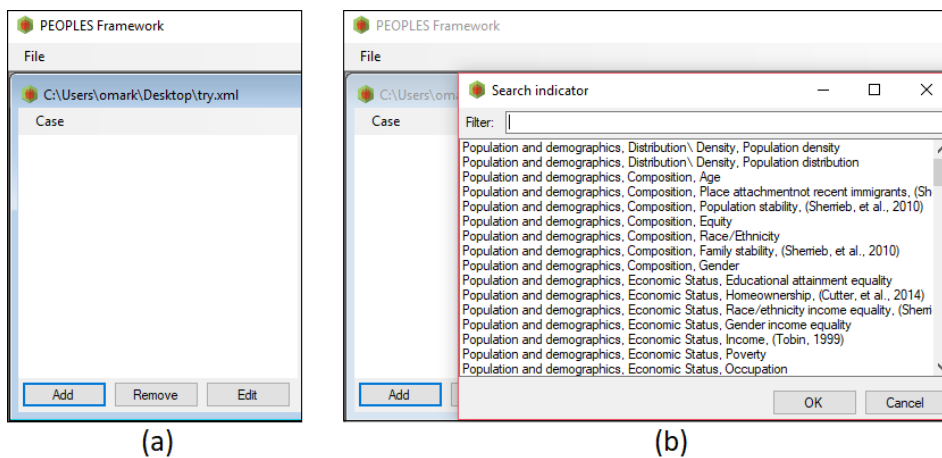


**Figure 4.14** Data entry for the PEOPLES indicators

The number of inputs required depends on the nature of the indicator. Static indicators require only two parameters for their evaluation ( $q_0$  and  $I$ ) (Figure 4.15(a)) whereas dynamic indicators need five inputs ( $q_0$ ,  $q_1$ ,  $q_f$ ,  $T_r$ , and  $I$ ) (Figure 4.15(b)). It is very important to note that, unlike the web app software introduced in the previous section, all the parameters  $q_0$ ,  $q_1$  and  $q_r$  MUST be normalized by the user (i.e., the user has to divide these quantities over  $SV$ ).

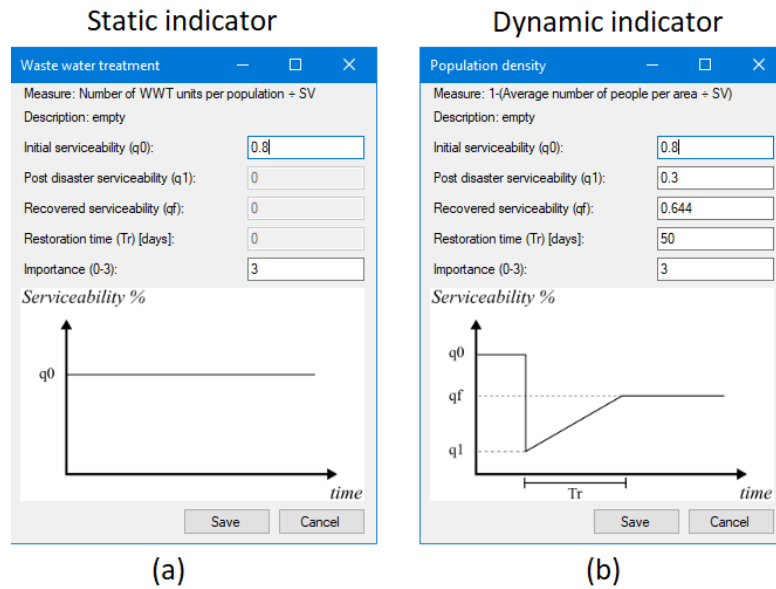


Figure 4.15 Data entry for the indicators

### 4.5.3 Results

The same case study introduced in Section 4.4 is applied in both software tools. Figure 4.16 and Figure 4.17 show the resilience curves obtained using the online and desktop software tools, respectively. The resilience indexes (LOR) of the physical infrastructure dimension obtained using the software tools are similar to that obtained in Section 4.4 (LOR=25.63%). This demonstrates that both software tools are implemented according to the methodology introduced in earlier in the chapter.

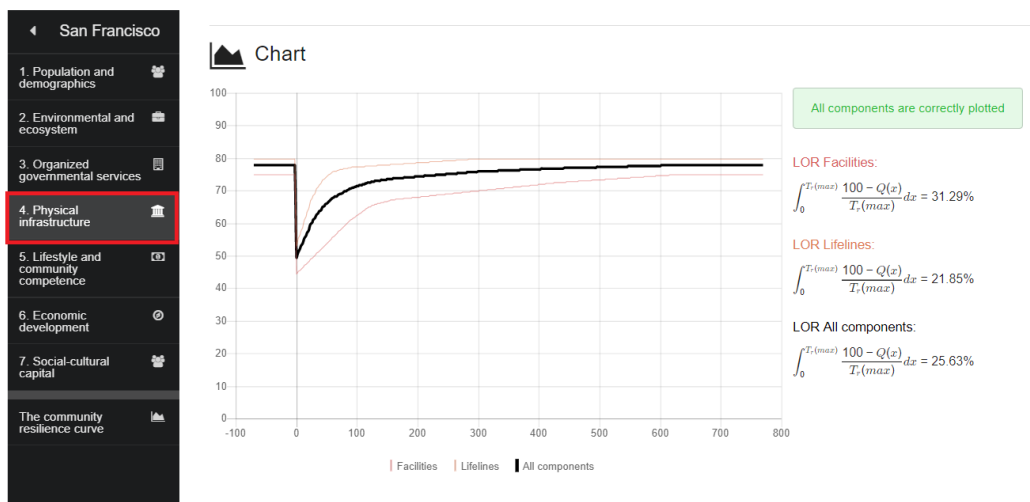


Figure 4.16 Functionality curves of the components “Facilities” and “Lifelines” and the dimension “Physical Infrastructure”

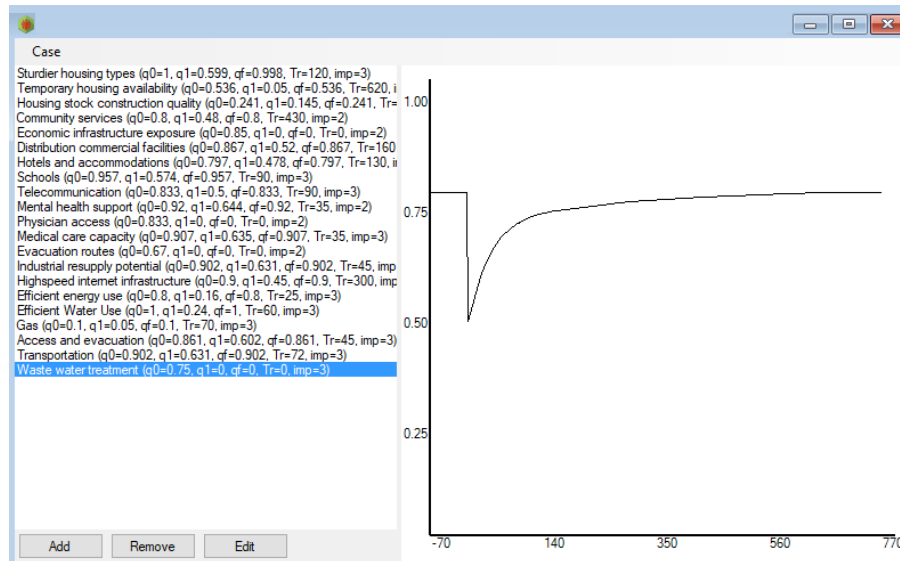


Figure 4.17 Functionality curves of the components “Facilities” and “Lifelines” and the dimension “Physical Infrastructure”

## 4.6 Method 2: simplified fuzzy logic resilience framework

The methodology previously described can serve as a powerful tool in preliminary decision-making processes related to natural catastrophic events. Nevertheless, this method is operable only if indicators can be numerically quantified, which may not be the case in some scenarios. In this section, a method that does not require deterministic data to compute the resilience of a community is proposed. The method exploits fuzzy logic-based modeling of PEOPLES indicators in order to deal with uncertainties and missing knowledge. In the following, the fuzzy modeling of PEOPLES indicators and the evaluation of community resilience using information gathered through the fuzzy inference system are discussed. Different approaches are proposed to match different levels of complexity, starting from a two- and four-parameter approaches and ending with a full translation of the PEOPLES framework.

### 4.6.1 Fuzzy logic

[Zadeh \(1965\)](#) introduced the concept of fuzzy set and the theory behind it. This theory comes with the absence of any mathematical framework that is able to describe the complexity and vagueness included in processes where human intervention is significant. While in the crisp logic the variables belong only to one class, in the fuzzy logic a variable  $x$  can be a member of several classes (fuzzy sets) with different membership grades ( $\mu$ ). Thus, each fuzzy set is characterized by a membership function that associates to any input  $x$  a real number ( $\mu$ ) ranging between 0 ( $x$  does not belong to the fuzzy set) and 1 ( $x$  completely belongs to the fuzzy set) ([Zadeh 1965](#)). The strength of inference systems based on fuzzy logic relies on the following two main aspects:

- fuzzy inference systems can handle both descriptive (linguistic) knowledge and numerical data;
- fuzzy inference systems exploit the approximate reasoning algorithm to formulate relationships between inputs by which uncertainties can be propagated throughout the whole process ([Tesfamariam and Saatcioglu 2008a](#)).

Designing a fuzzy logic-based system follows two fundamental steps: 1) defining the membership functions and the fuzzification process; 2) designing the fuzzy inference system. Fuzzy methods have been widely developed and applied in several fields ([Ross 2009](#)). In the context of earthquake engineering, fuzzy methods have been exploited in different applications (e.g. ([Tesfamariam and Saatcioglu 2008b](#); [Tesfamariam and Saatcioglu 2010](#); [Tesfamariam and Wang 2011](#))). Fuzzy methods have been widely used also for developing structural control systems. A clear procedure for the application of fuzzy logic can be found in ([Tesfamariam and Saatcioglu 2008a](#); [Tesfamariam and Saatcioglu 2008b](#)).

A fuzzy logic system (FLS) can be defined as the nonlinear mapping of an input data set to a scalar output data. A FLS consists of four main parts: fuzzifier, rules, inference engine, and defuzzifier (Figure 4.18). The process of fuzzy logic is: a crisp set of input data are gathered and converted to a fuzzy set using fuzzy linguistic variables, fuzzy linguistic terms and membership functions. This step is known as fuzzification. Afterward, an inference is made based on a set of rules. Lastly, the resulting fuzzy output is mapped to a crisp output using the membership functions, in the defuzzification step.

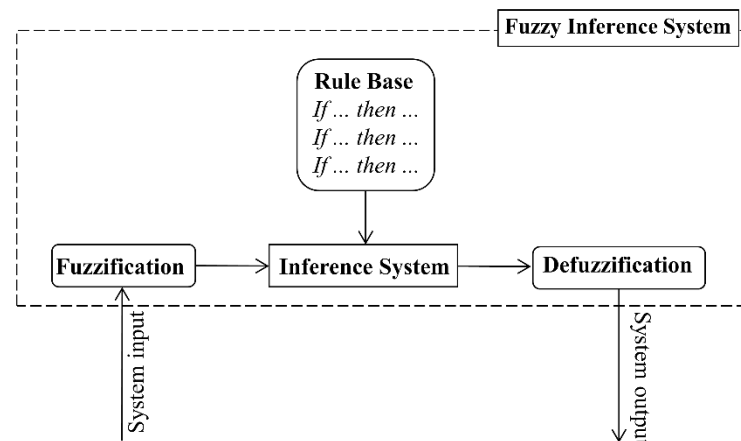


**Figure 4.18** Fuzzy inference system

#### 4.6.1.1 Fuzzification

The basic input parameters have a range of values that can be clustered into linguistic quantifiers, for instance, very low (VL), medium low (ML), medium (M), medium-high (MH) and very high (VH). The process of assigning linguistic values is a form of data compression and it is called *granulation*. The fuzzification step converts the input values into a homogeneous scale by assigning corresponding membership functions with respect to their specified granularities ([Tesfamariam and Saatcioglu 2008b](#)).

Membership functions are used in the fuzzification and defuzzification steps of an FLS, to map the non-fuzzy input values to fuzzy linguistic terms and vice versa. A membership function is used to quantify a linguistic term. Note that, an important characteristic of fuzzy logic is that a numerical value does not have to be fuzzified using only one membership function. In other words, a value can belong to multiple sets at the same time. There are different forms of membership functions such as triangular, trapezoidal, piecewise linear, Gaussian, or singleton. The most common types of membership functions are triangular, trapezoidal, and Gaussian shapes. The type of the membership function can be context dependent and it is generally chosen arbitrarily according to the user experience ([Mendel 1995](#)).

#### 4.6.1.2 Fuzzy rules

The fuzzy rule base (FRB) is derived from heuristic knowledge of experts or historical data to define the relationships between inputs and outputs. The most common type is the *Mamdani* type, which is a simple *if-then* rule with a condition and a conclusion. For instance, considering two inputs, the  $i^{\text{th}}$  rule has the following formulation:

$$R: \text{if } x_1 \text{ is } A_1 \text{ and } x_2 \text{ is } A_2 \text{ then } y \text{ is } B \quad (4.9)$$

where  $R$  is the rule number,  $x_1$  and  $x_2$  are the inputs variable,  $A_1$  and  $A_2$  are input sets,  $y$  is the output and  $B$  is the output set. The completeness of a fuzzy model is determined by the description of the behavior for all possible input values and requires a large number of rules. The rule base is the union of all the rules:

$$R = \bigcup_{i=1}^n R_i = R_1 \text{ also } R_2 \text{ also } \dots \text{ also } R_n \quad (4.10)$$

In some cases, it is possible to regulate the degree of influence of each rule on the final output. This can be done by adding weightings based on priority or consistency, in a static or in a dynamic way.

#### 4.6.1.3 Fuzzy inference system (FIS)

After evaluating the result of each rule, the results are combined to obtain a final output. This process is called *inference*. Several accumulation methods can be used to combine the results of the individual rules. The maximum algorithm is generally used for accumulation. The evaluations of the fuzzy rules and the combination of the results of the individual rules are performed using fuzzy set operations. The operations on fuzzy sets are different with respect to the operations on non-fuzzy sets.

#### 4.6.1.4 Defuzzification

After the inference step, the overall result is a fuzzy value. This result should be defuzzified to obtain a final crisp output. This is the purpose of the defuzzifier component of an FLS. The defuzzification represents the inverse of the fuzzification process. It is performed according to

the membership function of the output variable. There are several techniques to perform the defuzzification such as center of gravity, center of area, and mean of maximum methods.

### 4.6.2 Two- parameter approach

This approach adopts only two of the four functionality parameters described before, namely functionality initial drop  $q^*$  (previously referred to as  $q_0$ ) and recovery time  $T^*$  (previously referred to as  $t_0$ ). Fuzzy parameters have been chosen based on the research by [Bruneau et al. \(2003\)](#) who describes the resilience of a system using the following three indicators: reduced failure probability; reduced consequences from failure; reduced time to recovery. The reduced failure probability has not been considered as it is not easily related to the herein adopted mathematical definition of resilience, which considers only the failure consequence  $q^*$  and the repair time  $T^*$ . Figure 4.19 presents a hierarchy of the two-parameter approach where both *time* and *initial drop* variables are used as inputs for the fuzzy system. The inputs are combined using a set of rules to obtain the output variable *fuzzy resilience*. The fuzzy output is defuzzified to get a crisp value that serves as a resilience index for the corresponding indicator.

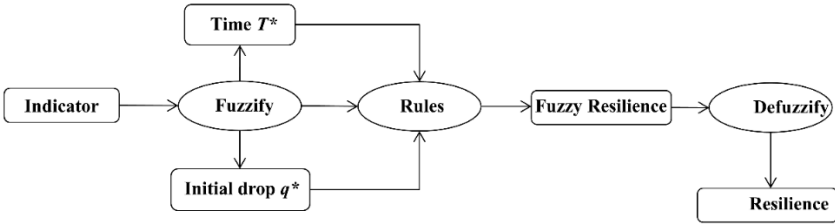


**Figure 4.19** Schematic representation of the *two-parameter* approach

#### 4.6.2.1 Evaluating initial functionality drop ( $q^*$ )

Two trapezoidal membership functions can be reasonably adopted in the present case. They are termed as “High” and “Low”. The fuzzification used for  $q^*$  is [High; Low]  $\rightarrow [(0, 0, 0.3, 0.7); (0.3, 0.7, 1, 1)]$ . The membership functions are graphically shown in Figure 4.20.

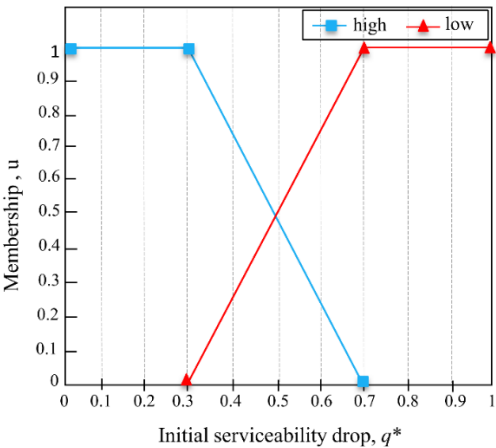


**Figure 4.20** Membership functions for the functionality variable  $q^*$

#### 4.6.2.2 Evaluating recovery time ( $T^*$ )

When speaking of recovery, the intention is *full* recovery. Outperforming, or non-complete recovery, as indicated by Cimellaro et al. (2010), are not generally predictable and therefore they are not included here. For the time variable  $T^*$ , three membership functions are suggested by the authors, namely: “short”; “long”; and “very long”. The time variable is normalized based on a 3-year time span, which is normally the time reference for civil applications (i.e., 3 years corresponds to 1 on the horizontal axis). Figure 4.21 shows the membership functions chosen by the authors. The membership functions are not symmetrical as they have been constructed to the favor of the “Long” and “Very Long” memberships. That is, high range of values of the restoration time  $T^*$  variable corresponds to the membership functions “Long” and “Very Long”.

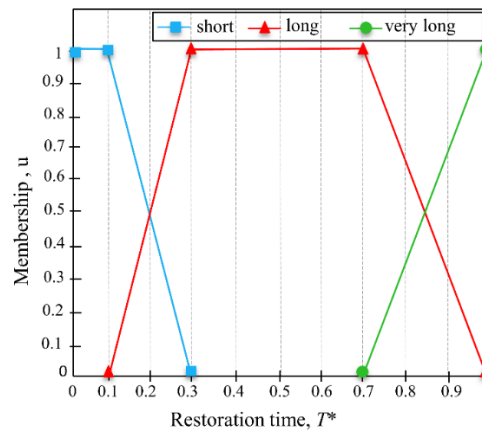


**Figure 4.21** Membership functions for the downtime variable  $T^*$

The aim is to translate the given input variables ( $q^*$  and  $T^*$ ) into one resilience measure  $R$ . This measure is itself fuzzy and so it is defined by a membership function. The chosen membership functions are depicted in Figure 4.22. Following the fuzzy approach, it is possible to define an output value calculated from the provided inputs on the basis of a set of rules. The rules adopted in this study to relate the inputs and the output are shown in Table 4.4.

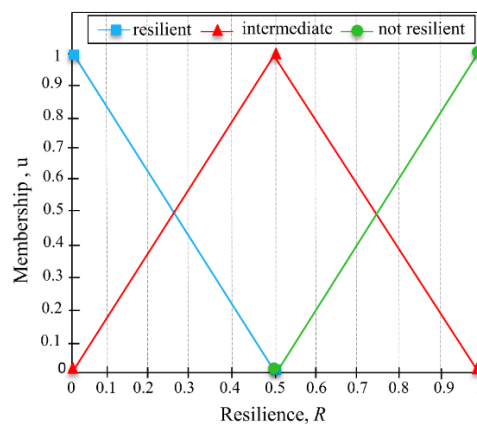


**Figure 4.22** Membership functions for the resilience variable  $R$

**Table 4.4** Fuzzy rule base for resilience

$T^*$	$q^*$	$R$
short	high	resilient
Long	high	resilient
Very long	high	intermediate
Short	low	intermediate
long	low	not resilient
Very long	low	not resilient

#### 4.6.2.3 Defuzzification

The fuzzy output variable is translated (defuzzified) into a numerical value that serves as a measure for resilience. Different methods for defuzzification can be used ([Manyena 2006](#)) such as center of gravity, weighted average, mean-max, center of largest area etc. The use of one method rather than another is dependent on the application. Here, the center of gravity method given in Eq. (4.11) is used.

$$CoA = \frac{\int_{x_{min}}^{x_{max}} f(x) \cdot x \, dx}{\int_{x_{min}}^{x_{max}} f(x) \, dx} \quad (4.11)$$

where  $f(x)$  is the function that shapes the output fuzzy set after the aggregation process and  $x$  stands for the real values inside the fuzzy set support ( $[0, 1]$ ). Practical examples on the application of the fuzzy method to several case studies can be found in ([Tsfamariam and Saatcioglu 2008a](#); [Tsfamariam and Saatcioglu 2008b](#)).

#### 4.6.2.4 Importance factor

The fuzzy logic introduced above applies to each indicator apart. It is often the case to aggregate different indicators into a single measure (i.e. community resilience) through a hierarchical structure. Usually, indicators are not equally important because they contribute differently towards resilience and this necessitates weighting them according to their contribution. The weighting scheme used in ([Kammouh et al. 2019b](#)) is here adopted. It can be performed by simply allocating an importance factor ( $I$ ) ranging between 1 and 3 to each indicator then applying the weighted average rule, as follows:

$$R = \frac{\sum_{i=1}^N I_i R_i}{\sum_{i=1}^N I_i} = \sum_{i=1}^N w_i R_i \quad (4.12)$$

where  $R$  is the community resilience measure,  $R_i$  is the resilience measure of the  $i^{th}$  indicator,  $I_i$  is the corresponding importance factor (which can be scaled to preference), and  $w_i$  is the weighting factor of the  $i^{th}$  indicator. The difference with what has been proposed previously in the chapter is that in this methodology the functionality functions are translated into resilience values before applying the weighting method (Figure 4.23). This simplifies the fuzzy system as it reduces the number of variables that need to be handled.

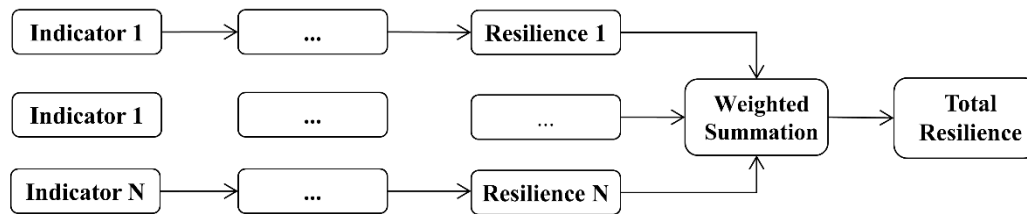


**Figure 4.23** Hierarchical scheme of the fuzzy system with the weighing process

### 4.6.3 Four-parameter approach

Considering only two parameters to represent a resilience indicator may in some cases be insufficient, thus affecting the mentioned benefits of using the Fuzzy approach. Moreover, this may oversimplify the problem especially when specific information about the structure itself is available and to be added. For this reason, in certain cases it may be beneficial to build up the resilience curve from fuzzy parameters other than the recovery time and the initial drop. In fact, it has been pointed out by [Comerio \(2006\)](#) that further distinction in the repair time is possible. According to his work, the following parameters should be taken into account:

- Construction repair time;
- Mobilization time;
- Economic conditions of the interested region;

The mobilization time, in particular, labeled as “irrational” in [Comerio \(2006\)](#) (e.g. financing, workforce availability, relocation of functions or regulatory changes), is often not properly accounted for and therefore it should be given special attention when evaluating downtime. These three indicators may be fuzzified with a structure similar to the one adopted for the recovery time  $T^*$ . The result is similar to that shown previously with the only difference that new rules and membership functions are to be assigned to the new variables. When resilience measures are calculated, weighting is performed to obtain the system (community) resilience.

### 4.6.4 Full PEOPLES

Most of the concepts described previously remain valid here. The only difference is that the approach introduced in this section includes the weighting of the variables within the fuzzy system. Normally, choosing adequate weighting factors is subjective and includes uncertainty. Although the inclusion of the weighting factors within the fuzzy system may add additional complexity as more variables are considered, it is certainly beneficial as it solves the uncertainty problem related to the weighting factors. To do that, two alternatives are proposed:

- Include the importance factor in the definition of the rules governing the fuzzy logic. In other words, assign rules such that the output is strongly related to the indicators with the highest importance;
- Translate the importance factor into a fuzzy variable itself and include rules for it.

In both cases, rules have to be adapted to account for the importance factors. In the former case, rules are firmly tight to the particular application (i.e. hard to modify and not flexible); the latter case is, in this respect, more flexible but at the cost of additional complexity since additional rules have to be added to include the effect of the importance factor. This approach will be further developed, and case studies will be added in future work. Figure 4.24 shows the logic flow where the weighting process is included as a separate variable in the first step before fuzzification.

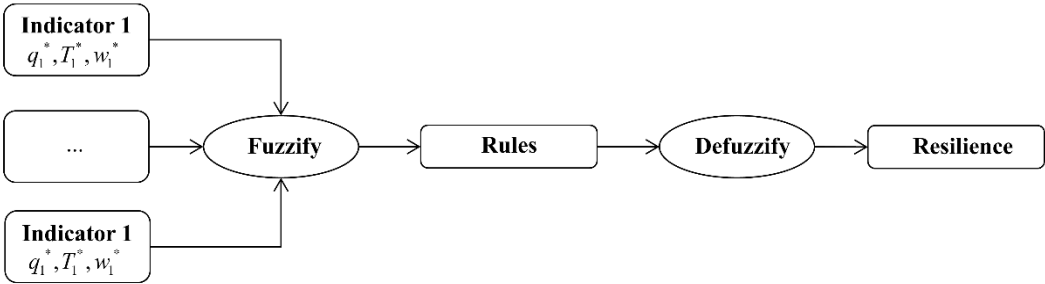


**Figure 4.24** Full PEOPLES approach general hierarchical scheme with the weighting process included in the fuzzy system as a separate variable

### 4.7 Discussion

The two methodologies introduced before, although applied in the same context, are used under two different conditions. The first “deterministic” method is used only when data on a previous disaster is available. Applying the methodology to a real disaster allows the user to assess the loss of resilience following that particular disaster, which may help to prepare for future disasters by focusing on the weak aspects. This method also has the potential of being probabilistic when data on many previous events are available. The second methodology is used for both assessment and planning when data does not actually exist (which is often the case). Of course, this method would yield less accurate results since it relies on expert judgments instead of actual data.

Choosing between the two methods depends on what we really need. If it is an actual assessment for a previous disaster, then the first method should be used (given that data is available). If the goal is to plan for future events without having data on previous events, then the fuzzy-based method should be used. The results of the first method are more accurate but it can be rather challenging to obtain data.

### 4.8 Concluding remarks

This chapter introduces two methods to compute the resilience of communities based on the PEOPLES framework. An indicator-based approach has been implemented as the core engine of both methodologies. The indicators used in the study, which are collected from well-known literary publications, are defined by weighted functionality functions.

The significance of the first resilience method lies in its graphical representation which helps decision makers take proper actions to improve their resilience. The method uses the structure of PEOPLES and it requires deterministic data for its implementation. The methodology has been partially applied to the city of San Francisco by considering one of the seven dimensions of PEOPLES. The indicators in the proposed methodology are modeled in a dynamic fashion. That is, the numeric value of the indicator changes with time. This allows reflecting the recovery rapidity of the indicator. Also, the interdependency among the variables at the same and different levels is considered through the proposed interdependency matrix technique. This method has been implemented in a user-friendly tool that allows the user to insert data on the different community indicators and get a resilience curve as a return.

The second method, on the other hand, does not need deterministic data for its implementation but rather descriptive knowledge, which can come in the form of a questionnaire. This method makes use of the fuzzy logic modeling to account for the uncertainty involved in the resilience parameters assessment.

Choosing between the two methods depends on the availability of data and on the level of complexity sought. The interdependency among the resilience variables in both methods has been considered by performing an interdependency analysis, which resulted in an importance factor allocated to each variable. The proposed methodologies move beyond the recoverability of a system to also incorporate hardness and adaptive capacity. For example, the hardness capacity is intrinsically reflected in the input parameter  $q_0$  (initial functionality), which can reach a value that is greater than the initial value. In addition, because of its inherent layer-based structure, the methodology permits performing diagnostic and sensitivity analysis to determine the critical indicators. This can be rather important in design problems.

While all previous works generally provide a single index to measure community resilience, the proposed methods indicate in detail whether the resilience deficiency is caused by the system's lack of robustness or by the slow restoration process. They identify where exactly resources should be spent to efficiently improve resilience. In the next two chapters, we will go in more details and we will tackle specific infrastructure systems (water and transportation networks). Different techniques (mostly simulation) will be presented to evaluate the resilience and functionality of the lifelines following a disaster event.

# Chapter 5

## 5. Resilience assessment of large-scale water distribution networks: a simulation approach

### 5.1 Introduction

The capacity of a community to resist an emergency situation is strictly related to the proper functioning of its own infrastructure systems. The resilience of a community can be determined by individually assessing the resilience of its infrastructure systems. This chapter continues the work done in the previous chapter by focusing on systems within a community. Here, we dive inside communities and tackle a specific infrastructure, namely Water Distribution Networks (WDN). Virtual cities can be a good tool to assess the resilience of infrastructures as well as their interdependencies; therefore, the use of a virtual city, namely IDEAL CITY, is adopted in this chapter. IDEAL CITY is a virtual city that consists of 890,000 inhabitants. The purpose of this virtual city is to integrate all critical infrastructures of a virtual community within the same model. Then, a seismic event will be applied to study several complex aspects, such as the interdependency among the infrastructures.

In this chapter, IDEAL CITY is used to evaluate the effect of a seismic event on the water distribution network. Multiple earthquake scenarios have been applied considering the time at which the earthquake happens (striking time). For each scenario, two resilience indexes have been evaluated. The first one is based on the number of people suffering outage of water supply and the second considers the drop in the total water available.

### 5.2 The resilience of Water Network Distribution

Currently, a standard procedure to evaluate the resilience of water networks is missing in the literature. High serviceability of a water distribution network implies a large water supply with acceptable water pressure. Generally, the water supply depends on the customer request

and on the water pressure in the pipes. The damage induced by an earthquake causes a reduction of the pressure, and this consequently causes a reduction in the water supply.

In this chapter, a 24-hour demand pattern is defined according to the customer request in the virtual city. Two serviceability functions  $F_1(t)$  and  $F_2(t)$  are presented. The first is related to the number of people without water while the second measures the ratio between water supply and water demand. The mathematical equation of the first performance measure is:

$$F_1(t) = 1 - \frac{\sum_i n_e^i(t)}{n_{tot}} \quad \text{for } i = 1, \dots, N \quad (5.1)$$

where  $n_e^i(t)$  is the number of people connected to node  $i$  (i.e., who get their demand from the water supply provided by node  $i$ ) suffering insufficient pressure;  $n_{tot}$  is the total number of people within the water distribution network;  $i$  is the generic node,  $N$  is the total number of nodes. The number of people without water at given node following a disaster event is assumed to be proportional to the water supply reduction at the same node:

$$n_e^i(t) = n_i \frac{w_{Lost}^i(t)}{w_i(t)} \quad (5.2)$$

where  $n_i$  is the total number of people connected to the node  $i$ ;  $w_{Lost}^i$  is the volume of water lost at node  $i$ ;  $w_i$  is the water demand at node  $i$  under normal operating conditions. The water loss and water demand at a given time step following a disaster event are computed as follows:

$$w_{Lost}^i(t) = \int_0^t [Q_{demand}(t) - Q_i(t)] dt \quad \text{for } i = 1, \dots, N \quad (5.3)$$

$$w_i(t) = \int_0^t Q_{demand}(t) dt \quad (5.4)$$

where  $Q_{demand}$  is the water demand at node  $i$ ,  $Q_i$  is the available water flow (water supply) at node  $i$ ,  $t$  is a generic time step. The second performance function  $F_2(t)$  is related to the water demand and is given by the following formula:

$$F_2(t) = \frac{\sum_i Q_i(t)}{Q_{Demand,tot}} \quad (5.5)$$

where  $Q_{demand,tot}$  is the total water demand in the city. The recovery time  $T_R$  is assumed to last 24 hours (Figure 5.1). The Control Time  $T_c$  is considered equal to  $T_R$  in an attempt to get a normalized value of resilience.

For each serviceability function, a resilience index is computed as the area below the function for the defined control time ([Cimellaro et al. 2016c](#)):

$$R = \int_{t_1}^{t_2} \frac{F(t)}{T_c} dt \quad (5.6)$$

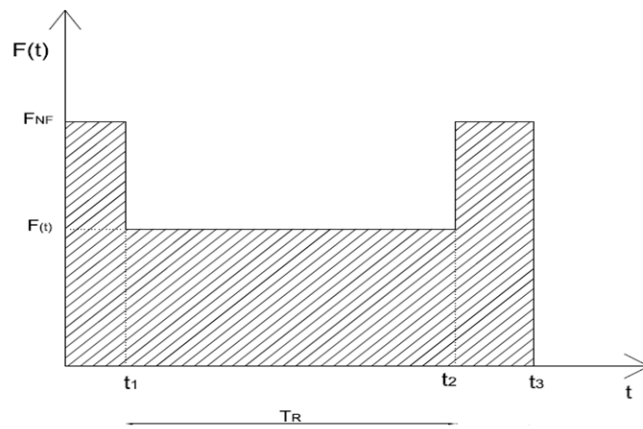


**Figure 5.1** Functionality of Water Distribution Network, adapted from ([Cimellaro et al. 2016c](#)).

### 5.3 IDEAL CITY: Virtual City for Resilience Analyses

Virtual city applications allow performing resilience analyses as the information and data on the infrastructure are readily available. Currently, IDEAL CITY (Figure 5.2) is a virtual city containing 890000 residents. The area is about 120 km<sup>2</sup> divided into 10 districts, inspired by the real subdivision of the city of Turin, Italy. The inhabitants have been assigned to the districts in a way to create different population densities. Data and information about the city infrastructure are provided as separate layers in a GIS environment using “ArcGIS” software ([ESRI 2011](#)).



**Figure 5.2** IDEAL CITY: 3D representation using “ArcGIS” software.

## 5.4 Model Description, Assumption and Calibration

The water network analyzed in this study is based on the urban water network of the city of Turin. Elevations of the grounds have been obtained from Google Maps ([Google](#)). Several assumptions had to be made to build the water network model. The geometry of the water network is assumed to overlap with the transportation network of the city as it was not possible to get the exact map of the water network due to security reasons. The water network model (Figure 5.3) has been built using the Epanet-Matlab toolkit, which allows controlling Epanet 2.0 using MATLAB ([Eliades](#) ; [MathWorks](#) ; [USEPA](#)).

The EPANET model comprises 19654 ductile iron pipes (1,285,007 m of total length) with a Darcy-Weisbach roughness coefficient  $\varepsilon$  equal to 0.26 mm, 14996 nodes, 9 valves, 38 pumps, 19 reservoirs, and 26 tanks. Nodes are situated 1.2 m below the ground surface. Ground elevations range between 207.76m and 340.68 m above sea level. Water sources are aquifer (82%) and rivers/surface water (18%) with an average total daily demand of 353.38Ml/day.

The water demand at each node (junction) depends on the number of people who are served by that node. In fact, in the model, the nodes are connected to the households and not to the population. Therefore, it is first necessary to find the population density per each unit volume of household, which also depends on the district as the population density is not the same among all districts. This is done using the following formula:

$$\rho_j = \frac{P_j}{V_j} \left[ \frac{\text{people}}{m^3} \right] \quad (5.7)$$

where  $P_j$  is the household population density in district  $j$  (number of people per a unit volume of a household located in district  $j$ ),  $P_{e_j}$  is the number of people in district  $j$ ,  $V_j$  is the total volume of the households located in district  $j$ .

The water network is considered as a mesh model formed by the pipes' interconnections. Each mesh element (closed shaped) is assigned a water demand based on the total volume of household located inside:

$$q_{j,w} = \rho_j \cdot \delta \cdot V_w \quad (5.8)$$

where  $q_{j,w}$  is the water demand in a mesh element  $w$  in a district  $j$ ,  $\delta$  is the city water supply per inhabitant (equal to 315 l/capita/days) ([Piemonte](#)),  $V_w$  is the volume of the households within mesh element  $w$ .

The total water demand per mesh element  $q_i$  is distributed equally among the adjoining nodes (Figure 5.4 (a)). In other words, the water demand for each node is the sum of the demand contribution of the adjoining mesh elements (Figure 5.4 (b)):

$$q_i = \sum_{w=1}^{n_{w,i}} \frac{q_{w,j}}{n_{i,w}} \quad (5.9)$$

where  $q_i$  is the water demand at node  $i$ ,  $q_{w,j}$  if the water demand of the mesh element  $w$  which is located in district  $j$ ,  $n_{w,i}$  is the number of mesh elements adjoining node  $i$ ,  $n_{i,w}$  is the number of the nodes adjoining mesh  $w$ .



**Figure 5.3** Global view of the water network.



**Figure 5.4** (a) Water demand  $q_{j,w}$  within a mesh element  $w$ , (b) Water demand at a node  $i$ .

The calibration of a WDN of such size brings on several difficulties. It is a fundamental issue to ensure an accurate and realistic simulation for both the flow velocity and pressure. The pipes diameters and the positions of the valves, pumps, reservoirs, and tanks have been determined with the following constraints in mind (Figure 5.5):

$$0.5m / s \leq Velocity \leq 2m / s \quad (5.10)$$

$$40m \leq Pressure \leq 80m \quad (5.11)$$

The calibration procedure adopted in this chapter is iterative. Future work will be oriented to apply a systematic parametric calibration for large scale water networks ([Ormsbee and Lingireddy 1997](#); [Afshar and Kazemi 2012](#); [Parehkar et al. 2015](#)).

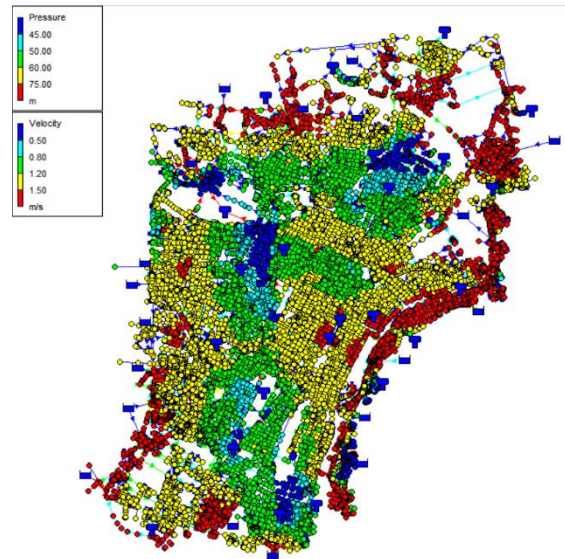


**Figure 5.5** Calibrated water pressure and velocity in the WDN

## 5.5 Seismic Hazard and Earthquake Damage of Pipes

The seismic hazard is evaluated according to the Probabilistic Seismic Hazard Analysis (PSHA) ([Protezionecivile](#) ; [Baker 2013](#)). In the context of this work, the hazard is defined as the occurrence probability of a seismic event of specific characteristics within a certain period of time. The corresponding ground motion (peak ground acceleration PGA) is said to have a P probability of exceedance in T years, where T is the return period ([Protezionecivile](#)). In this work, the return period is 2475 years with a probability of exceedance of 2% in 50 years.

According to the attenuation law by Sabetta and Pugliese ([Sabetta and Pugliese 1996](#)), the *PGV* value is influenced by the soil local condition and it is a function of *M* and *R*:

$$\text{Log } PGV = a + bM + c \text{Log} \sqrt{R^2 + h^2} + e_1 S_1 + e_2 S_2 \pm \sigma \quad (5.12)$$

where *a*, *b*, *e*<sub>1</sub>, *e*<sub>2</sub>, are parameters determined through non-linear regression, *h* is a function of the epicenter depth,  $\sigma$  is the standard deviation of log (PGV), *S*<sub>1</sub> and *S*<sub>2</sub> depends on the geological soil conditions, *M* and *R* are respectively the magnitude and the epicenter distance of the earthquake, respectively. In the case study, the PVG value is 35.84cm/s, assumed constant across the entire region of interest.

## 5.6 Vulnerability Analysis of Water Pipes

The reliability of a water network is strictly connected to the concept of vulnerability of its elements. Herein, the focus is given to the pipes, the most important components in a pipe

network because it is the most challenging part to inspect and replace. The seismic vulnerability of the buried pipelines introduced in the American Lifelines Alliance (ALA 2001) (Eidinger 2001) is adopted in this work. Vulnerability functions are entirely empirical and are based on reported damage from historical earthquakes. Damage is expressed in terms of pipe repair rate  $RR$ , defined as the number of repairs per 1,000 m of pipe length exposed to a certain level of seismic intensity.

$$RR = 0.00187 \cdot K_I \cdot PGV \quad (5.13)$$

where  $K_I$  is a coefficient that depends on the pipe material, pipe diameter, joint type, and soil condition. Once the repair rate is known, the failure probability  $P_{f,j}$  of a pipeline is evaluated through the Poisson exponential probability distribution, as follows:

$$P_{f,j} = 1 - e^{-RR \cdot L} \quad (5.14)$$

where  $L$  is the length of pipe and  $e^{-RR \cdot L}$  is the probability of zero breaks along the pipe. In this chapter, three different  $K_I$ 's are considered in order to investigate the influence of the pipe material on the failure probability  $P_{f,j}$ :  $K_I = [0.5; 0.8; 1]$ . The seismic wave propagation induces strains to the pipes due to the soil-pipe interaction: strains could produce damage if the pipe strength is exceeded. When pipe damage occurs, the pipe is assumed to break in the middle.

Pipe damage is modeled with EPANET 2.0 as follows: the pipe is divided into two equal parts and two reservoirs are added at their endpoints in order to simulate the water leakage through the crack (Figure 5.6). The reservoirs have a total head equal to the elevation of the middle point of the pipe (assuming that the pipe breaks in the middle). A check valve is inserted so that water only flows towards the reservoirs.

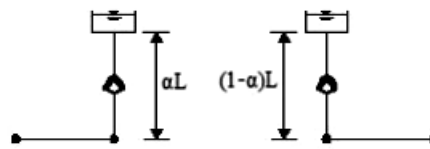


**Figure 5.6** Pipe break simulation in EPANET 2.0.

A demand-driven analysis (DDA) is carried out in a standard manner using the software EPANET. The problem with DDA is that it fixes the demands at the nodes. However, in the case of pipe damage, the pressure at some nodes drops, and this affects the water supply. Thus, a pressure-driven analysis PDA is needed to account for the dependence of water supply on pressure. To do so, a standard DDA is first performed. Then, nodes with pressure below the value required to satisfy the demand are converted in Emitter nodes. An Emitter is a node whose demand is proportional to a fractional power of the pressure according to the following equation:

$$Q_i = C_i (H_i - z_i)^\alpha = C_i \cdot p_i^\alpha \quad (5.15)$$

where  $Q_i$  is the actual demand flow;  $C_i$  is the emitter coefficient;  $H_i$  is the actual total head of the  $i_{th}$  node;  $z_i$  is the elevation of the  $i_{th}$  node;  $p_i$  is the actual pressure of the node;  $\alpha$  is the emitter exponent (0.5 if no other information is available). The emitter coefficient is evaluated as:

$$C_i = \frac{Q_{demand}}{(H_{r,i} - z_i)^\alpha} = \frac{Q_{demand}}{p_{r,i}^\alpha} \quad (5.16)$$

where  $Q_{demand}$  is the demand flow;  $H_{r,i}$  and  $p_{r,i}$  are the total head and the pressure required to satisfy  $Q_{demand}$ , respectively. In this work, 20 m of water column is considered as the minimum value to satisfy the demand at any node. The model is run again with the emitters inserted. The PDA procedure is applied during the breakage. Three cases can occur:

- If  $Q_i \leq 0$ , the actual demand flow at the node is set to zero,
- If  $0 \leq Q_i \leq Q_{demand}$ , the actual demand flow is set equal to  $Q_i$ ;
- If  $Q_i \geq Q_{demand}$ , the actual demand flow is set equal to  $Q_{demand}$ .

## 5.7 Definition of the event scenarios

Resilience is a dynamic quantity characterized by a lack of certainty. Uncertainties are crucial both for risk management and resilience analysis ([Bozorgnia and Bertero 2004](#)). To study the uncertainty, a Monte Carlo approach has been applied to generate a large number of simulations using a Matlab code provided in ([Fragiadakis et al. 2012](#)). The code requires pipes diameters, pipes lengths, start and end nodes, and pipes failure probabilities. In addition, an importance factor has been assigned to each pipeline: “2” is assigned to main pipelines, “1.5” to the pipes within the districts, and “1” to the pipes connecting the districts. The number of scenarios  $N_S$  is set to 5000, which yielded a stable distribution of the results (Figure 5.7).

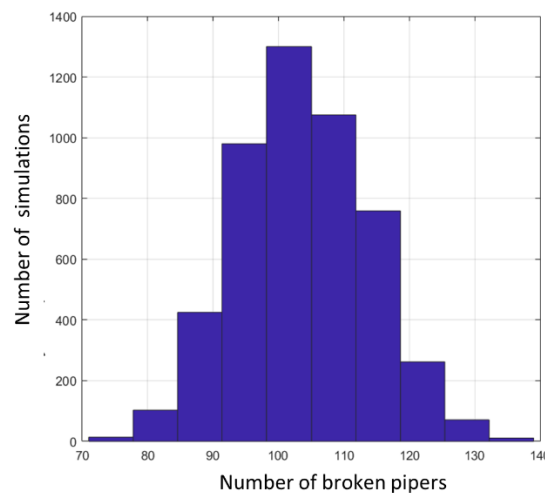


**Figure 5.7** Distribution of the simulation results. ( $N_S = 5000$ ,  $K_1 = 0.5$ ).

## 5.8 Numerical results

Serviceability functions  $F_1(t)$  and  $F_2(t)$  are evaluated for the 5000 simulation scenarios and for three values of  $K_I$ . The simulations considered a random occurrence time of the earthquake. For each of them, two resilience indexes have been computed using Eq. (5.6). At each earthquake occurrence time, the mean value of the resilience indexes has been computed with its standard deviation (Figure 5.8). Pipes with ductile material (low  $K_I$ ) show a more resilient behavior than pipes with fragile material (high low  $K_I$ ). The highest resilience indexes correspond to  $K_I=0.5$ .

It is clear that the resilience indicators are not very sensitive to the time at which the earthquake occurs. In addition, the value  $R$  follows the water demand pattern: it is lower when damage occurs during high water demand periods. Moreover, from Figure 5.8, the resilience index  $R_Q$  (referring to the variation of water supply) is more sensitive than the index  $R$  (referring to people suffering from water outage).

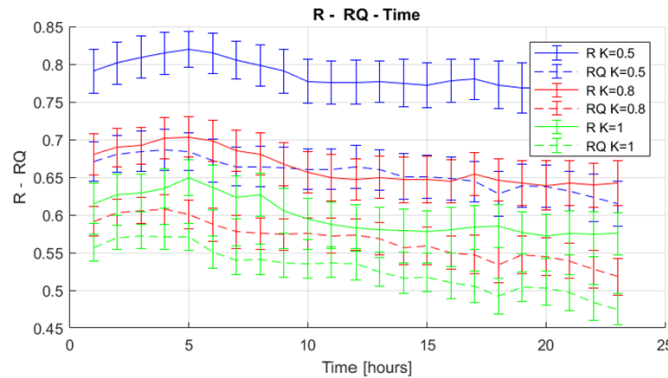


**Figure 5.8** Resilience indexes  $R$  and  $R_Q$  for three  $K_I$  values (pipe material).

## 5.9 Concluding remarks

Two resilience indexes to measure the performance of a water distribution network after an earthquake are proposed. The methodology presented here considers the pipes as the only element of the WDN that can be affected by an earthquake. The methodology has been applied to a virtual city, namely IDEAL CITY. Two serviceability functions have been identified:  $F_1(t)$  is related to the number of users suffering water outage and  $F_2(t)$  is related to the reduction in the total water supply. The resilience indexes are evaluated as the area under the performance curves. The resilience indexes showed different values but they both followed the daily water demand trend.

The introduced methodology can serve as a decision-making tool for water distribution systems in communities. Future work will aim at generalizing the methodology. Since water demand pattern, time control, and recovery time affect the evaluation of resilience, future work will focus on a parametric study to understand the effect of each parameter on the resilience evaluation. The methodology will also be generalized to include the possibility of changing the seismic input and the geometry of the network. Next chapter will deal with another

infrastructure system in a community (Transportation network). The functionality of large-scale transportation networks following a disaster event will be studied. Different coding algorithms will be proposed to simulate and analyze transportation networks.

# Chapter 6

## 6. Resilience assessment lifeline networks: application to a large-scale transportation system

### 6.1 Introduction

Infrastructure systems are crucial for the development of communities as they provide essential services to the population. To improve the resilience of such systems, their intrinsic properties need to be understood and their resilience state needs to be identified. This chapter tackles another important infrastructure system in a community, namely the transportation network. Transportation networks need to provide continuous service for communities, and this necessitates a good understanding of their resilience and reliability states. For instance, understanding how the topology of the network changes under disruptive events can be fundamental in the decision-making process. It could also speed up rescue operations and help in evaluating cascading effects on other interdependent networks. This chapter explores mostly the reliability of large-scale networks. Reliability is a very broad concept and its application is extended to all engineering fields. In general terms, network reliability can be defined as the probability of connecting the nodes of the network ([Chang and Li 2014](#)). Other authors consider reliability as the quality of the transportation system in terms of optimal travel time; i.e. the probability that a trip between two nodes takes less than a certain time ([Immers et al. 2002](#)). Another widely used concept is the capacity reliability, which is the probability that the network capacity can accommodate a certain traffic volume at a required level of service ([Chootinan et al. 2005](#); [Chen et al. 2013](#); [Niu et al. 2017](#)). Reliability has also been studied under specific situations, such as the emergency response, using ideas of both travel time and level of service ([Edrissi et al. 2015](#)). Looking at graph theory, [Guidotti et al. \(2017\)](#) have used the connectivity measures as a tool to determine whether a network is reliable or not.

In this work, the reliability of the transportation network of a large-scale virtual city is evaluated. The reliability definition adopted in ([Gertsbakh and Shpungin 2008](#); [Gertsbakh and Shpungin 2009](#); [Gertsbakh and Shpungin 2012](#)) is considered in this study. According to the researchers, reliability is related to the probability that some nodes, called terminals, remain connected. Thus, the system fails when the terminals are no more connected. The terminal nodes are strategic nodes with pre-defined survival probabilities. Knowing these probabilities helps greatly in improving the network ([Peeta et al. 2010](#)). However, it can be rather difficult to identify those probabilities. For this reason, a different failure criterion has been selected in this work. Another performance parameter, the Birnbaum Importance Measure (BIM), is considered in this chapter to study the behavior of the analyzed network. This parameter represents the importance of the network's components ([Gertsbakh and Shpungin 2012](#)). Components with a high BIM index are vulnerable components. Determining the reliability and BIM indexes is relatively simple for small networks, but when applied to a large-scale network, the computational effort becomes unaffordable. To overcome the computational problems, two coding algorithms are presented in the chapter.

This study helps increase the resilience of communities. Identifying the vulnerable components in a network makes infrastructure operators focus on them, and thus improve the overall resilience of the infrastructure in an efficient manner.

## 6.2 Network reliability and components' importance

### 6.2.1 Destruction spectrum

The Destruction spectrum, or simply D-spectrum, is a representation of a network's structure and its failure definition ([Gertsbakh and Shpungin 2009](#)). The system in Figure 6.1 is used to introduce the concept of the D-spectrum. The nodes in the system are assumed reliable while the links are unreliable; that is, only links are subject to failure. In this example, the system's failure is defined as the loss in connectivity between the terminal nodes *a* and *c*.

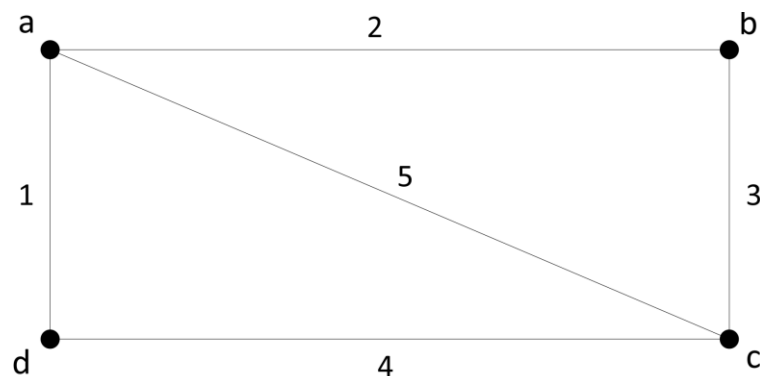


**Figure 6.1:** A simple network with two critical nodes.

The system's failure can be reached through different sequences of failing components. For instance, if the links (1; 2; 5; 3; 4) fail, the two nodes  $a$  and  $c$  become disconnected, and thus the system fails. Another permutation leading to the same result can be (3; 5; 4; 1; 2). The failing component at which the system becomes down is called the anchor of the permutation. In the two permutations above, links 5 and 4 are the anchors, respectively. The total number of failure permutations in a system is  $k!$ , where  $k$  is the number of unreliable elements. After identifying all failure permutations, the D-spectrum set of the network is computed as follows:

$$D = \left\{ d_1 = \frac{x_1}{k!}, d_2 = \frac{x_2}{k!}, \dots, d_k = \frac{x_k}{k!} \right\} \quad (6.1)$$

where  $d_i$  is the  $i^{\text{th}}$  component of the spectrum,  $x_i$  is the total number of permutations whose anchor's order is  $i$ ,  $k$  is the total number of unreliable components. It is obvious from the equation above that the summation of all elements is 1 ( $\sum_{i=1}^k d_i = 1$ ).

It is worth to note that the failure probability of each link is not considered in the D-spectrum. One may simply consider a random removal of the links in the sense that all links have the same failure probability. Otherwise, a strategic link removal can be considered but it requires additional analyses. For instance, in transportation networks, the removal of a link (road) may be linked to the level of damage of the adjacent buildings. This requires fragility analysis to determine the level of damage each building is subject to.

## 6.2.2 Network reliability

Generally, a network can be considered reliable when it offers a certain level of service or performance, even during emergency situations. Most of the reliability definitions that can be found in the literature deal with the concept of reliability in probabilistic terms. According to the definition of [Gertsbakh and Shpungin \(2008\)](#), each element of the network (nodes and links) is given a probability  $p$  of being available and a probability  $q=1-p$  of being unavailable. These probabilities contribute to quantifying the network's reliability. The formulation used to calculate the reliability index  $R(N)$  is given in Eq.(6.2). The equation is valid when all unreliable components have the same failure probability.

$$R(N) = 1 - \sum_{i=1}^k y_i \frac{k! q^i p^{k-1}}{i!(k-i)!} \quad (6.2)$$

where  $y_i$  is the cumulative D-spectrum, given by the following equation:

$$y_i = \sum_{b=1}^i d_b \quad (6.3)$$

### 6.2.3 Components' importance

The Birnbaum Importance Measure (BIM) is a parameter that describes the importance of the network's components. The vulnerability of the components is what determines their corresponding value of BIM. This measure can be a tool to identify the critical components of a network in order to strengthen them. The following equation is used to compute the BIM index of a single component  $j$ :

$$BIM_j = \sum_{i=1}^k \frac{k!(z_{i,j}q^{i-1}p^{k-i} - (y_i - z_{i,j})q^i p^{k-i-1})}{i!(k-i)!} \quad (6.4)$$

where  $z_{i,j} = Z_{i,j} / k!$ , in which  $Z_{i,j}$  is the number of permutations satisfying two conditions: (a) if the first  $i$  elements of the network are down, then the network is down; (b) element  $j$  is among the first  $i$  elements of the permutation. By doing some manipulation, the expression in Eq.(6.4) can be written in a different form, shown in Eq.(6.5). It is worth to note that both reliability and BIM indexes share a common factor in their equations, and this provides a unique characteristic to compute both indexes in a single operation.

$$BIM_j = \sum_{i=1}^k \frac{k!q^i p^{k-1}}{i!(k-i)!} \cdot \left( \frac{z_{i,j}}{q} - \frac{y_i - z_{i,j}}{p} \right) \quad (6.5)$$

## 6.3 Method: application to large scale networks

Theoretical reliability analyses are not always applicable to large problems. For instance, the applications of the above-mentioned equations are limited to small networks with a defined number of components. This is due to the presence of *factorial* in the denominator of the spectrum set (Eq.(6.1)). The same problem appears when computing the reliability index  $R$ , although we know in advance that this is a number between 0 and 1, regardless of the network's size. In this section, we present a computational strategy to apply the D-spectrum to large scale networks and then compute their reliability index and BIM-spectra.

### 6.3.1 D-spectrum for large networks: A Monte Carlo approach

We propose the use of a Monte Carlo approach to generate the failure permutations needed to compute the D-spectrum. Hereafter, the algorithm of the Monte Carlo simulation is presented.

### 6.3.1.1 Algorithm 1: *D-spectrum*

- 1) Define a failure criterion for the network (e.g. number of failed components, disconnected nodes, etc.).
- 2) Set the permutation number to  $n=1$ .
- 3) Choose a random number from 1 to  $k$  and store it (i.e. the chosen number represents a failed component).
- 4) Check if the network's failure criterion is met:
  - a) if yes, stop and store the permutation and go to step 5;
  - b) otherwise, choose another number from 1 to  $k$  excluding the numbers chosen in previous steps and then go again to 4.
- 5) Set  $n=n+1$ .
- 6) Repeat the steps 3-5  $M$  times to generate  $M$  permutations.
- 7) Categorize the permutations according to their anchor's value (i.e., the anchor value coincides with the vector's length of the permutation).
- 8) Compute the  $D$ -spectrum using Eq.(6.1).

In case of strategic removal, the unreliable network's components should be linked with certain removal probabilities or lifetime distributions. In this case, step 3 is adjusted so that the removal process is not random.

## 6.3.2 Reliability and BIM indexes for large scale networks: Incremental calculation

Practically, computing the reliability and BIM indexes is not possible for moderate to large networks. The reason is that both numerator and denominator in the second term of the reliability index (Eq.(6.2)) and in the first term of the BIM index (Eq.(6.5)) are too large. However, it is known in advance that the reliability index is a number that ranges between 0 and 1 regardless of the network's size, and this property represents the key solution. In this section, we propose *incremental computation* to solve the numerical problem. The proposed method can handle large numerators and denominators given that their division is a real number that is not too large. The key idea is that neither the numerator nor the denominator is allowed to exceed a certain number and yield to infinity. To go more deeply, let  $M$  denote the common term of the reliability and BIM equations, which represents the problematic part (Eq.(6.6)). First, all the parameters in the  $M$  equation ( $K!$ ;  $q^i$ ;  $p^{k-i}$ ;  $i!$ ;  $(k-i)!$ ) are classified according to the criterion whether they increase or reduce  $M$ . The calculation starts by injecting the parameters that increase  $M$ , and whenever  $M$  reaches a defined upper limit, the terms that decrease  $M$  are injected until  $M$  reaches a lower limit. This is done repeatedly until all terms are exhausted. The calculation is done for a single  $i$  and repeated for  $i=1, 2, 3, \dots, k$ . More details about the numerical method are presented in Algorithm 2.

$$M_i = \frac{k!q^i p^{k-i}}{i!(k-i)!} \quad (6.6)$$

### 6.3.2.1 Algorithm 2: Incremental computation

- 1) Define upper and lower thresholds (e.g.,  $10^{10}$  and  $10^{-10}$ ).
- 2) Classify the parameters in  $M$  in two categories: Category A includes the parameters that contribute to increasing  $M$ , and Category B for the parameters that contribute to decreasing  $M$ . In our case, there is only one parameter that falls under category A ( $k!$ ), while the other parameters fall under B ( $q^i, p^{k-i}; i!; (k-i)!$ ).
- 3) Each of the parameters is written in an expanded form, as follows:
  - $k!=[1;2;3;\dots;k]$ ;
  - $q^i=[q,q,q,\dots,q]$  ( $i$  times);
  - $p^{k-i}=[p;p;p,\dots;p]$  ( $(k-1)$  times);
  - $i!=[1;2;3;\dots;i]$ ;
  - $(k-i)!=[1;2;3;\dots;k-1]$ .
- 4) Set  $i = 1$  and start calculating  $M$  progressively by injecting the parameters above. One can start multiplying the numbers inside the parameter  $k!$  until  $M$  reaches the upper threshold (e.g.  $1 \times 2 \times 3 \times \dots \times n > 10^{10}$ ). The used numbers cannot be used again, and they must be removed from the set once used. Whenever  $M$  reaches the upper thresholds, the sets of the parameters in category B are injected until  $M$  reaches the lower threshold. The order of the terms is not important, so the user can exploit the terms in any order until they are exhausted. The terms should be used in the same way they are in  $M$ , so multiplication terms ( $k!; q^i, p^{k-i}$ ) are multiplied by  $M$  while division terms ( $i!; (k-i)!$ ) are used to divide  $M$ .
- 5) Repeat Step 4 for  $i=1, 2, 3, \dots, k$ .
- 6) Find  $Z_{ij}$  using the permutations obtained from *Algorithm 1* and following the criteria introduced in Section 2.3.
- 7) Compute the reliability index and BIM index as follows:

$$R = 1 - \sum_{i=1}^k y_i \cdot M_i \quad (6.7)$$

$$BIM_j = \sum_{i=1}^k M_i \cdot \left( \frac{z_{i,j}}{q} - \frac{y_i - z_{i,j}}{p} \right) \quad (6.8)$$



critical nodes are disconnected, the network becomes down. This criterion is applicable to small scale networks. When dealing with large networks, a huge computational effort would be needed to identify whether the nodes are connected or not. In this work, a simpler network failure criterion is adopted. The network is considered unavailable when at least 5% of the nodes are isolated (not connected to any link).

### 6.4.3 Results

The methodology introduced in Section 3 has been applied to the case study. Due to the large size of the analyzed network, the results are not shown using vectors or matrices, but rather using graphs.

First, *Algorithm 1* has been used to generate the failure permutations of the links. The number of permutations considered in this case study is 3.5 million. The generated permutations have been subsequently used in the calculation of the D-spectrum. The result of the D-spectrum is shown in Figure 6.3. It can be clearly seen that there are only a few non-zero elements in the distribution, and they are all gathered in a small range. The distribution of the D-spectrum is a perfectly normal distribution. The location of the distribution's peak depends greatly on the chosen failure criterion of the network and on the number of components forming the network. More study will be dedicated to knowing the reason for having a normal distribution and to identify the effect of the failure criterion and number of components on the position of the distribution's peak. Moreover, looking at the definition of the D-spectrum, the sum of all its elements is 1. This is verified in Figure 6.4, which shows the distribution of the cumulative D-spectrum.

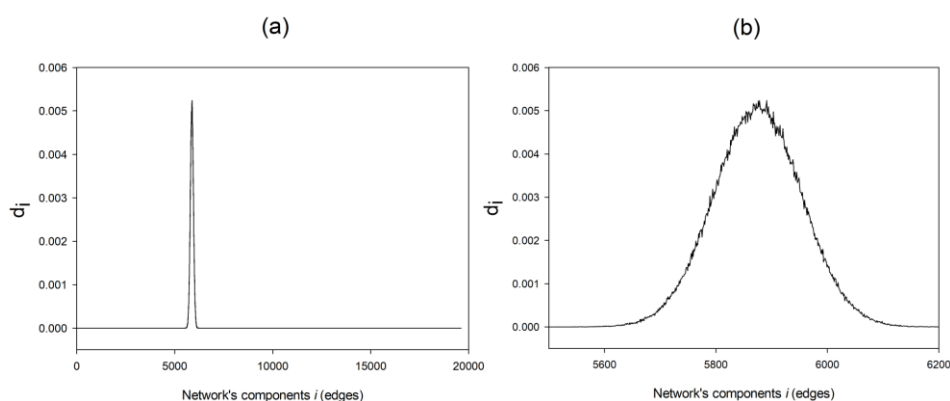


**Figure 6.3:** (a) The D-spectrum of all components of the case study network; (b) a zoomed view at the distribution peak.

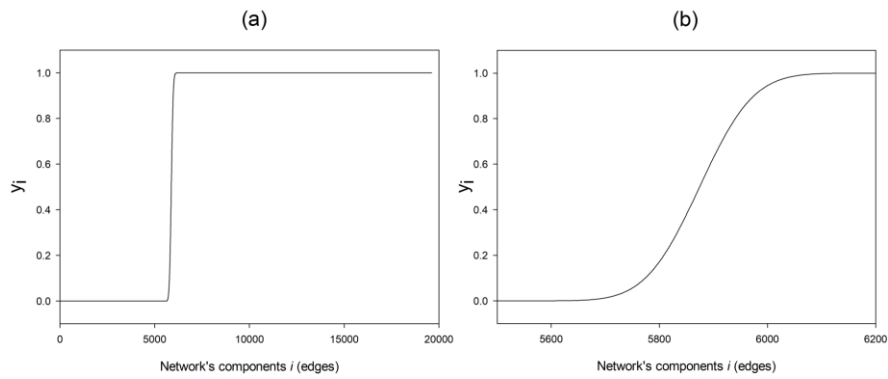


**Figure 6.4:** (a) The cumulative D-spectrum of all components the case study network; (b) a zoomed view at the transitional part.

Following the D-spectrum, the BIM index of the network's components and the network reliability index  $R$  have been evaluated using Algorithm 2. The BIM index results of the networks' components have been normalized with respect to the maximum value. Figure 6.5 shows the BIM results of the first 100 components. The BIM indexes of the other components range between the upper the lower bounds, 1 and 0.98 respectively. This implies that the variance in the results is very small. In fact, the importance index of the link is ruled by the network configuration and the failure probability of the link. In our network, we considered an equal failure probability for the links, which was represented by the random removal process. The small difference in the importance of the links was only due to the network's configuration.

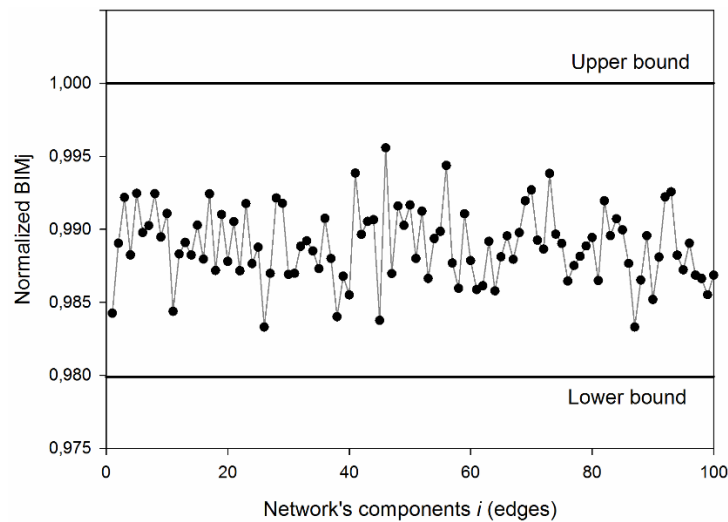


**Figure 6.5:** The BIM spectra of the network's components.

The reliability of the network was computed using Eq. (6.7). It is worth to mention that the network reliability depends mainly on the following factors: (a) the network size (number of components in the network  $k$ ); (b) the component's failure probability  $q$ ; (c) the network's failure criterion (embedded in the cumulative D-spectrum term  $y$ ); (d) and the network's

topography (embedded in the cumulative D-spectrum term  $y$ ). The reliability of the analyzed network was found to be 46%. However, this number considers equal failure probabilities for all network components. This is rarely the case because usually the effect of disruptive events on a network system is not spatially uniform.

## 6.5 Concluding remarks

This chapter presented a methodology to evaluate multiple performance indexes for large scale networks. In the literature, several methods to evaluate networks reliability and resilience can be found. The application of such methods to large scale networks is not feasible due to the computational complexity. In this chapter, the case of large-scale networks is tackled. The case study considered in this work is the transportation network of a virtual city. First, the road map of the city is transformed into an undirected graph, which consists of 15012 nodes and 19614 links. Random removal of the links is applied as a failure mechanism until the network's failure point is reached. The network reliability is then calculated using the Destruction Spectrum (D-spectrum) approach assuming the same failure probability for all links. A Monte Carlo approach is used to generate failure permutations which are necessary for evaluating the D-spectrum. In addition, the network's links have been ranked from the most to the least important by applying the Birnbaum Importance Measure (BIM). To overcome the computational obstacles, two algorithms have been presented and discussed.

The results obtained in this study are used to identify the vulnerable components of the network. The vulnerable components are the ones that should be focused on to improve the overall resilience of the infrastructure. The analysis concept adopted in this study is applicable to all network-based infrastructure systems such as water, gas, transportation, etc. Future work is geared towards replicating the analysis methodology to the case of strategic link removal. The link removal mechanism will be linked to the buildings' damage assuming a certain destructive event.

While still considering resilience at the infrastructure level, next chapter will consider another aspect of resilience, namely restoration time. Restoration fragility curves showing the time needed by different infrastructure systems to recover from a disaster event of a certain magnitude will be presented.

# Chapter 7

## 7. Downtime assessment of infrastructure systems following earthquakes

*Part of the work described in this chapter has been previously published:*

Kammouh, O., Cimellaro, G. P., and Mahin, S. A. (2018). "Downtime estimation and analysis of lifelines after an earthquake." *Engineering Structures*, 173, 393-403.  
<https://doi.org/10.1016/j.engstruct.2018.06.093>.

### 7.1 Introduction

In the seismic resilience, downtime is “the time necessary to plan, finance, and complete repair facilities damaged by earthquakes or other disasters and is composed by rational and irrational components” ([Comerio 2005](#)). Generally, several factors are involved in the downtime estimation, such as the characteristics of the exposed structure, the earthquake intensity, and the amount of human force that is assigned to recover the damaged structure. With these factors, the process of estimating the downtime becomes harder. Therefore, it is crucial to have a simple model for estimating the downtime of infrastructures ([Kammouh and Cimellaro 2017](#)).

Resilience is composed of two main components, damage incurred after the disastrous event and the restoration time of the system hit by the event. The previous two chapters focused on assessing the damage incurred to infrastructure systems following an earthquake event. This chapter is complementary to the previous chapters as it analyzes the missing component of resilience (Restoration time). The aim of this study is to develop a probabilistic model to evaluate the downtime of lifelines following a seismic event. Four different types of lifelines are analyzed in this work, namely power, water, gas, and telecommunication. First, a large database has been collected from a wide range of literature. The database contains real restoration data for many seismic events that occurred in the last century. Probabilistic restoration functions have been constructed using the gamma distribution, which has been selected because of its good fit to the empirical data.

For each of the four lifelines, a group of fragility curves has been developed based on several factors, such as the earthquake magnitude, development level of the affected country, and countries with enough data. The restoration curves have been presented in terms of probability of recovery and time; the longer is the time after the disaster, the higher is the probability of the infrastructure to recover its functionality.

## 7.2 Downtime data analysis and interpretation

Figure 7.1 shows the location of all 32 earthquakes considered in this study. Approximately, 90% of the earthquakes analyzed in this research took place along the Ring of Fire of the Pacific Ocean, a string of volcanoes and seismic activity sites. The other 10% of the earthquakes took place along the Alpide belt, a line that passes through the Mediterranean region, Turkey, Iran, and northern India. The database was gathered from renowned authors and official institutions and belongs to earthquakes that have occurred after the 60s because there was little or no reliable information about the damage caused by earlier earthquakes.



**Figure 7.1** Location of the earthquakes considered in the study

Table 7.1 lists all the earthquakes considered in this work along with the year in which they occurred, the country they hit, and their intensity in terms of Richter magnitude. Several other damaging earthquakes that occurred around the same period have also been collected but not included in this study because no engineering damage reports could be obtained for those events. Nevertheless, the events included in this study are sufficient to provide useful illustrations for the recovery behavior of the examined lifelines.

**Table 7.1** Summary of the analyzed earthquakes

Earthquake	Year	Country	Magnitude	Reference
<i>Loma Prieta</i>	1989	USA	6.9	( <a href="#">Schiff 1998</a> )
<i>Northridge</i>	1994	USA	6.7	( <a href="#">Schiff 1995</a> )
<i>Kobe</i>	1995	Japan	6.9	( <a href="#">Kuraoka and Rainer 1996</a> )
<i>Niigata</i>	2004	Japan	6.6	( <a href="#">Dynes et al. 1964</a> )
<i>Maule</i>	2010	Chile	8.8	( <a href="#">Evans and McGhie 2011</a> )
<i>Darfield</i>	2010	New Zealand	7.1	( <a href="#">Knight et al. 2012</a> )

<i>Christchurch</i>	2011	New Zealand	6.3	( <a href="#">Giovinazzi et al. 2011</a> )
<i>Napa</i>	2014	USA	6	( <a href="#">Brocher et al. 2015</a> )
<i>Michoacán</i>	1985	Mexico	8.1	( <a href="#">O'Rourke 1996</a> )
<i>Off-Miyagi</i>	1978	Japan	7.4	( <a href="#">Katayama 1980</a> )
<i>San Fernando</i>	1971	USA	6.6	( <a href="#">Jennings 1971</a> )
<i>The Oregon Resilience Plan</i>	2013	USA	9	( <a href="#">Recovery 2013</a> )
<i>LA Shakeout Scenario</i>	2011	USA	7.8	( <a href="#">Jones et al. 2008</a> )
<i>Tohoku</i>	2011	Japan	9	( <a href="#">Nojima 2012</a> )
<i>Niigata</i>	1964	Japan	7.6	( <a href="#">Scawthorn et al. 2006c</a> )
<i>Illapel</i>	2015	Chile	8.4	( <a href="#">ONEMI 2015</a> )
<i>Nisqually</i>	2001	USA	6.8	( <a href="#">Reed and Park 2004</a> )
<i>Kushiro-oki</i>	1993	Japan	7.8	( <a href="#">Yamazaki et al. 1995</a> )
<i>Hokkaido Toho-oki</i>	1994	Japan	8.2	( <a href="#">Yamazaki et al. 1995</a> )
<i>Sanriku</i>	1994	Japan	7.5	( <a href="#">Yamazaki et al. 1995</a> )
<i>Alaska</i>	1964	USA	9.2	( <a href="#">Eckel 1967</a> )
<i>Luzon</i>	1990	Philippines	7.8	( <a href="#">Sharpe 1994</a> )
<i>El Asnam</i>	1980	Algeria	7.1	( <a href="#">Nakamura et al. 1983</a> )
<i>Tokachi-oki</i>	1968	Japan	8.3	( <a href="#">Katayama et al. 1977</a> )
<i>Valdivia</i>	1960	Chile	9.5	( <a href="#">Edwards et al. 2003</a> )
<i>Nihonkai-chubu</i>	1983	Japan	7.8	( <a href="#">Yasuda and Tohno 1988</a> )
<i>Bam</i>	2003	Iran	6.6	( <a href="#">Ahmadizadeh and Shakib 2004</a> )
<i>Samara</i>	2012	Costa Rica	7.6	( <a href="#">C.N.E. 2012</a> )
<i>Arequipa</i>	2001	Peru	8.4	( <a href="#">Edwards et al. 2003</a> )
<i>Izmir</i>	1999	Turkey	7.4	( <a href="#">Gillies et al. 2001</a> )
<i>Chi-Chi</i>	1999	Taiwan	7.6	( <a href="#">Soong et al. 2000</a> )
<i>Alaska</i>	2002	USA	7.9	( <a href="#">EERI 2003</a> )

Figure 7.2 shows the distribution of the analyzed earthquake in terms of location. Most of the collected data belong to earthquakes that took place in the USA, Japan, and South America. This is because damage data are continuously collected and reported by the competent authorities in these regions, mainly to allow this data to be used by scholars to improve community resilience.

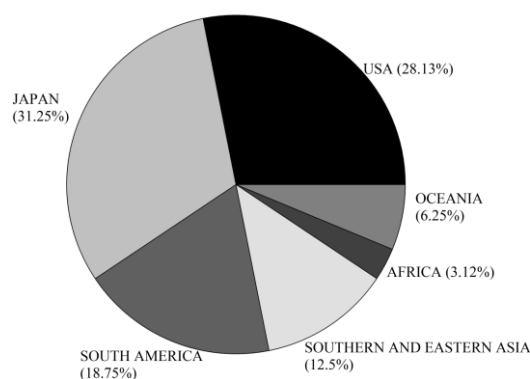


**Figure 7.2** Distribution of the analyzed earthquakes by location

Data related to infrastructure damage caused by earthquakes is reported in the literature in both qualitative and quantitative forms. The challenge faced during the data collection process was to have a normalized database that can be combined and used in the downtime analysis. It has been decided that only scholarly

publications reporting numerical data were to be considered. Reports with exclusively qualitative data have not been considered in the analysis, which mainly improved the quality of the developed curves. Another reason why qualitative data has been excluded is that such data reflects only the degree of damage of the infrastructures, and not the restoration function or the recovery speed. For instance, countries that already have a restoration plan and allocate enough resources to the recovery process would bounce back to a functional state in a short time regardless of how severely their infrastructures were damaged. Moreover, transforming the infrastructures damage into restoration time would require several assumptions that cannot be verified and could make the results biased. Since the objective of this research is to have a tool to estimate the downtime of infrastructures for a given location and a given earthquake magnitude, only documents reporting the actual time needed to restore the infrastructure service have been examined. The restoration time and the restoration speed of the infrastructures depend on several factors, such as the size of the infrastructure, the interdependency with other systems, the allocated financial and human resource for restoration, the level of initial damage suffered by the infrastructure, etc. Although these factors can vary among countries and even regions, the authors decided not to extrapolate restoration curves related to these parameters due to the paucity of data. Splitting the available data based on these factors would result in unreliable outputs as the data sets would be very small to carry out a probabilistic study. Instead, other parameters are considered in the study, such as the earthquake magnitude, development level of the affected country, and countries with enough data. The normalization of the raw data was not necessary as it is expressed on the same scale and can be combined (i.e., number of days required to restore the service). The normalization of data would be necessary if the qualitative damage data was considered because qualitative and linguistic terms vary between reports and include intrinsic subjectivity.

Recovery in the context of this work means returning full service to the population (i.e. the number of users served before and after the disaster event is the same, regardless of the state of the infrastructure). Table 7.2 lists the complete database used to create the restoration curves of the lifelines. The different earthquakes are listed in a random order. It is notable that each earthquake has caused damage to multiple infrastructure systems at the same time. For instance, in the city of Loma Prieta, the earthquake caused damage to two power plants, ten water systems, five gas stations, and six telecommunication systems. The affected infrastructures needed different times to recover even when the infrastructures are of similar types. For example, the two power plants that were affected by the Loma Prieta earthquake needed 2 and 0.5 days respectively to recover. There were some cases where either the damage information was not available, or no damage was recorded. Such cases are marked with a dash (-) inside the table. In total, the number of affected infrastructure units analyzed in this chapter are: 63 power systems; 84 water systems; 47 gas systems; and 34 Telecommunication systems. In the following, the raw data of three selected earthquakes is presented to show how the

restoration times of the damaged infrastructures were extracted from the source text. The raw data of the rest of the earthquake events can be found in the references reported in Table 7.2.

**Table 7.2** The number of affected infrastructures and the corresponding downtime for each lifeline

Earthquakes	Lifelines affected							
	Power		Water		Gas		Telecom.	
	No.	DT (days)	No.	DT (days)	No.	DT (days)	No.	DT (days)
<i>Loma Prieta</i>	2	(2), (0.5)	10	(14), (4), (3), (1.5), (2), (1), (3), (3), (7), (4)	5	(30), (16), (11), (10), (10)	6	(3), (4), (0.1), (3), (3), (1.5)
<i>Northridge</i>	3	(3), (0.5), (2)	6	(7), (2), (58), (12), (67), (46)	4	(7), (30), (5), (4)	3	(1), (2), (4)
<i>Kobe</i>	5	(8), (3), (2), (5), (6)	3	(0.5), (8), (73)	3	(84), (11), (25)	3	(1), (5), (7)
<i>Niigata</i>	4	(11), (4), (1)	3	(14), (28), (35)	3	(28), (35), (40)	-	-
<i>Maule</i>	6	(14), (1), (3), (10), (14)	4	(42), (4), (16), (6)	2	(10), (90)	4	(17), (7), (3), (17)
<i>Darfield</i>	3	(1), (2), (12)	2	(7), (1)	1	(1)	3	(9), (2), (3)
<i>Christchurch</i>	3	(14), (0.16)	1	(3)	2	(14), (9)	2	(15), (9)
<i>Napa</i>	1	(2)	6	(20), (0.9), (0.75), (2.5), (12), (11)	1	(1)	-	-
<i>Michoacán</i>	4	(4), (10), (3), (7)	4	(30), (14), (40), (45)	-	-	1	(160)
<i>Off-Miyagi</i>	2	(2), (1)	1	(12)	3	(27), (3), (18)	1	(8)
<i>San Fernando</i>	1	(1)	-	-	2	(10), (9)	1	(90)
<i>The Oregon Resil. Plan</i>	1	(135)	1	(14)	1	(30)	1	(30)
<i>LA Shakeout Scenario</i>	1	(3)	1	(13)	1	(60)	-	-
<i>Tohoku Japan</i>	7	(45), (3), (8), (2), (2), (4)	8	(4.7), (47), (1), (26), (7), (1), (47), (47)	6	(54), (2), (30), (3.5), (13), (18)	3	(49), (21), (49)
<i>Niigata</i>	2	(24)	3	(15), (4), (10)	2	(180), (2)	-	-
<i>Illapel</i>	1	(3)	1	(3)	-	-	-	-
<i>Nisqually</i>	3	(2), (6), (3)	-	-	-	-	-	-
<i>Kushiro-oki</i>	1	(1)	3	(6), (3), (5)	2	(22), (3)	-	-
<i>Hokkaido Toho-oki</i>	1	(1)	3	(9), (3), (5)	-	-	-	-
<i>Sanriku</i>	1	(1)	3	(14), (12), (5)	-	-	-	-
<i>Alaska</i>	3	(2), (0.75), (1)	5	(14), (5), (1), (7), (14)	3	(1), (5), (2), (14)	2	(1), (21)
<i>Luzon</i>	3	(7), (20), (3)	3	(14), (14), (10)	-	-	3	(5), (10), (0.4)
<i>El Asnam</i>	-	-	1	(14)	-	-	-	-
<i>Tokachi-oki</i>	1	(2)	-	-	2	(30), (20)	-	-
<i>Kanto</i>	2	(7), (5)	1	(42)	2	(180), (60)	1	(13)
<i>Valdivia</i>	1	(5)	1	(50)	-	-	-	-
<i>Nihonkai-chubu</i>	1	(1)	1	(30)	1	(30)	-	-
<i>Bam</i>	1	(4)	3	(14), (10)	-	-	1	(1)
<i>Samara</i>	1	(1)	1	(2)	-	-	1	(1)
<i>Arequipa</i>	1	(1)	3	(32), (34)	-	-	-	-
<i>Izmit</i>	1	(10)	2	(50), (29)	1	(1)	1	(10)
<i>Chi-Chi</i>	3	(40), (14), (19)	1	(9)	1	(14)	1	(10)
<i>Alaska 2002</i>	2	(2), (0.5)	10	(14), (4), (3), (1.5), (2), (1), (3), (3), (7), (4)	1	(3)	6	(3), (4), (0.1), (3), (3), (1.5)

Note: No = the number of affected infrastructures; DT = the downtime in days.

## 7.2.1 Valdivia 1960, Chile ([Edwards et al. 2003](#))

The Valdivia earthquake was the strongest shaking ever recorded, with a magnitude of 9.5 on the Richter scale and an intensity of XI to XII on the Mercalli

scale. This earthquake shocked all South America and destroyed the Chilean city of Valdivia. More than 5.000 people died, and more than 2 million people were forced to leave their homes. The shock was so strong that new lakes were formed and some rivers shifted their course. After the big shake, a huge tsunami devastated all the coastline of Valdivia city, destroying houses, bridges, boats, and ports. Despite the power of the earthquake, the Chilean utilities of the region performed quite well, mainly due to the preparation of the country to this kind of hazards. One electrical system was affected by the earthquake, and it took five days to recover its function. The water system was also affected, and it fully recovered after exactly 50 days. As for the gas and telecommunication infrastructures, no damage was reported as the two systems functioned normally after the earthquake.

### **7.2.2 El-Asnam 1980, Algeria ([Nakamura et al. 1983](#))**

An earthquake of magnitude 7.1 and a focal depth of 15 km struck the city of El-Asnam in northern Algeria on the 10<sup>th</sup> of October 1980. 23.5% of the buildings of the city collapsed during the 1980 quake. More than 6.500 people died after the shock and 9.000 were injured. This event was an example of a poor post-earthquake study. Only information regarding the downtime of the water system was reported. The water system remained inoperative for two weeks following the deadly earthquake.

### **7.2.3 Niigata 1964, Japan ([Scawthorn et al. 2006c](#))**

On June 16, 1964, Japan was jarred by the strongest earthquake to hit the country since the Kanto Earthquake in 1923. The shake, which measured 7.7 on the Richter scale, was felt in over two-thirds of the main Japanese island of Honshu, but the most affected region was the Niigata prefecture. The earthquake destroyed more than 8.000 houses, disrupted all public utilities, severely interrupted all the communication systems, and put out of commission almost all the land, sea, and air transport facilities. The region of Niigata stayed with partial power supply for 24 days until the power system was recovered. The earthquake affected three water systems in the city, and they took 15, 4, and 10 days to recover, respectively. Two gas systems were damaged by the quake; the first was heavily affected, and it remained inoperative for 6 full months, while the second was slightly damaged, and it took only 2 days to recover. No major damage in the telecommunication infrastructure was recorded as no drop-in service was experienced by the users.

## **7.3 Methodology**

The main challenge faced in this work is to illustrate the gathered data in the form of restoration curves. Typically, real data is complex to handle because they are exposed to a series of errors that vary in nature and magnitude. In this chapter, the collected restoration raw data are fitted with a statistical distribution. Choosing

the right distribution can be a difficult task due to the relevant number of distributions available in the literature. To characterize new raw data with a distribution, four questions need to be asked. The first question is whether the data is discrete or continuous. The second is whether the data is symmetric or if there is asymmetry in the distribution. The third question relates to the presence of upper or lower limits on the data. The last question deals with the possibility of observing extreme values in the distribution. Answering these questions can be fundamental in fitting the right distribution.

Different distribution families that satisfy the characteristics of the infrastructure restoration process have been selected. The parameters of the distributions have been estimated using the maximum likelihood estimation method. The distribution with the optimal fit has been identified (1) visually using the probability paper visual test, and (2) statistically using the Kolmogorov-Smirnov (K-S) and Chi-Square tests for Goodness-of-fit. In the following, the statistical distribution selection procedure is discussed in detail.

### 7.3.1 Parameters estimation

Different methods for estimating the parameters of a distribution can be used; among these are the *method of moments* and the method of *maximum likelihood* ([ANG H-S and TANG 1975](#); [Tang and Ang 2007](#)). In this work, the method of maximum likelihood is used to estimate the parameters of the distributions. The likelihood of a set of data is the probability of obtaining that particular set of data given the chosen probability distribution model. This expression contains the unknown model parameters. The values of these parameters that maximize the sample likelihood are known as the Maximum Likelihood Estimator MLEs ([Sematech/NIST](#)). Unlike the method of moments, the maximum likelihood method derives the point estimator of a parameter directly. The maximum likelihood estimate (MLE) of a parameter possesses many desirable properties. In particular, for large sample size, the maximum likelihood estimator is often considered to provide the best estimate of a parameter ([Tang and Ang 2007](#)).

### 7.3.2 Fitting analysis

Visual testing is the easiest and simplest way to test a distribution. This is done by comparing the histogram of the raw data to the distribution. To either accept or reject a distribution, the cumulative frequency of the empirical data is compared to the cumulative distribution function (CDF) of the theoretical distribution. Alternatively, one can use probability paper to check if a given distribution conforms to the empirical data ([Tang and Ang 2007](#)). A probability paper is usually constructed using a transformed probability scale in such a way to obtain a linear graph between the cumulative probabilities of the underlying distribution and the values of the random variable. The probability paper procedure has minimized our choices to only three distributions: The *exponential*, *lognormal*, and *gamma* distributions.

When a particular distribution is determined to model a phenomenon using a given probability paper by simple visual inspection, the validity of the theoretical distribution can be verified statistically using *goodness-of-fit* tests. There are multiple tests to verify the goodness-of-fit in the literature, such as the Kolmogorov-Smirnov (or K-S), the chi-square, and the Anderson-Darling (or A-D). The latter, in particular, is useful when the tails of distribution are important. Therefore, only the K-S and chi-square goodness-of-fit tests are performed in this chapter and the results are presented in the following section.

### 7.3.3 The distribution with optimal fit

Dating back to 1967, The Kolmogorov-Smirnov test (K-S) is considered one of the oldest and most useful tests of fit for distributions ([Chakravarti et al. 1967](#)). The basic idea of the *Kolmogorov-Smirnov* test is to compare the experimental cumulative frequency with the CDF of an assumed theoretical distribution. If the maximum difference between the experimental and theoretical frequencies is larger than a certain value for a given sample size  $n$ , the theoretical distribution is not acceptable for modeling the underlying population; conversely, if the difference is less than a critical value, the theoretical distribution is acceptable at the defined significance level  $\alpha$  ([Tang and Ang 2007](#)). Mathematically, it is represented as follows:

$$D_n = \max_x |F_X(x) - S_n(x)| \quad (7.1)$$

where  $D_n$  is a random variable,  $F_X(x)$  is the CDF of the theoretical distribution,  $S_n(x)$  is the stepwise empirical cumulative frequency function. For a significance level  $\alpha$ , the K-S test compares the observed maximum difference  $D_n$  with the critical value  $D_n^\alpha$ , which is defined for a significance level  $\alpha$ , as follows:

$$P(D_n \leq D_n^\alpha) = 1 - \alpha \quad (7.2)$$

In this chapter, the K-S test analysis for only two data sets is presented. Table 7.3 shows the data sets considered in the analysis, extracted from Table 7.2. Both sets correspond to the events with an earthquake magnitude within the range EM 6-6.9.

**Table 7.3** Downtime data points and corresponding frequencies for the water and power infrastructures with EM 6-6.9

WATER	DT (days)	0.5	0.7 5	0.9	1	1.5	2	2.5	3	4	7	8	10	11	12	14	15	20	28	30	35	46	58	67	73
	Freq.	1	1	1	1	1	3	1	4	1	2	1	1	2	2	2	1	1	1	1	1	1	1	1	1
POWER	DT (days)	0.5	0.6	1	2	3	4	5	6	8	11	14													
	Freq.	2	1	2	4	4	2	1	2	1	1	1													

Figure 7.3 shows the cumulative step function of (a) the water distribution infrastructure, and (b) the power network infrastructure for the data corresponding to EM 6-6.9. The Gamma, exponential, and lognormal cumulative distributions functions are plotted against the stepwise function for each data set to visualize the distribution fit. As we can see in the figure, it is very hard to rely on visual interpretation to choose the distribution with the best fit; therefore, the goodness-of-fit testing is necessary.

Table 7.4 shows the goodness-of-fit tests for the two data sets. For both infrastructures, all theoretical distributions are acceptable as the value of  $D_n$  is always lower than the critical value  $D_n^\alpha$  for a significance level  $\alpha=0.05$ . From the table, the gamma distribution yields the best results (i.e. lowest  $D_n$ ).

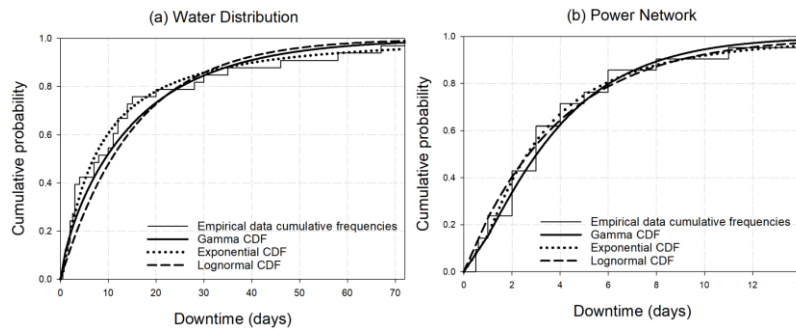


**Figure 7.3** Cumulative frequencies with three theoretical CDF fitting distributions for (a) the water distribution infrastructure, and (b) the power network infrastructure for the data corresponding to EM 6-6.9

**Table 7.4** Kolmogorov-Smirnov goodness-of-fit test for the water and power infrastructures for EM=6-6.9

Theoretical distribution	The water distribution network for EM=6-6.9		The power network for EM=6-6.9	
	$D_n$	$D_n^\alpha$ ( $\alpha=0.05$ , $n=24$ )	$D_n$	$D_n^\alpha$ ( $\alpha=0.05$ , $n=11$ )
Gamma distribution	0.098	0.245	0.0745	0.395
Exponential distribution	0.122		0.0811	
Lognormal distribution	0.216		0.0837	

Similarly, the Chi-square goodness of fit test has been performed to consolidate our distribution choice. The Chi-square goodness-of-fit test compares the observed frequencies  $n_1, n_2, \dots, n_k$  of  $k$  values (or in  $k$  intervals) of the variate with the corresponding theoretical frequencies  $e_1, e_1, \dots, e_k$  calculated from the assumed theoretical distribution model. The assumed theoretical distribution is an acceptable model if the following equation is satisfied:

$$\sum_{i=1}^k \frac{(n_i - e_i)^2}{e_i} < c_{1-\alpha, f} \quad (7.3)$$

where  $C_{1-\alpha, f}$  is the critical value of the chi-square distribution at the cumulative probability of  $1-\alpha$ ,  $f = k-1$  is the number of degrees-of-freedom (d.o.f.), where  $f$  must be reduced by one for every unknown parameter that must be estimated.

Figure 7.4 shows the frequency histogram plot of the downtime data corresponding to (a) the water distribution infrastructure and (b) the power network infrastructure for earthquake magnitudes EM 6-6.9. The probability density function (PDF) of the Gamma, exponential, and lognormal theoretical distributions are displayed and compared against the empirical data points. Table 7.5 presents the goodness-of-fit tests for the two downtime data sets. For the water distribution system, the chi-square test results ( $\chi_f^2$ ) for the three theoretical distributions are below the maximum threshold ( $C_{1-\alpha, f}$ ). This signifies that all three distributions can be used to model the downtime data. For the power network, however, only the gamma distribution is acceptable because the chi-square tests for the exponential and lognormal distributions exceed the given threshold for a 5% significance level  $\alpha$ .

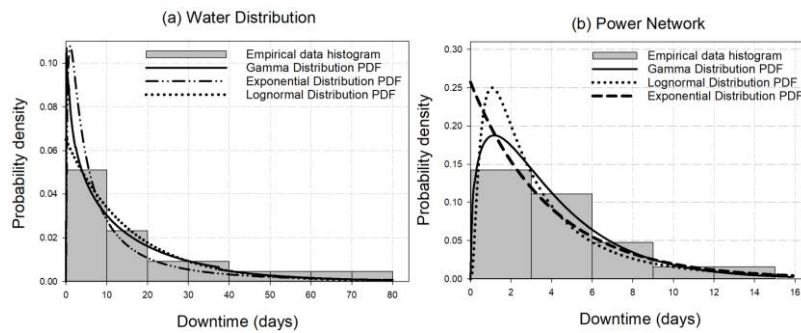


**Figure 7.4** Histograms and PDF fitting distributions for (a) the water distribution infrastructure, and (b) the power network infrastructure for the data corresponding to EM 6-6.9

**Table 7.5** Chi-square goodness-of-fit test for the water and power infrastructures for EM=6-6.9

Theoretical distribution	Water distribution system, EM=6-6.9			Power network, EM=6-6.9		
	Chi-square $\chi_f^2$	$f = k - 1$	$C_{1-\alpha, f}$ ( $\alpha = 0.05$ )	Chi-square $\chi_f^2$	$f = k - 1$	$C_{1-\alpha, f}$ ( $\alpha = 0.05$ )
Gamma distribution	6.23	5	11.07	5.45	3	7.81
Exponential distribution	7.8	4	9.48	13.98	2	5.99
Lognormal distribution	10.51	5	11.07	15.08	3	7.81

In conclusion, among the three, the gamma distribution was found to be the optimal fit, having passed the goodness-of-fit tests for the remaining data sets. Hence, it is hereafter used to build the restoration curves. The restoration curves for each lifeline have been created using the distribution fitter toolbox in MATLAB®

([Guide 1998](#)), which uses the maximum likelihood estimation method to estimate the parameters of the theoretical distribution.

## 7.4 Results: the restoration curves

Restoration curves were developed for the power, water, gas, and telecommunications systems using the collected downtime data. The variables considered to plot the curves are: (i) the number of days required to restore full service to customers (horizontal axis) and (ii) the probability that the utility is completely restored to the customers (vertical axis). To provide a better understanding of the restoration process, the collected data has been divided based on different categories, as follows:

1. *Earthquake magnitude (EM)*: Although it is not the only parameter, the earthquake intensity plays a primary role in defining the infrastructure damage and the downtime. This classification assumes that the earthquake magnitude is fully correlated with the induced damage. The collected data has been classified into four groups of Richter magnitude scale (strong 6-6.9; Major 7-7.9; Severe 8-8.9; and Violent 9-9.9). For each lifeline, a group of restoration curves considering the four EM ranges have been developed.
2. *First world countries vs developing countries*: developing restoration curves for every single country is not feasible due to the relatively small amount of available data. As an alternative, the data was divided based on the level of development of countries. Countries were classified as either first world countries or developing countries. For each group, lifelines restoration curves have been created.
3. *Countries with a large database*: it is interesting to see how specific countries are performing in terms of disaster recovery. Restoration curves for the US, Japan, and countries in South America have been developed since a large portion of the collected data belongs to these three regions.

### 7.4.1 Category 1: Earthquake magnitude

Figure 7.5 shows the restoration curves for the four lifelines based on the earthquake magnitude. The intensity of the earthquake is a key parameter in defining the downtime, and this is shown in Figure 6 where most of the times the lifeline restoration rate follows the earthquake magnitude.

The restoration curves of the lifelines are characterized by similar behavior. The only difference lies in the restoration rate. The power system has a very high probability to recover within 60 days, unlike the other infrastructures that need at least 100 days to reach the same probability. This outcome is expected because all lifelines need the power to function, and thus the power system is always the first to recover. The telecommunication system, on the other hand, is heavily dependent on the power network, and this delays its restoration until the power system is recovered. Similarly, the water system reaches a restoration probability close to 1

after approximately 100 days. Table 7.6 shows the distributional parameters used in the statistical analysis of each lifeline derived using the maximum likelihood estimation method.

**Table 7.6** The distributional parameters derived for Category 1 restoration curves

Parameters	Power system				Water system			
	M=6- 6.9	M=7- 7.9	M=8- 8.9	M=9- 9.9	M=6- 6.9	M=7- 7.9	M=8- 8.9	M=9- 9.9
$\alpha$	1.4319	0.9497	1.1901	0.6270	0.749	0.901	1.022	0.950
$\beta$	2.7136	5.8436	4.2713	17.342	20.51	27.24	17.817	19.805
Parameters	Gas system				Telecommunication system			
	M=6- 6.9	M=7- 7.9	M=8- 8.9	M=9- 9.9	M=6- 6.9	M=7- 7.9	M=8- 8.9	M=9- 9.9
$\alpha$	1.5745	0.9971	3.2153	1.0926	0.622	3.075	0.4755	1.1745
$\beta$	12.009	20.786	5.909	15.147	16.10	3.511	92.001	25.967

Note: M = the earthquake magnitude in the Richter scale.

In standard fragility analysis, the fragility functions for the different damage states within the same data sample should not intersect. The intersection of fragility curves may occur when each curve corresponding to a specific damage state is fitted independently of one another ([Shinozuka et al. 2000](#)). In order to avoid the intersection of fragility curves corresponding to different damage states, the same standard deviation is usually assumed ([Shinozuka et al. 2000](#)), where the parameters of the distribution functions representing different states of damage are simultaneously estimated by means of the maximum likelihood method. In that method, the parameters to be estimated are the median of each fragility curve and one value of the standard deviation that is assumed the same for all fragility curves. In the loss analysis, however, the intersection of the functions could happen. Losses do not necessarily follow a specific pattern (i.e. it may cost more to repair a lower damage state). Restoration times are even more dependent on the invested resources (i.e. severe damage may be recovered quickly due to engagement of overwhelming resources, for example, using military resources to construct temporary bridges). This Justifies the intersection of the curves in Figure 6.

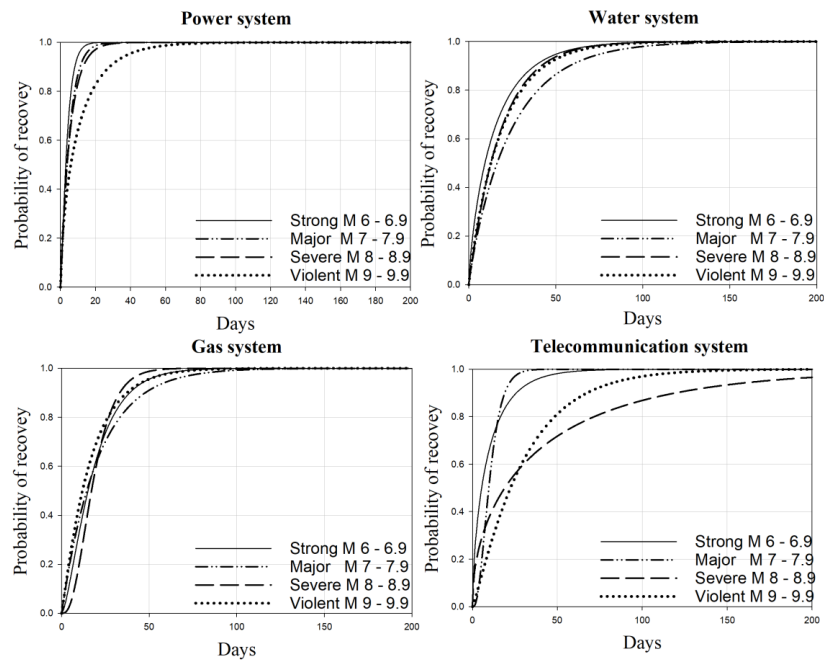


**Figure 7.5** Restoration curves of the lifelines based on the earthquake magnitude

## 7.4.2 Category 2: First world countries vs developing countries

Table 7.7 classifies the countries according to their level of development. USA, Japan, and New Zealand have been considered as “first world countries” while the remaining countries have been grouped under “developing countries”. Figure 7.6 shows the restoration curves of the database grouped according to the level of development of the affected countries. For all infrastructures, the developed countries tend to have a higher recovery probability at a given downtime. This means that the developed countries are more likely to recover the lifelines in a shorter period. For both groups, the restoration curve of the power system reaches a high probability of recovery quicker than the other lifelines, usually because the functionality of the different lifelines is greatly dependent on the power network. Table 7.8 presents the statistical parameters of the theoretical distributions derived using the maximum likelihood estimation.

**Table 7.7** Classification of the countries based on their level of development

First world countries	developing countries
<i>USA</i>	<i>Chile</i>
<i>Japan</i>	<i>Mexico</i>
<i>New Zealand</i>	<i>Philippines</i>
	<i>Algeria</i>
	<i>Chile</i>
	<i>Iran</i>
	<i>Costa Rica</i>
	<i>Peru</i>
	<i>Turkey</i>
	<i>Taiwan</i>

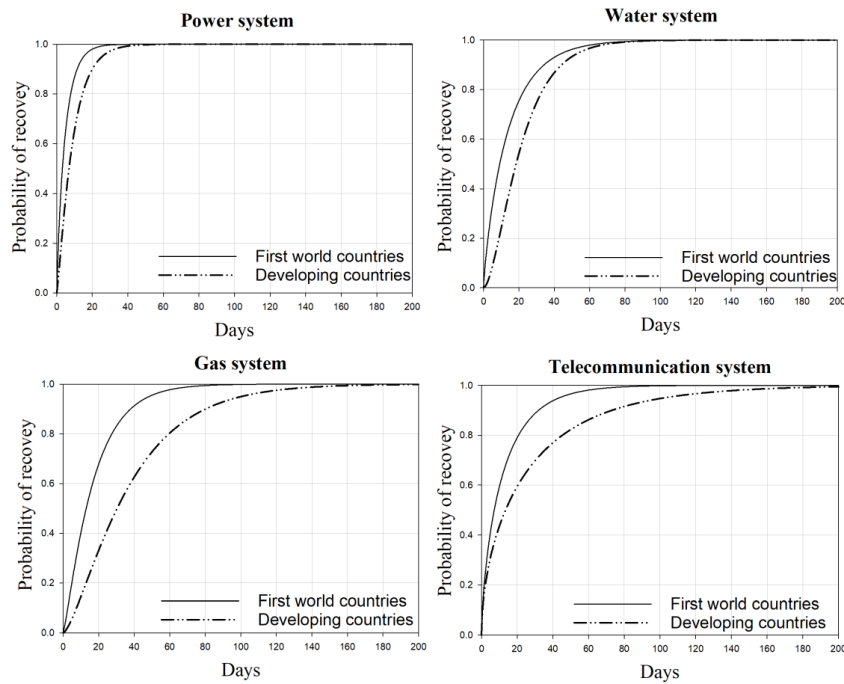


**Figure 7.6** Restoration curves of the lifelines based on the level of development of the countries

**Table 7.8** The distributional parameters derived for Category 2 restoration curves

Parameters	Power system		Water system	
	<i>First world countries</i>	<i>Developing countries</i>	<i>First world countries</i>	<i>Developing countries</i>
$\alpha$	0.883805	1.25039	0.845769	1.86575
$\beta$	5.46925	7.35006	16.8706	11.963
Parameters	Gas system		Telecommunication system	
	<i>First world countries</i>	<i>Developing countries</i>	<i>First world countries</i>	<i>Developing countries</i>
$\alpha$	1.23635	1.50336	0.671797	0.546505
$\beta$	14.0461	25.6092	18.7854	50.4214

### 7.4.3 Category 3: countries with a large database (USA, Japan, and countries in South America)

A large portion of the collected downtime data belongs to the three regions USA, Japan, and South America. Data related to these countries was large enough to develop independent recovery curves, except for telecommunication infrastructure in the region of South America. Table 7.9 presents the parameters of the gamma distribution CDFs used for building the restoration curves. Figure 7.7 compares the restoration rate of the lifelines in the three regions, regardless of the earthquake intensity. The USA takes the lead in the recovery of all lifelines, while Japan comes second. Finally, countries in South America are the last to recover the infrastructure. South America generally experienced earthquakes of larger magnitudes in history than the other countries, and this can be a possible factor for this result.

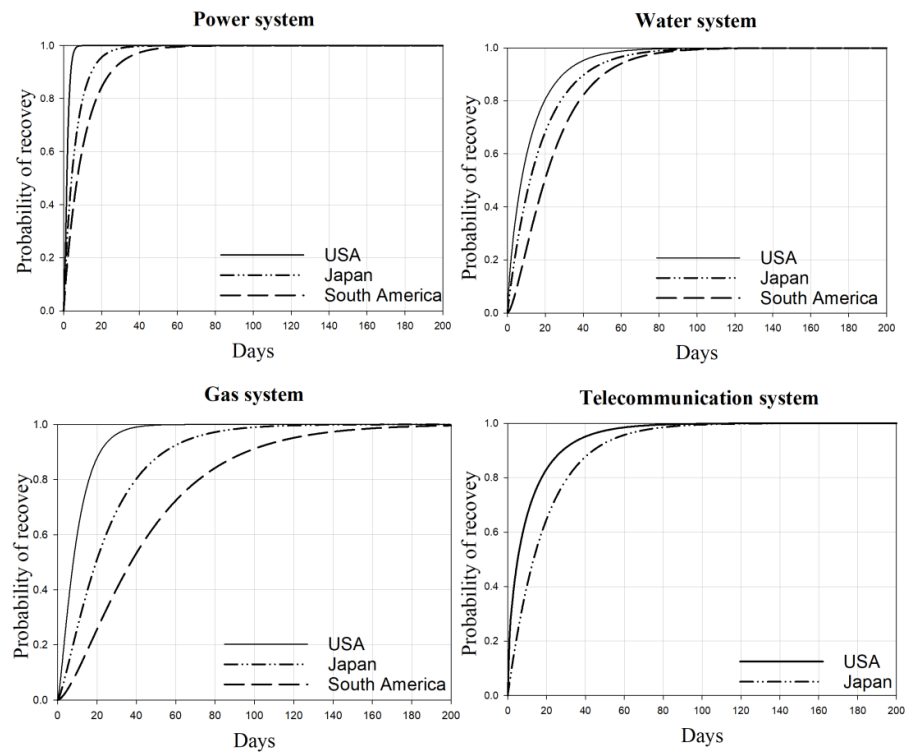


**Figure 7.7** Restoration curves of the lifelines of the USA, Japan, and countries in South America

**Table 7.9** The distributional parameters derived for Category 4 restoration curves

Parameters	Power system			Water system		
	<i>USA</i>	<i>Japan</i>	<i>South America</i>	<i>USA</i>	<i>Japan</i>	<i>South America</i>
$\alpha$	2.24621	0.931013	0.936271	0.774639	0.973	1.5892
$\beta$	0.881828	6.71312	11.4201	15.4265	17.924	15.4952
Parameters	Gas system			Telecommunication system		
	<i>USA</i>	<i>Japan</i>	<i>South America</i>	<i>USA</i>	<i>Japan</i>	<i>South America</i>
$\alpha$	1.40685	1.36345	1.59156	0.535494	1.00736	0.497757
$\beta$	7.26358	18.6439	29.3214	19.7517	18.9853	135.943

## 7.5 Discussion

The results presented above show some interdependencies and coupling behaviors among the lifelines. The power system was always the first infrastructure to recover its normal functions following the disaster, usually because all lifelines depend on the power system, and so right after the event, it should restore as soon as possible. For the telecommunication system, the restoration process starts fast, but then the probability of restoration in the following days after the earthquake becomes less than that of the power system. This is probably due to the interdependency of the two systems; that is, if the power system is not fully restored, the telecommunication service will not be restored as well. The water and gas networks show a lower recovery rate, where both infrastructures are dependent on the power system for service transmission. In most cases, the gas distribution

system is the utility that takes longer to be completely restored. One reason can be the mandatory tests and investigations required after a hazardous event, which force the utility to be closed for extra days.

Generally, estimating the recovery delay caused by infrastructures interdependencies can be a challenging task due to the complexity involved in the process. In this work, the lack of information regarding systems interdependencies has prevented such an analysis.

The downtime depends on several factors, such as the size of the infrastructure and the development level of the country (i.e. developed countries have a higher degree of infrastructure interdependency). Identifying all variables that affect the downtime can be an approach for normalizing and estimating the dependent downtime. In our work, the interdependency of the analyzed infrastructures are embedded in the results and they are behind the introduced restoration curves. In addition, the work presented here is an empirical study based on a probabilistic analysis; therefore, parameters such as the interdependency can be considered as an intrinsic characteristic of the data.

The main challenge faced while creating the database was to deal with different studies, with a different analysis, and different formats. There is not yet an international standard to collect the performance of the utilities after hazardous events, and this led to exclude several studies because the damage data reported was not scaled and cannot be combined. That is, some data points were qualitative and biased, and consequently, they did not qualify to be included in the study. A standard procedure to analyze the performance of lifelines following natural disaster remains a need to improve community resilience.

Data classification and categorization is another challenge faced in this work. The collected data has been divided based on one criterion at a time. The considered criteria are the earthquake magnitude, development level of the affected country, and countries with enough downtime data. For each of the three categories, a group of restorations curves has been developed for each infrastructure type. Distinguishing the data based on several criteria at once would lead to small data sets whose analysis would not be statistically defensible. Nevertheless, this will be considered in future research once enough data is gathered.

## **7.6 Concluding remarks**

Downtime is one of the most difficult parameters to estimate disaster resilience. Estimating the resilience of infrastructures due to earthquakes has been studied in the past; however, none of the studies highlighted a clear procedure to estimate the disruption time of damaged systems. This chapter provides an empirical model for estimating the downtime of damaged infrastructures following an earthquake. The model uses a large database for earthquake events that occurred over the last few decades. Different types of statistical distributions have been tested and then the gamma distribution has been selected because of its good fit to the empirical data. Four main lifelines were considered in this work (power, water, gas, and

telecommunication). For each of them, a group of restoration curves has been derived. The restoration curves were presented in terms of the number of days required to restore full service to customers (horizontal axis) and the probability that the utility will be completely restored to the customers (vertical axis). the longer is the time after the disaster, the higher is the probability of the infrastructure to recover its functions.

Given that such a model is still missing in literature, this work provides a useful tool to estimate the downtime of infrastructures hit by earthquakes. It allows evaluating the infrastructures' resilience, given that the downtime is a key parameter in the resilience estimation process. Future work will be oriented towards extending the database to include more earthquakes. In addition, special attention will be given to the infrastructure interdependency, which can increase the accuracy of the restoration curves. Other lifelines such as the transportation system will also be analyzed once satisfactory data is collected.

In the previous chapters, different methodologies and techniques to evaluate the resilience of specific systems have been presented. Next chapter will introduce a general methodology to evaluate the resilience of any engineering system. The methodology accounts for the dynamic nature of the system by considering the temporal dimension.

# Chapter 8

## 8. Probabilistic resilience assessment of engineering systems

*Part of the work described in this chapter has been previously published:*

Kammouh, O., Gardoni, P., and Cimellaro, G. P. (2019). "Resilience assessment of dynamic engineering systems." *MATEC Web Conf.*, 281, 01008.

### 8.1 Introduction

Resilience can be an outcome (static), a process (dynamic) ([Cutter et al. 2008b](#)). While most of the current researches are focusing on quantifying the engineering resilience from a static point of view, there is a significant gap in assessing the dynamic nature of resilience through quantitative approaches. This chapter first proposes a static framework to model systems of static nature (e.g., assessing a system's performance at a specific instance of time) ([Kammouh et al. 2019a](#)). It employs the BN as a tool to quantify the system's resilience. The framework is illustrated using a case study in which the resilience of a country, namely Brazil, is assessed. In general, BN is good to assess a physical-causal model; however, learning and updating a BN requires an extensive computational load. Updating a BN is necessary for resilience modeling, especially in monitoring the possibility of disruptive events. Thus, this chapter also presents a universal dynamic probabilistic framework to quantitatively assess the resilience of systems of dynamic nature (i.e., critical infrastructures, buildings, communities, etc.) The framework can be used to assess the resilience of multiple systems at once and it adopts the DBN as an inference tool. In fact, a DBN model can be obtained by expert knowledge, from a database using a combination of machine-learning techniques, or both. These properties make the DBN formalism very useful in the disaster resilience domain as this domain has an abundance of both expert knowledge and databases records. Moreover, a DBN allows performing a transient analysis of the system after the occurrence of disruption until the system was recovered from its disruptive states. The transient analysis can be rather useful to model the restoration process of the damaged system.

The proposed resilience framework is presented in the form of a mathematical formulation that integrates the probability distribution of all variables' states. A case study of a transportation network is used to illustrate the proposed methodology. Results show the ability of the framework to dynamically model complex systems, even when data are scarce.

## 8.2 Bayesian and Dynamic Bayesian Networks

Bayesian and Dynamic Bayesian networks are probabilistic graphical models that use Bayesian inference for probability computations. Bayesian networks typically model conditional dependence using links in a directed graph. Through these relationships, one can efficiently conduct inference on the random variables in the graph through the use of factors. In the following, Bayesian and Dynamic Bayesian networks are explained in details.

### 8.2.1 Bayesian Network (BN)

The Bayesian Network, also known as Bayesian Belief Network, is a graphical model that allows the design of stochastic relationships among a group of variables. Applications of BN can be found in a variety of fields, from social to economic and biological disciplines ([Ismail et al. 2011](#); [Schultz and Smith 2016](#)). BN permits the usage of different types of knowledge, both quantitative and qualitative, and can cope with missing data considering the uncertainty embedded in the system ([Balbi et al. 2014](#)). To construct a BN, several hypotheses have to be made. Each hypothesis is decomposed into a set of random variables. Each variable can take values within a finite set of states (also known as beliefs), mutually exclusive and complementary exhaustive (MECE) ([Grover 2013](#)). The dependency of one variable on another is represented in the network as a directed edge (or link). The relationships between the variables in a BN are expressed in terms of family relationships. The link starts from the so-called father node and points at the son node, which is the impacted variable. The set of edges and nodes builds a directed acyclic graph. The network itself is normally learned from data or specified by experts who not only provide the main hypotheses (and consequently the variables to be considered in the model), but also the dependencies between the variables. The foundation and the inference process of BN are set in the Bayes' Theorem. Given a state  $b$  for a variable  $B$  and a number  $k$  of MECE states  $a_j, i = 1, \dots, k$  for a variable  $A$ , the updated probability is computed as:

$$P(a_j | b) = \frac{P(b | a_j)P(a_j)}{P(b)} \quad (8.1)$$

where  $P(a_j | b)$  is the probability that  $b$  is observed under the hypothesis  $a_j$ ,  $P(b | a_j)$  is the probability that  $a_j$  is true given that the state  $b$  is observed, also called priori probability ([Laskey 1995](#)). The dependencies of one variable (the son node) on another (the father node) are usually quantified using a Conditional Probability

Table (CPT), where the likelihood of the son node to assume a certain state under a certain father node state is assigned ([Grover 2013](#)). In the case of a variable with no parents, the probabilities are reduced to the unconditional probability. The quantitative part of the BN starts by assigning conditional probability distributions (CPD) to the nodes. Each node in a BN has a CPT that determines the CPD of the random variable. The CPTs provide information on the probability of a node given its parents ([Murphy and Russell 2002](#)).

Once the BN is constructed, we pinpoint that the outcome is highly dependent on the assigned probabilities ([Ismail et al. 2011](#)). To test the robustness of the model and the dependency of the outcome on each father node, a sensitivity analysis is usually performed. This allows identifying the most important and impactful variables, leading to consequent emphatic attention in the collection of data for the concerned variables ([Laskey 1995](#)). For more details, several examples of BN applications can be found in the literature ([Ismail et al. 2011](#); [Cockburn and Tesfamariam 2012](#); [Kabir et al. 2015](#); [Siraj et al. 2015](#); [Kabir et al. 2016](#)).

## 8.2.2 Dynamic Bayesian Network (DBN)

BNs are used when the analyzed system is in a static state. This is often not the case in a dynamic, continuously changing world. This raises the need for a tool that is capable of accounting for system changes, such as the Dynamic Bayesian Network. DBN is a Bayesian network extended with additional mechanisms that are capable of modeling influences over time ([Murphy and Russell 2002](#)). It extends the classical BN by adding the time dimension.

In principle, a Dynamic Bayesian Network (DBN) works exactly as a Bayesian Network (BN): once you have a directed graph that represents correlations between variables, we can learn conditional probability tables (the parameters) from a dataset. The main difference is that a DBN represents a phenomenon that develops through time; so, while in a regular BN you might have a node representing variable “A” that influences variable “B”, in a DBN you might have variable “A” at time=1 that influences variable “A” at time=2.

DBN is suitable for describing dynamic systems where the performance fluctuates (e.g. before and after a disaster). Like the BN, the DBN is a directed acyclic graphical model used for statistical processes. A DBN consists of multiple BNs (often referred to as time-slices or time steps), each with its own variables. The variables within a single or successive time-slices are connected using links. A DBN can be defined as  $(B_1, B_{\rightarrow})$ , where  $B_1$  is a BN that specifies the initial distribution of the variable states  $P(Z_1)$  ([Murphy and Russell 2002](#)), where  $Z_t = (U_t, X_t, Y_t)$  is the input, hidden, and output variables of the model at time step  $t$ , while  $B_{\rightarrow}$  is called a “two-slice temporal Bayesian network” (2TBN), which defines the transition model  $P(Z_t|Z_{t-1})$ , as in Eq. (8.2). The nodes in the first slice of the 2TBN network do not have parameters associated with them, while CPTs are required for the nodes in the second slice.

$$p(Z_t | Z_{t-1}) = \prod_{i=1}^N p(Z_t^i | Pa(Z_t^i)) \quad (8.2)$$

where  $Z_t^i$  is the  $i^{th}$  node at time  $t$  and could be a component of  $X_t$ ,  $Y_t$ , or  $U_t$ .  $Pa(Z_t^i)$  are the parents of  $Z_t^i$ , which can be in the same or the previous time-slice.

The process in a DBN is stationary and the structure repeats after the second time-slice, so the variables for the slices  $t=2,3,\dots,T$  remain unchanged. This allows expressing the system using only two slices (i.e., the first and the second time-slices). Therefore, an unbounded sequence length could be modeled using a finite number of parameters. The probability distribution for a sequence of time-slices can be obtained by unrolling the 2TBN network, as follows:

$$p(Z_{1:T}) = \prod_{t=1}^T \prod_{i=1}^N p(Z_t^i | Pa(Z_t^i)) \quad (8.3)$$

The DBN is often seen as a generalization of other temporal reasoning developments, such as the hidden Markov model (HMM) and the Kalman filter model (KFM) ([Hulst 2006](#)). These models, which can be expressed in a compact form, are popular for their fast learning and fast inference techniques. In fact, DBNs generalize HMMs by expressing the state space in not only a single discrete random variable but also in a factored form.

#### 8.2.2.1 Temporal plate and contemporal nodes

The temporal plate is the area within the DBN model that includes temporal information (i.e., information that changes from a time step to another). The temporal plate includes the variables that evolve over time. These variables are part of the DBN that can be unrolled. However, nodes that have a constant value at every time step are considered a waste of memory and computational power if copied in each time step. Therefore, it is wise to introduce these nodes outside the temporal plates. The collection of these nodes is called the contemporal space, and the nodes are called contemporal nodes ([Murphy and Russell 2002](#)).

#### 8.2.2.2 Anchor and terminal nodes

One extension of the original DBN formalism was established in ([Hulst 2006](#)), where the author introduced nodes that are only connected to the first and last time slices of the DBN. Such variables do not affect the intermediate time slices like the contemporal nodes.

- Anchor node (A): a node that is outside the temporal plate but has at least one child inside the temporal plate in the first time slice of the unrolled DBN.
- Terminal node (T): a node that is outside the temporal plate and has at least one parent inside the temporal plate in the last time slice of the unrolled DBN.

Figure 8.1(a) presents a single time slice of a DBN (a snapshot of the system) where all variables appear to be static. This is a typical Bayesian network where the time dimension is not considered. Figure 8.1(b) shows a general DBN where the variables that are in the temporal plate (the dotted rectangle) are those that are repeated when the DBN is unrolled, and the variables that are outside the temporal plate are the static (contemporal, anchor, or terminal) nodes. Figure 8.1(c) shows the unrolled DBN where the variables that are inside the temporal plate are connected with one another through temporal arcs and appear in every time-step, while the other variables appear only once since their value is constant. The transition model of the DBN can be represented as follows:

$$P(Z_t | Z_{t-1}, Z_{t-2}, \dots, Z_{t-k}, C) = \prod_{i=1}^N P(Z_t^i | Pa(Z_t^i), C^i) \quad (8.4)$$

where  $Pa(Z_t^i)$  is the parents of  $Z_t^i$  inside the temporal plate,  $C^i$  for  $i=1, \dots, N$  are the contemporal variables that are a parent of  $Z_t^i$ . The joint distribution of a DBN sequence of length  $T$  including the additional variables (A) and (T) is given as follows:

$$P(A, C, Z_{1:T}, T) = P(C).P(A|C) \prod_{i=1}^N P(Z_1^i | Pa(Z_1^i), A^i, C^i) \prod_{t=2}^T \prod_{i=1}^N P(Z_t^i | Pa(Z_t^i), C^i) \prod_{i=1}^N P(T^i | Z_T^i, C^i) \quad (8.5)$$

where  $A^i$  is the anchor variables that are a parent of  $Z_1^i$ ,  $T^i$  is the terminal variables that are a child of  $Z_T^i$ .

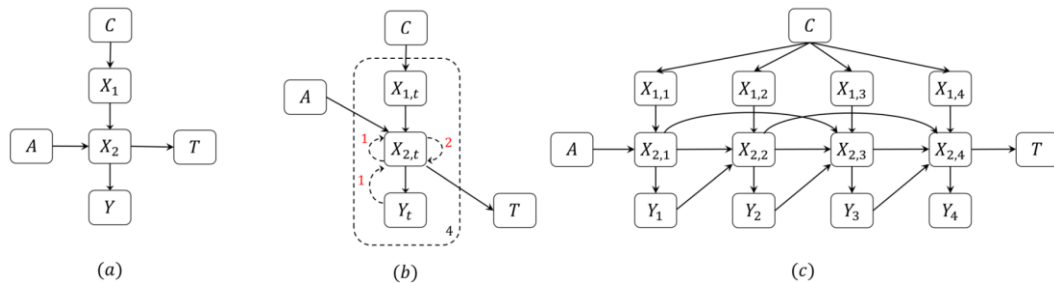


**Figure 8.1** (a) The initial network of a DBN (typical Bayesian network), (b) the 2TBN or a second order DBN, (c) the unrolled DBN model for  $T=4$  slices.

## 8.3 Quantifying Resilience Using Bayesian Network

### 8.3.1 Static resilience model

In this work, we adopt a model based on the resilience definition provided by [Bruneau et al. \(2003\)](#) and [Bruneau and Reinhorn \(2007\)](#), who describe the resilience of a system using the following three indicators (hereafter we call them the three resilience pillars): reduced failure probability (*reduced vulnerability*); reduced

consequences from failure (*robustness*); and reduced time to recovery (*recoverability*) (Figure 8.2):

- Reduced vulnerability: the reduced likelihood of damage & failure to critical infrastructure systems and components ( $P_1$ );
- Robustness: the damage level, in terms of injuries, lives lost, physical damage, and negative economic and social impacts ( $P_2$ );
- Recoverability: the time required to restore a specific system or a set of systems to the normal or pre-disaster level of functionality ( $P_3$ ).

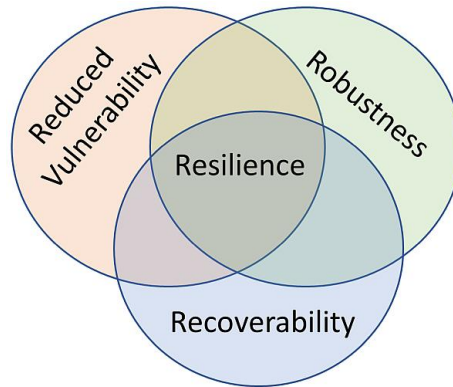


**Figure 8.2** The three resilience pillars

A system with a low probability of failure, high robustness, and high recoverability capacity is considered resilient. The three resilience pillars can be typically described using a set of indicators representing the analyzed system. The choice of indicators can be made by experts in the relevant field. Figure 8.3 shows a general resilience functionality curve where the three resilience pillars are allocated to three time-spans:

- The pre-disaster time span: defined by the system's probability of failure;
- The disaster time span: determined by the robustness level of the system;
- Post-disaster time span: defined by the recovery capacity of the system.

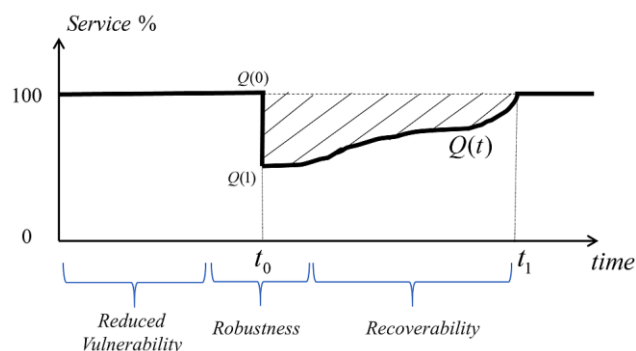


**Figure 8.3** A general resilience function of a system

### 8.3.2 Network structure and elements connectivity

Assume that we have a system that is composed of 7 indicators ( $X_1, X_2, \dots, X_7$ ). The indicators are connected to the three resilience pillars according to their

relevance. Such connections can be obtained from past experience or expert knowledge. One indicator can contribute to multiple pillars, as shown in the Bayesian network in Figure 8.4 where indicator  $X_4$  is connected to  $R_1$  and  $R_2$  while  $X_7$  is connected to  $R_2$  and  $R_3$ . The final output (*resilience index*) represents a combination of all factors that contribute towards the resilience pillars.

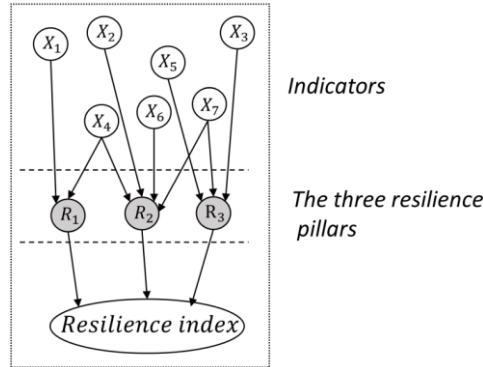


**Figure 8.4** Bayesian network to compute the resilience index of a static system

### 8.3.3 Joint probability distribution

Each node in a Bayesian network is characterized by a probability distribution. All probabilities together form the joint probability distribution (JPD) of the BN. The JPD of a BN can be written as follows:

$$P(Z) = \prod_{i=1}^N P(Z^i | Pa(Z^i)) \quad (8.6)$$

where  $Z$  is the set of all variables,  $P(Z)$  is the joint probability of the variables,  $Pa(Z^i)$  is the set of variables that are parents of  $Z^i$ ,  $P(X_i | Pa(X_i))$  is the local probability distribution. Considering the system in Figure 8.4, the JPD can be calculated using Eq. (8.7).

$$\begin{aligned} P(X, R, Re) = & P(X_1) \cdot P(X_2) \cdot P(X_3) \cdot P(X_4) \cdot P(X_5) \cdot P(X_6) \cdot P(X_7) \cdot \\ & P(R_1 | X_1, X_4) \cdot P(R_2 | X_2, X_4, X_6, X_7) \cdot P(R_3 | X_3, X_5, X_7) \cdot \\ & P(Re | R_1, R_2, R_3) \end{aligned} \quad (8.7)$$

## 8.4 Case study 1: resilience evaluation of the state of Brazil

### 8.4.1 Model definition: Hyogo Framework for Action

Given the increase in the number of natural and man-made disasters, the United Nations (UNISDR) have formulated a structured approach to help communities cope with unexpected disruptions. The conceived framework, firstly presented in the 2005 UNISDR report ([ISDR 2005](#); [UNISDR 2008](#)), is known as the Hyogo

Framework for Action (HFA). It is now considered a global blueprint for minimizing risk associated with natural hazards through the implementation of national laws for risk management and control. The HFA was originally conceptualized in Kobe, Japan with the goal of encouraging countries to implement resilient measures in their respective laws. The lifespan for the implementation was from 2005 to 2015. After that, each of the participating countries was required to submit a report (a detailed questionnaire) on their own progress. A score was then given by the UN to each of the submitted reports based on the progress each country had made ([UNISDR 2011](#); [Kammouh et al. 2018b](#)). The progress recorded by every country is computed on the basis of a five-point scale for each indicator, where ‘one point’ indicates weak progress while ‘five points’ implies a great endeavor and commitment in that specific area. Table 3.4 reports the scores of the 22 indicators for 37 countries assessed by the United Nations.

The objective of the HFA is the significant reduction in losses after disasters. Following the resilience model introduced in Section 8.3.1, the HFA indicators are unfolded under the three resilience pillars:

- **Reduced Vulnerability:** includes consideration of disaster risk that is aimed at preventing and mitigating disaster as well as reducing vulnerability;
- **Robustness:** Strengthening of institutions and mechanisms at all level aiming at increasing resilience;
- **Adaptive and Recovery capacity:** Structural embedding of risk reduction methods for emergency preparation, response, and recovery.

To increase the level of detail and to convert the strategic goals into operationalizable activities, the UNISDR introduces five priorities:

1. Ensure disaster risk reduction;
2. Identify, assess and monitor disaster risks and enhance early warning;
3. Use available physical and non-physical resources to build a culture of safety and resilience;
4. Reduce the underlying risk factors;
5. Strengthen disaster preparedness for effective response.

Each of the five priorities is further disaggregated into four to six indicators, summing up to a total of twenty-two (Table 8.1). The indicators refer to the implementation of activities, mechanisms, or policies with the aim of risk reduction, preparation, and recovery.

## **8.4.2 Network structure and elements connectivity**

To build the network, a conceptual linkage between the indicators and the resilience pillars is needed. Despite not being present in the UNISDR report ([ISDR 2005](#); [UNISDR 2008](#)), the assignment of the activity to one of the resilience pillars is performed as follows:

- If the indicator clearly refers to a regulatory requirement or action with proactive intent of risk reduction, it is assigned to P<sub>1</sub>;
- If the indicator clearly refers to the implementation of institutional mechanisms or the building of resources for the proactive establishment of resilience capabilities, it is assigned to P<sub>2</sub>;
- If the indicator clearly refers to the implementation of practices, mechanisms, and programs for emergency response and recovery, it is assigned to P<sub>3</sub>. Note that it is possible for an indicator to affect more than one resilience pillar.

Table 8.1 shows a list of the indicators of the HFA grouped by priority. The BN is built following the procedure described in Section 8.3.2 (Figure 8.5). It can be seen that P<sub>1</sub> is influenced by seven indicators (Q<sub>1</sub>, Q<sub>2</sub>, Q<sub>13</sub>, Q<sub>14</sub>, Q<sub>15</sub>, Q<sub>16</sub>, and Q<sub>19</sub>), P<sub>2</sub> is influenced by eleven indicators (Q<sub>3</sub>, Q<sub>4</sub>, Q<sub>5</sub>, Q<sub>6</sub>, Q<sub>8</sub>, Q<sub>9</sub>, Q<sub>11</sub>, Q<sub>12</sub>, Q<sub>19</sub>, Q<sub>21</sub>, and Q<sub>22</sub>), while strategic P<sub>3</sub> is impacted by eight indicators (Q<sub>7</sub>, Q<sub>8</sub>, Q<sub>10</sub>, Q<sub>11</sub>, Q<sub>17</sub>, Q<sub>18</sub>, Q<sub>20</sub>, and Q<sub>21</sub>). Only four indicators present an overlap between different resilience pillars: Q<sub>8</sub>, Q<sub>11</sub>, Q<sub>21</sub> (between P<sub>2</sub> and P<sub>3</sub>) and Q<sub>19</sub> (between P<sub>1</sub> and P<sub>2</sub>).

**Table 8.1** List of indicators of the Hyogo Framework for Action grouped by priority (UNISDR 2011).

Priority	Indicator	Resilience pillar
(1) Ensure that disaster risk reduction (DRR) is a national and a local priority with a strong institutional basis for implementation	Q1- National policy and legal framework for disaster risk reduction exist with decentralized responsibilities and capacities at all levels.	P1
	Q2- Dedicated and adequate resources are available to implement disaster risk reduction plans and activities at all administrative levels	P1
	Q3- Community Participation and decentralization is ensured through the delegation of authority and resources to local levels	P2
	Q4- A national multi-sectoral platform for disaster risk reduction is functioning.	P2
(2) Identify, assess and monitor disaster risks and enhance early warning	Q5- National and local risk assessments based on hazard data and vulnerability information are available and include risk assessments for key sectors.	P2
	Q6- Systems are in place to monitor, archive and disseminate data on key hazards and vulnerabilities	P2
	Q7- Early warning systems are in place for all major hazards, with outreach to communities.	P3
(3) Use knowledge, innovation, and education to build a culture of safety and resilience at all levels	Q8- National and local risk assessments take account of regional/transboundary risks, with a view to regional cooperation on risk reduction.	P2-P3
	Q9- Relevant information on disasters is available and accessible at all levels, to all stakeholders (through networks, development of information sharing systems etc.)	P2
	Q10- School curricula, education material, and relevant training include disaster risk reduction and recovery concepts and practices.	P3
	Q11- Research methods and tools for multi-risk assessments and cost-benefit analysis are developed and strengthened.	P2-P3
(4) Reduce the underlying risk factors	Q12- Countrywide public awareness strategy exists to stimulate a culture of disaster resilience, with outreach to urban and rural communities.	P2
	Q13- Disaster risk reduction is an integral objective of environment-related policies and plans, including for land use natural resource management and adaptation to climate change.	P1
	Q14- Social development policies and plans are being implemented to reduce the vulnerability of populations most at risk.	P1
	Q15- Economic and productive sectorial policies and plans have been implemented to reduce the vulnerability of economic activities	P1
	Q16- Planning and management of human settlements incorporate disaster risk reduction components, including enforcement of building codes.	P1
	Q17- Disaster risk reduction measures are integrated into post-disaster recovery and rehabilitation processes	P3
(5) Strengthen disaster preparedness for effective response at all levels	Q18- Procedures are in place to assess the disaster risk impacts of major development projects, especially infrastructure.	P3
	Q19- Strong policy, technical and institutional capacities and mechanisms for disaster risk management, with a disaster risk reduction perspective, are in place.	P1-P2
	Q20- Disaster preparedness plans and contingency plans are in place at all administrative levels, and regular training drills and rehearsals are held to test and develop disaster response programs.	P3
	Q21- Financial reserves and contingency mechanisms are in place to support effective response and recovery when required.	P2-P3
	Q22- Procedures are in place to exchange relevant information during hazard events and disasters, and to undertake post-event reviews	P2

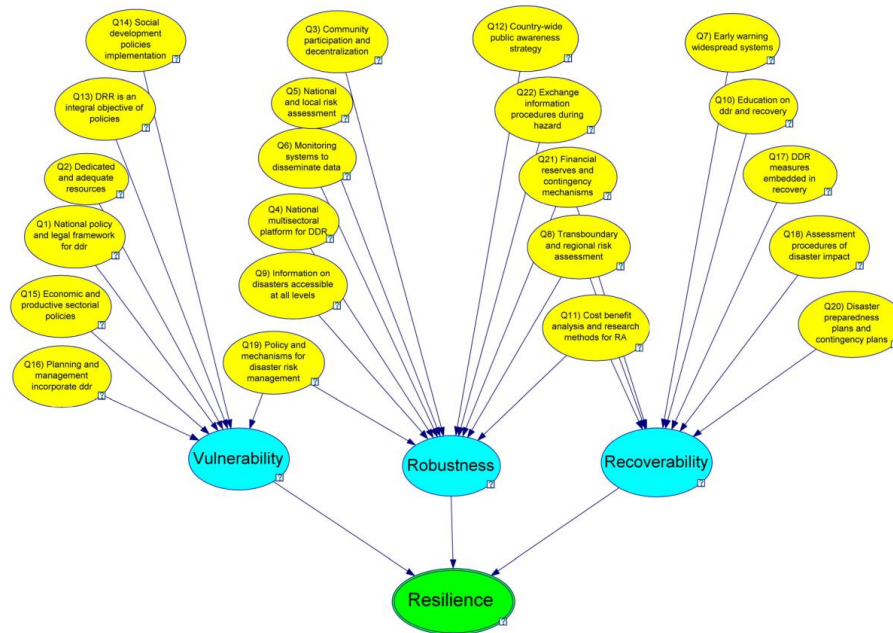


**Figure 8.5** Bayesian Network of the Hyogo framework indicators

### 8.4.3 Probability tables and inference

#### 8.4.3.1 Unconditional Probability Tables for the father nodes (indicators)

A five-level spectrum is assigned to each indicator: High (H), Good (G), Medium (M), Low (L), and Vulnerable (V). We have opted for a five-level scale for the indicators as proposed in (UNISDR, 2011), who assessed the indicators based on a 5-point scale. In the case study, the indicators take deterministic values, which are the values obtained from the collected data following the study done in (ISDR 2005) (see Table 3.4). For the sake of this study, the results obtained by the United Nations are translated into performance levels ( $5 = High$ ,  $4 = Good$ ,  $3 = Medium$ ,  $2 = Low$ ,  $1 = vulnerable$ ). The indicators are assumed equally weighted since assigning different weights to the indicators can be arbitrary and not defensible. Note that in the case of total lack of information, a uniform distribution can be assigned to the indicator states.

#### 8.4.3.2 Conditional Probability Tables for the son nodes (resilience pillars)

Once the connections between the son nodes (i.e. resilience pillars) and the father nodes (i.e. indicators) are completed, the CPTs of the resilience pillars given the indicators' states must be defined. Only three levels are assigned to each resilience pillar node (High (H), Medium (M), and Low (L)) to maintain a low complexity of the network. To define the CPTs of the pillars, the five states of the indicators, high, good, medium, low, and vulnerable have been coded as 4, 3, 2, 1, 0 respectively. The sum of the numerical values of the father nodes under a son node is computed and then divided for the maximum value, building as a global relative value  $x$  for the son node Eq. (8.8).

$$x = \frac{\sum_{i=1}^n y_i}{\sum_{i=1}^n \max_i} = \frac{\sum_{i=1}^n y_i}{n \times \max} \quad (8.8)$$

where  $x$  is the global relative value for the analyzed son node,  $i$  is the father node index,  $n$  is the number of father nodes under a son node,  $y_i$  is the value of the father node  $i$ ,  $\max_i$  is the maximum value a father node  $i$  can take (fixed for all nodes).

To illustrate in an example, consider three father nodes [A; B; C] each with a three-level scale (High, Medium, and Low), converted to (2, 1, and 0) respectively. Assuming a combination of [Medium, Medium, High] respectively for the three father nodes [A; B; C], which is equivalent to [1; 1; 2], the value  $x$  is computed as follows:

$$x = \frac{1+1+2}{2+2+2} = 0.667 \quad (8.9)$$

For each combination of father nodes values, the distribution among the three levels (High, Medium and Low) of the son node S is calculated as  $x^2$ ,  $2x(1-x)$ , and  $(1-x)^2$  respectively. This distribution ensures the normalization of the distribution and a suitable continuous parametrization, being a binomial distribution where the probability of success is  $x$  (Lewis 2011). A portion of the CPT of the son node S is presented in Table 8.2.

**Table 8.2** A CPT of a Son node given the states of the father nodes

Father nodes			Global value	States distribution of the Son Node S		
P1	P2	P3	$x = \frac{\sum_{i=1}^n y_i}{n \times \max}$	High $x^2$	Medium $2x(1-x)$	Low $(1-x)^2$
2	2	2	1.00	1.0000	0.0000	0.0000
2	2	1	0.83	0.6944	0.2778	0.0278
2	2	0	0.67	0.4444	0.4444	0.1111
2	1	2	0.83	0.6944	0.2778	0.0278
2	1	1	0.67	0.4444	0.4444	0.1111
2	1	0	0.50	0.2500	0.5000	0.2500
2	0	2	0.67	0.4444	0.4444	0.1111
2	0	1	0.50	0.2500	0.5000	0.2500
2	0	0	0.33	0.1111	0.4444	0.4444
1	2	2	0.83	0.6944	0.2778	0.0278
...	...	...	...	...	...	...

For the final output (resilience node in Figure 8.5), five states have been defined: High, Good, Moderate, Low, and Vulnerable. In this case, five degrees are preferred for a more accurate understanding of the output level. The same procedure described in the previous paragraphs applies here with the resilience node being the son node and the resilience pillars being the father nodes.

## 8.4.4 Results

Figure 8.6 shows a Bayesian network applied to the data of the country “Brazil” (row 26 in Table 3.4). The analysis has been done using GeNIe modeler, a graphical user interface that allows for interactive model building and learning based on the Bayes’ inference theory (BayesFusion ; BayesFusion 2016). The top level of the network presents the main activities to be performed at the national and local levels, the intermediate level includes the three resilience pillars, and the bottom level node is the output of the network (i.e., resilience).

As can be noticed in Figure 8.6, the three resilience pillars have a probability distribution for their different states despite that the indicators are deterministic. This is caused by the CPTs we previously defined as well as the characteristics of the Bayesian inference adopted in the study. The final output of resilience presents a range of uncertainty (16% *High*, 28% *Good*, 31% *Moderate*, 19% *Low*, and 7% *Vulnerable*) (Note: the sum is 101 instead of 100 because the tool used in the analysis rounds the values to the nearest whole number). In the analyzed scenario, the resilience state of the country Brazil is most likely to be *Moderate* given that this state has obtained the highest probability.

The Bayesian network can also be employed in a backward analysis. A deterministic resilience state can be set (for instance *Good*) and the output would be the levels of the indicators required to achieve the assumed resilience state. This is rather useful in case of system design or system improvement.

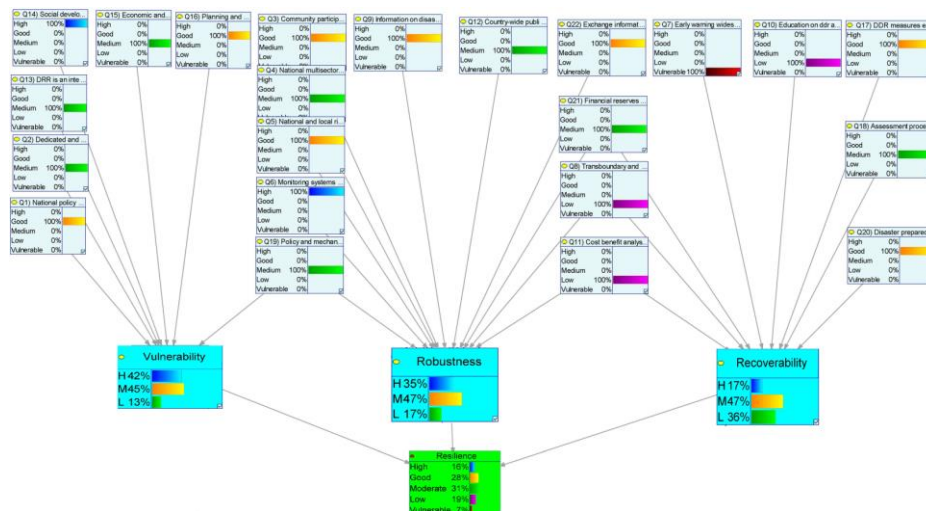


Figure 8.6 BN analysis and resilience results of the country “Brazil”

## 8.5 Time-dependent resilience analysis using DBN

In general, the resilience of a system tends to be a process rather than a state; thus, accounting for the performance variation of a system can be important. Ordinary Bayesian Networks are unable to account for the time dimension in the

analysis as they are limited to static systems. In this section, we propose a new methodology to assess the resilience of engineering systems in a dynamic manner.

### 8.5.1 Dynamic resilience model

The resilience model used in the dynamic resilience analysis is based on the resilience definition by [Bruneau and Reinhorn \(2007\)](#) who describe the resilience of a system using four components, also called the four Rs of resilience (4R's):

- *Robustness* ( $R_1$ ): refers to the ability of a system to stand a certain level of stress preserving its functionality;
- *Redundancy* ( $R_2$ ): indicates the alternative resources in the recovery stage when the primary ones are inadequate;
- *Rapidity* ( $R_3$ ): the capacity to contain losses and avoid future disruption. It represents the slope of the functionality curve during the recovery phase;
- *Resourcefulness* ( $R_4$ ): considers the human factor and the capacity to move needed resources.

This model is more detailed and more suitable to study dynamic events than the one described in Section 8.3.1; therefore, this model will be used hereafter. As shown in Figure 8.7, the first two resilience components ( $R_1$  and  $R_2$ ) define the damage level the system may encounter if exposed to a certain hazard. Robust and redundant systems would most likely experience less damage and function almost normally after the disaster. On the other hand, once damage occurs, the system's recovery starts. The recovery process is defined by the recovery capacity and resources availability, such as human resources. Thus, the other two components ( $R_3$  and  $R_4$ ) interfere during the recovery stage as they are the main drivers of the system's recovery.

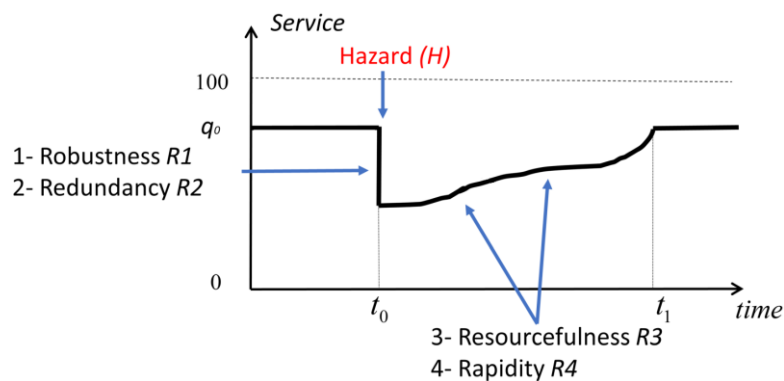


**Figure 8.7** The four resilience components (4R's) and their interaction with the resilience curve

### 8.5.2 Network structure and elements connectivity

DBN is a series of Bayesian networks with changing conditions. The elements connectivity within a single time step of a DBN is treated similarly to what introduced before (see Section 8.3.2 and Figure 8.4). One main characteristic of

DBN is that elements are connected through different time-steps. For example, element  $A_t$  can be linked to element  $B_{t+1}$  using a temporal link if element  $B_{t+1}$  has a dependency on  $A_t$ , where  $t$  is the time step. The connections between elements at different time steps are done using expert knowledge or from past data. Figure 8.8 shows a DBN where the individual networks at different time steps are connected with one another. In our methodology, an element in a BN at time-step  $t$  can only affect itself at time-step  $t+1$  (i.e.,  $A_t$  affects  $A_{t+1}$  and  $B_t$  affects  $B_{t+1}$ ).

Regarding the four resilience components (4R's), they are incorporated in the network at different time-steps. In Figure 8.8, the first step ( $t=1$ ) corresponds to the initial state of the system (i.e., before hazard occurrence). At this stage, none of the 4R's is involved as the aim here is to assess the initial performance of the system. The second step ( $t=2$ ) is dedicated to assessing the damage that would incur if a hazard of a certain magnitude occurs. The level of damage, or the drop in the functionality, can be determined by acquiring information about the hazard (H) and the system's characteristics (i.e.,  $R_1$  and  $R_2$ ). The combination of the parameters H,  $R_1$ , and  $R_2$  can provide valuable information on how a system with a predefined initial state would behave. Thus, the two resilience components  $R_1$  and  $R_2$  are thus connected to the DBN at the second time-step ( $t=2$ ). Once the drop in the functionality is determined, the recovery needs to be evaluated. Since recovery is not an instantaneous action, several Bayesian networks are needed. The recovery period is divided into a finite number of time-steps, each with a Bayesian network. Information about the rapidity and the resourcefulness ( $R_3$  and  $R_4$ ) of the system is integrated at all recovery time-steps as they will define how the variables (i.e., the indicators) will evolve from one step to another. Therefore, the same Bayesian network is copied from time-step  $t=3$  until time step  $t=T$ .

The result of each BN is a performance point. The collection of the performance points creates a resilience function that shows the changes in the system's performance, starting from a stable state (the first uniform part of the function in Figure 8.8) and ending with a stable state, when the system is fully recovered (the second uniform part of the function). Once obtained, the resilience function can be used to get a resilience index. One method uses the area above the resilience curve and links it to the notion "loss of Resilience" ([Bruneau and Reinhorn 2007](#); [Cimellaro et al. 2010](#)) while other methods consider other metrics to quantify the resilience ([Sharma et al. 2018](#)).

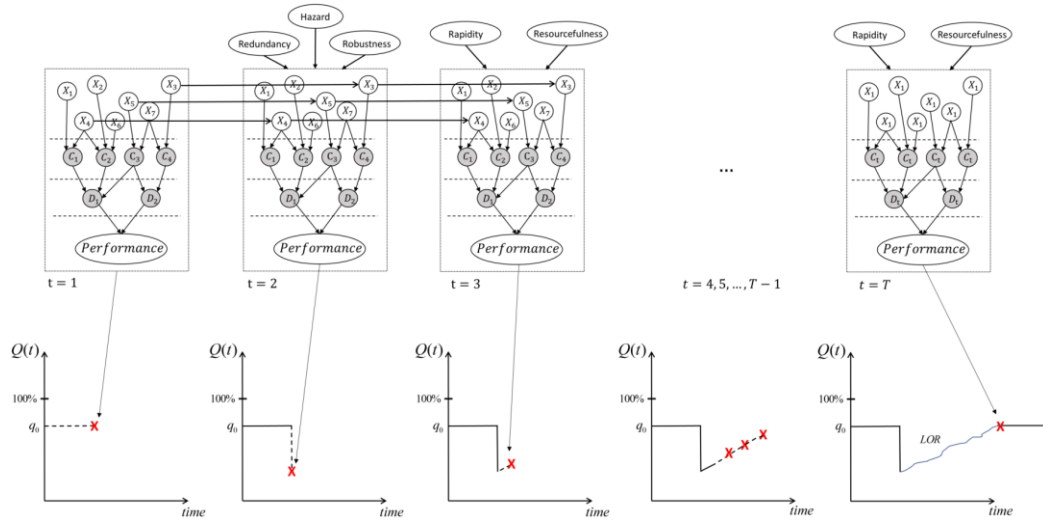


**Figure 8.8** Dynamic Bayesian network of an engineering system considering external factors such as the resilience characteristics (4R's) and the Hazard

### 8.5.3 Joint probability distribution

The proposed dynamic resilience analysis using the DBN approach can be mathematically written in probabilistic terms, as follows:

$$\begin{aligned}
 P(C, Z_{1:T}, H, R1, R2, R3, R4) = & \left[ P(C) \cdot \prod_{i=1}^N P(Z_{t=1}^i | Pa(Z_{t=1}^i), C^i) \right] \\
 & \cdot \left[ P(H) \cdot P(R1) \cdot P(R2) \prod_{i=1}^N P(Z_{t=2}^i | Pa(Z_{t=2}^i), C^i, H^i, R1^i, R2^i) \right] \\
 & \cdot \left[ P(R3) \cdot P(R4) \prod_{t=3}^T \prod_{i=1}^N P(Z_t^i | Pa(Z_t^i), C^i, R3^i, R4^i) \right]
 \end{aligned} \quad (8.10)$$

where  $C$  is the set of all static variables (contemporal variables),  $Z$  is the set of all dynamic variables (temporal variables),  $P(C)$  is the joint probability of the static variables,  $Pa(Z_i)$  is the set of variables that are children of  $Z_i$ ,  $H$  is the hazard variable,  $R_1$  is the Redundancy variable,  $R_2$  is the Redundancy variable,  $R_3$  is the Rapidity variable,  $R_4$  is the Resourcefulness variable,  $N$  is the number of dynamic indicators,  $T$  is the total number of time steps.

The first term on the right-hand side of Eq. (8.10) refers to the joint probability of the variables at the first time-step, the second term refers to the joint probability of the variables at the second time-step, while the third part of the equation considers the remaining time steps.

## 8.6 Case study 2: resilience evaluation of a transportation network

### 8.6.1 Model definition: Modeling the physical aspect of a transportation network

To illustrate the dynamic methodology introduced above, a case study of a typical transportation system is performed. The resilience of engineering systems can be systematically described using a layered diagram. Figure 8.9 shows a schematic representation of a general engineering system, being *resilience* the top level. The resilience node is defined using a set of dimensions. Each dimension is divided into components, and the components are further divided into indicators. The lower level of the diagram is the “Measures” layer, which provides descriptions of how the indicators can be numerically evaluated. Having different layers allows for a detailed description of the system.

For the sake of this study, a general indicator-based model to describe transportation systems is proposed. The model consists of Seven dimensions divided into 21 Components. The components are further divided into 78 indicators, which are allocated with measures to provide practical information on the computation of each indicator. The indicators included in the model have been collected from exclusively renowned literary publications. The authors have also proposed some indicators when needed to ensure the exhaustiveness of the model.

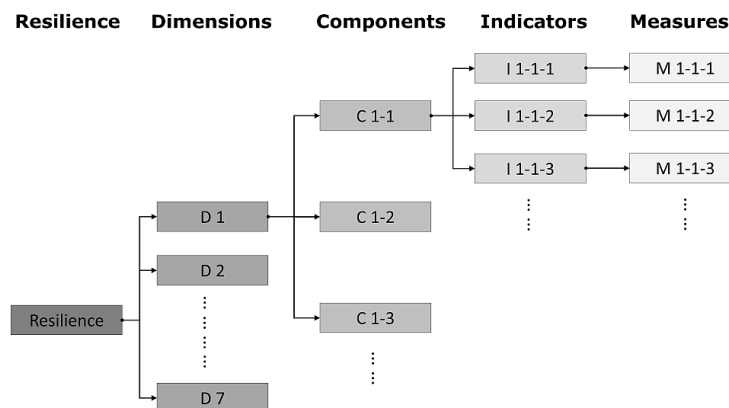


**Figure 8.9** An indicator layered-model to systematically describe engineering systems

Table 8.3 presents the seven dimensions of the proposed model: (1) Physical infrastructure, (2) User’s behavior, (3) Resources, (4) Plan, (5) Organization and management, (6) Social-economic characteristics, and (7) Environment and climate. To keep it simple, only the first dimension (Physical infrastructure) is used in this case study, and therefore only the first dimension is expanded with the list of components, indicators, and measures (Table 8.3). The last two columns in the table represent the importance factor (I) and the Nature (Nat) of the indicators, respectively. The importance factor provides a tool to weight the variables. Several methods for defining the importance factors exist in the literature. For example, ([Kammouh et al. 2019b](#)) proposed a matrix-based methodology to compute the

weight of variables based on the level of interdependency with other variables. That is, if many variables depend on a certain variable, the latter is assigned a high importance factor. Other methods suggest a subjective assignment of the weighting factors by an expert in the related field. This process is simpler but can produce inaccurate results. The Nature of the indicator (Nat) divides the indicators according to their type “static” or “dynamic”.

Figure 8.10 shows a graphical representation of a static and dynamic indicator. For static indicators, the functionality remains constant with the time given that they are not affected by hazards. Dynamic indicators, on the other hand, are affected by hazards, and consequently their functionality changes with time. Dynamic indicators are defined using a set of variables ( $q_0, q_1, T_r, q_f$ ) where  $q_0$  is the normalized functionality before the event,  $q_1$  is the residual functionality after the disaster,  $q_f$  is the functionality after recovery,  $T_r$  is the restoration time or the time needed to finish the recovery process.

Each indicator is normalized with respect to a fixed quantity, the target value (TV). The target value is an essential quantity that provides the baseline to measure the resilience of a system. The system’s existing functionality at any instance of time is compared to the target value to know how much functionality deficiency is experienced by the system.

**Table 8.3 Variables of the proposed transportation network model with corresponding importance factors (I) and nature (Nat)**

Dimension/ component/ indicator	The measure ( $0 \leq \text{value} \leq 1$ )	Reference	I	Nat
1- Physical infrastructure			3	
1-1- Links/ Connectors			3	
-Accessibility	Number of links/passageways per destination $\div$ TV	(Ip and Wang 2011)	3	D
-Road density	Number of alternative links between an origin and destination $\div$ TV	(Jenelius 2009)	3	D
-Road width	The average width of road $\div$ TV	(Jenelius 2009)	2	S
-Lanes of road	Number of lanes available $\div$ TV	(Litman 2006)	2	D
-Link (road, track, etc.) condition	% links with full functionality during the event		3	D
1-2- Vehicles			2	
-Mode of transport	Number of multi-mode choices per destination $\div$ TV	(Ip and Wang 2011)	3	D
-Service level	The average speed of vehicles in normal condition $\div$ TV		1	S
-Characteristics of vehicles	The degree of preference for specific vehicles (regarding performance, comfort level, etc.) $\div$ TV		1	S
1-3- Other Facilities/ Structures			3	
-Quality of facilities	1- (% deficiency of facilities in past events $\div$ TV)	(Tamvakis and Xenidis 2012)	3	S
-Critical components	Number of roundabout/emergency lanes $\div$ TV		2	S

-Maintenance of facilities	Number of maintenances during an interval of time $\div$ TV	( <a href="#">Tamvakis and Xenidis 2012</a> )	3	S
-Essential infrastructure robustness	% infrastructures that remained operational during emergencies in past events	( <a href="#">Reduction 2012</a> )	2	S
-Traffic load capacity	Number of excessive capacity (emergency lanes, tracks, airlines, etc.) $\div$ TV	( <a href="#">Cox et al. 2011</a> )	3	D
-Urban form	Number of city centers per 100,000 people $\div$ TV	( <a href="#">Mishra et al. 2012</a> )	3	S
-Size of the network (connectivity)	Number of connectivity of intersection $\div$ TV	( <a href="#">Zhang et al. 2011</a> )	2	D
-Size of the network (betweenness)	1- (Number of betweenness of intersections $\div$ TV)	( <a href="#">Zhang et al. 2011</a> )	2	D
1-4- Accessories			1	
-Tool kit inside vehicles	1 (Presence of tool kits, like extinguisher, escape hammer, etc.); 0 (otherwise)		2	S
-Path environment	Number of safety elements (isolation strips, traffic lights, etc.) per km $\div$ TV	( <a href="#">Soltani-Sobh et al. 2016</a> )	2	S
1-5- Serviceability			2	
-Characteristics of traffic lines	Frequency and capacity of each line $\div$ TV	( <a href="#">Dorbritz 2011</a> )	3	D
-Travel time reliability	number of punctual services assisted by control system $\div$ total number of service	( <a href="#">Leu et al. 2010</a> )	2	S
2- User's behavior				
3- Resources				
4- Plan				
5- Organization and management				
6- Social-economic characteristics				
7- Environment and climate				

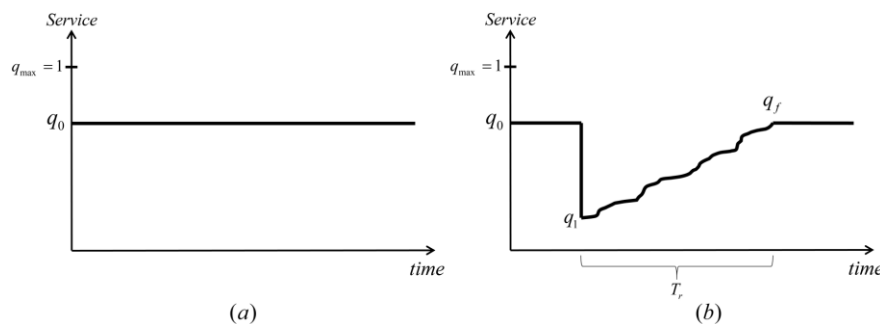


**Figure 8.10** a) Event-non-sensitive indicator (static) b) event-sensitive indicator (dynamic)

## 8.6.2 Network structure and elements connectivity

Figure 8.11 presents the network structure and elements connectivity using the software GeNIe ([BayesFusion 2016](#)). The network has been built following the information provided in Section 8.5.2. A color code is used to distinguish the variables in the network. Variables that are outside the box are static variables. They are assigned unconditional probability tables (UPTs) that do not change throughout the analysis. Variables inside the green box are dynamic variables. The dynamic

indicators (i.e., variables inside the green box and colored in yellow) are assigned UPTs for the first time-step and CPTs for the remaining time steps. The CPTs are used to define the functionality of the indicator at time  $(t+1)$  given its functionality at time  $(t)$  and given external variables (i.e., damage and recovery variables). The damage variables  $H$ ,  $R_1$ , and  $R_2$  are used to determine the amount of damage the indicators are exposed to following the hazard. Therefore, the damage variables interfere only at the second time-step (see Figure 8.8) and their effect is reflected in the CPTs of the dynamic indicators at time slice 2. On the other hand, the recovery variables  $R_3$  and  $R_4$  feed the dynamic indicators from time slice 3 until the last time-slice (see Figure 8.8). The effect of these variables is reflected in the CPTs of the dynamic indicators for all time slices starting from time slice 3. For the first time-slice, the system is assessed for its initial condition. That is, the effect of the damage and recovery variables is not considered, and so the dynamic indicators have no father nodes for this time slice. The software used for the analysis allows determining at what step each variable should interfere.

Other variables inside the green box are the variables colored in Orange (components) and Blue (dimensions). such variables are dynamic, and their value is defined using CPTs that consider the values of their father nodes. The father nodes of the components are the indicators while the father nodes of the dimensions are the components. The damage and recovery variables do not affect the components or the dimensions directly. Their effect is transmitted through the indicators to the lower levels of the network. The connectivity between the indicators and the components or between the components and the dimensions can be defined using expert knowledge and experience.

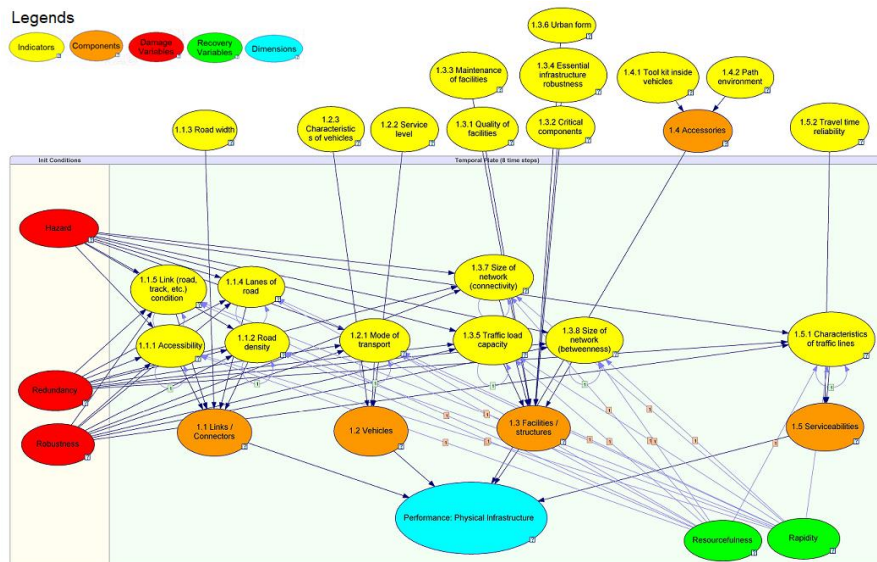


Figure 8.11 DBN connectivity of the transportation network model

### 8.6.3 Probability tables and inference

In the dynamic analysis, CPTs are assigned to variables that have father nodes in the same or different time-slice as well as the damage and recovery variables, depending on the time-slice. For example, “components” are assigned CPTs that

consider their father nodes (i.e., indicators), while each dynamic indicator (i.e., indicator that has a temporal link) is assigned a CPT that considers the indicator itself at a previous time-slice. The same procedure used in Section 8.4.3 can be used to conclude all CPTs and UPTs of the model’s variables.

## 8.6.4 Results

Five scenarios have been implemented for comparative reasons. Table 8.4 summarizes the inputs of the damage and recovery variables for the different scenarios. For the sake of simplicity, each variable is assigned a three-level scale (high, medium, and low). For all scenarios, the states of the static indicators are assigned a uniform probability distribution. This is usually done when little or no information about the variables is available. However, when data is available, different probability distribution among the three states can be set. The result of the analysis is the performance level of the system. Since the analysis is dynamic, the result is a curve showing the variation of the performance in time. Four time-steps (or time-slices) are assigned to the analysis as a time interval. In the following, each scenario is tackled separately then a comparison between the scenarios highlighting the effect of the different variables on the performance level of the system is performed.

**Table 8.4** Values for the different input variables

Input	Scenario 1 (Figure 8.12)	Scenario 2 (Figure 8.13)	Scenario 3 (Figure 8.14)	Scenario 4 (Figure 8.15)	Scenario 5 (Figure 8.16)
Hazard (H)	High	High	Low	Low	High
Redundancy (R <sub>1</sub> )	Low	Low	High	High	Low
Robustness (R <sub>2</sub> )	Low	Low	High	High	Low
Resourcefulness (R <sub>3</sub> )	High	Low	Low	High	Medium
Rapidity (R <sub>4</sub> )	High	Low	Low	High	Medium

Note: the red color implies a negative impact on the performance, the green color implies a positive impact, and the orange color implies a medium impact.

### 8.6.4.1 Scenario 1

Figure 8.12 shows the result of the first scenario. The states of the damage and recovery variables are set according to Table 8.4: the damage variables are set to negative impact (i.e., H is set to *high* while R<sub>1</sub> and R<sub>2</sub> are set to *low*) while the recovery variables are set to positive impact (i.e., R<sub>3</sub> and R<sub>4</sub> are set to *high*). To discuss the analysis results, we will focus on the node “Performance” (i.e., node in Blue color). The result is presented as a probability variation for each of the three states of the variable. From Figure 8.12, we can see that the probability for the node “Performance” being high starts very low then it increases rapidly to reach a stable state. This result is expected since our initial input for the damage is set to a *negative impact*, which caused the probability for the system’s performance of being high to be low in the beginning. On the other hand, the recovery variables have been set to *positive impact*, and this caused the probability of the system’s performance of being high to increase rapidly over time. The probability does not reach 1 because of the uncertainties introduced in the static indicators, which have been transmitted

throughout the network. As a complementary, the probability of being low starts relatively high then it reduces over time with the same rate.

#### 8.6.4.2 Scenario 2

In the second scenario (Figure 8.13), the damage variables are kept as before (high damage or negative impact) but the recovery variables have been changed from *high* to *low*. The effect of setting the recovery variables to *low* is reflected in the performance node. We can see that the initial probabilities are exactly like the first scenario, as the damage variables are the same, but the probabilities do not evolve similarly with time. The probability of being high starts low and remains low for all time steps, unlike in the first scenario where there was a noticeable increase in this probability. This is due to the recovery variables which have been set to *low*, where *low* stands for limited or no recovery activities.

#### 8.6.4.3 Scenario 3

As for the third scenario, the damage variables have been switched from negative impact to positive impact. This is done by setting H to *low* and both R<sub>1</sub> and R<sub>2</sub> to *high* (Figure 8.14). On the other hand, the recovery variables are kept *low*. The Performance node appears to start with a high probability of being high and remains constant with time. This is because, as the inputs suggest, the damage is low and there is no recovery. No recovery is observed for two reasons: a) there is no damage margin to recover, and b) the recovery variables are set to *low*.

#### 8.6.4.4 Scenario 4

In the fourth scenario, the damage variables are kept as in the third scenario (i.e., positive impact) while the recovery variables are switched back to *high* (i.e., negative impact). The result is shown in Figure 8.15 where the probability of being high starts relatively high and then slightly increases before it becomes stable. The only difference between the result in this scenario and the previous scenario is the slight increase in the performance. This slight increase in the probability is due to the high recovery capacity of the system. However, the high recovery capacity of the system was not needed in this case as there was not a damage margin to recover.

#### 8.6.4.5 Scenario 5

The last scenario is similar to the first scenario with the only difference that the recovery variables are set to *medium* instead of *high* (Figure 8.16). As a return, the increase in the probability of being high of the performance node in this scenario is less than that in scenario 1. We can see a steady increase in the probability until it reaches a stable state at the end of the curve.

In all the cases, we can see that the state “*medium*” of the performance node has a certain probability. As mentioned before, this is due to the uncertainty introduced in the static indicators which are propagated in the network. Moreover, the dynamic variables inside the box (i.e., dynamic indicators and dynamic components) are impacted by external variables such as the static indicators and the

damage/recovery variables. The dynamic indicators, in particular, are affected by the indicators themselves at previous time steps due to the presence of temporal links (arrow going from the indicator to itself).

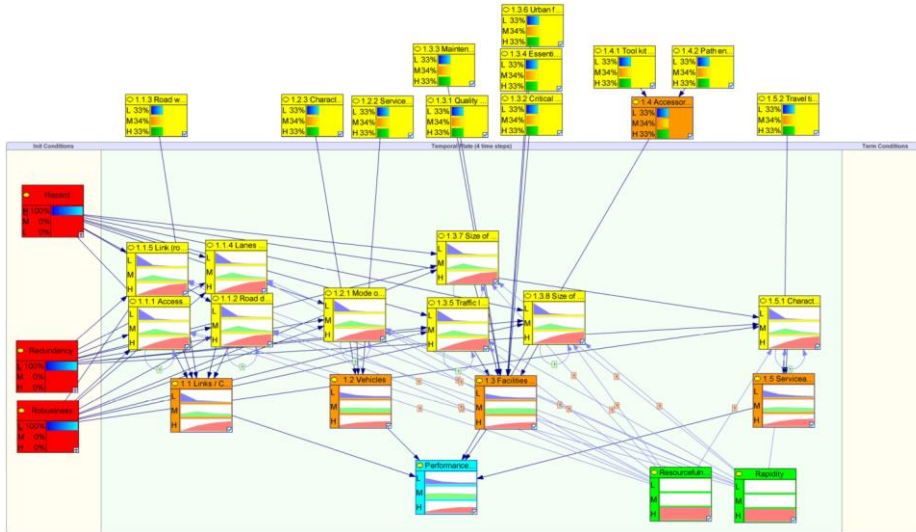


**Figure 8.12** System's performance results for the first scenario of the simulation (high damage, high recoverability)

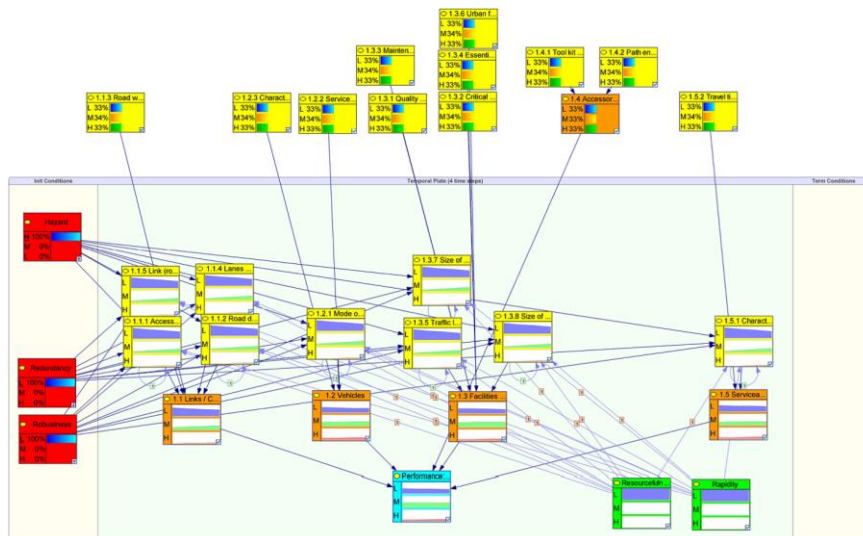


**Figure 8.13** System's performance results for the second scenario of the simulation (high damage, low recoverability)

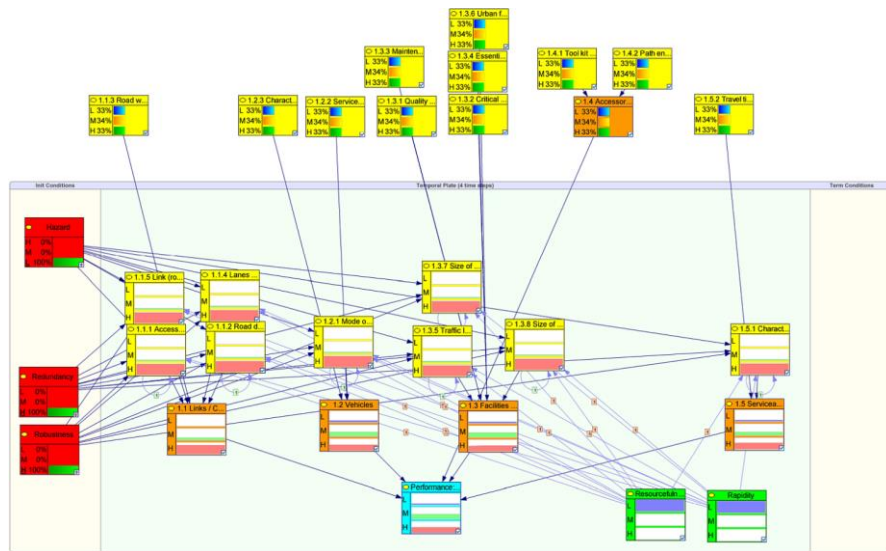


**Figure 8.14** System's performance results for the third scenario of the simulation (low damage, low recoverability)

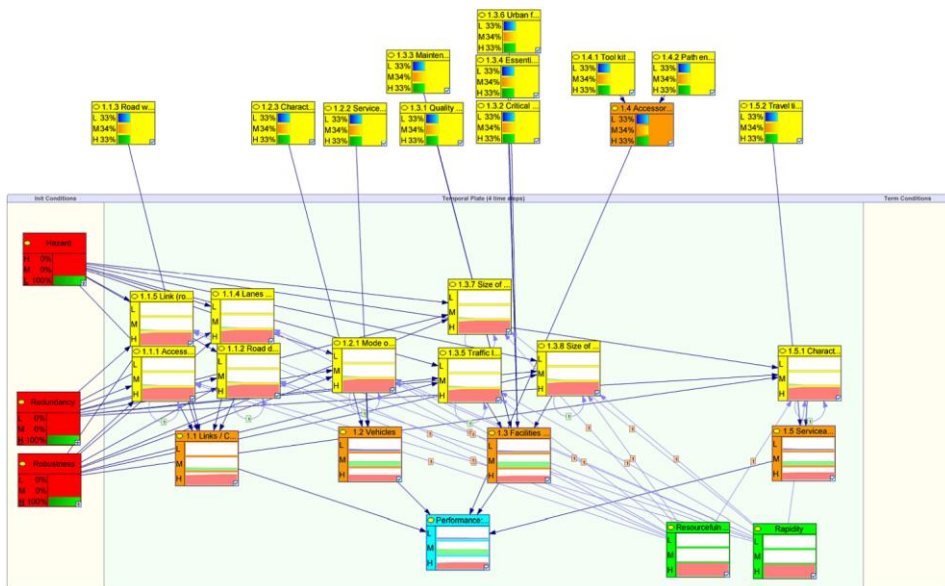


**Figure 8.15** System's performance results for the fourth scenario of the simulation (low damage, high recoverability)

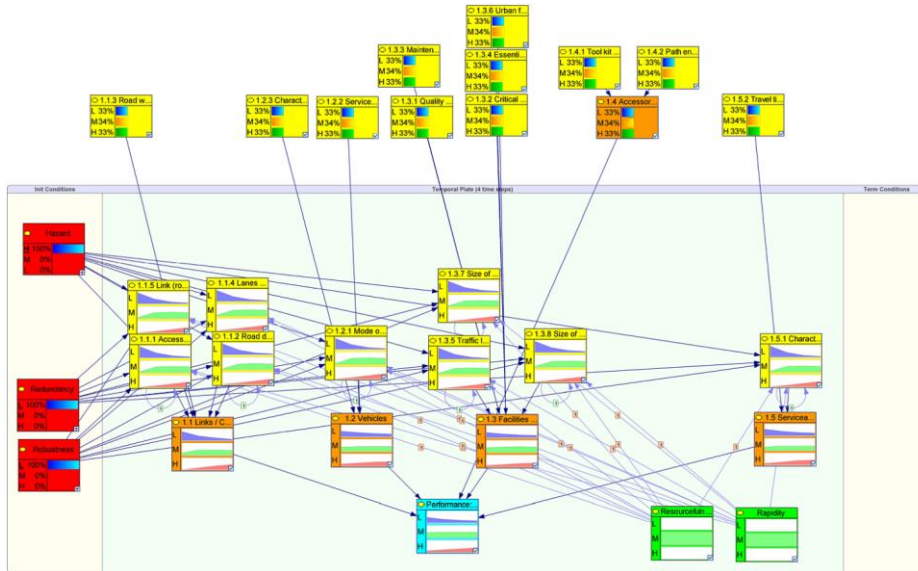


**Figure 8.16** System's performance results for the fifth scenario of the simulation (high damage, medium recoverability)

### 8.6.5 Further considerations

In our formulation in Eq. (8.10), we assume that only one hazard event can occur. The work can be extended to include a sequence of multiple hazards (e.g. foreshock and aftershock). In this case, the damage variables (H, R1, and R2) would appear in other time slices. This is shown in Figure 8.17 where the resilience function no longer has two drops in functionality instead of one drop due to the presence of two hazards. In such a case, the joint probability formation introduced before should be rewritten to account for the damage variables at other time slices. There would also be some instances where both damage and recovery variables interfere together.

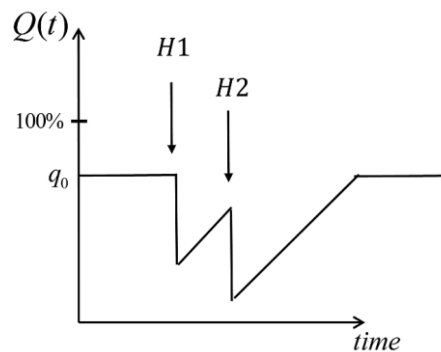


**Figure 8.17** Resilience function with multiple hazards

Moreover, the damage and recovery variables have been expressed using a single variable. However, each of the variables can be described in a separate network that consists of several variables. This allows considering more details that would not be possible to be included if only one variable is considered. Eq. (8.11) presents the damage variables as joint probabilities of other variables.

$$\begin{cases} P(H) = P(H^1, H^2, \dots, H^k) \\ P(R_1) = P(R_1^1, R_1^2, \dots, R_1^m) \\ P(R_2) = P(R_2^1, R_2^2, \dots, R_2^m) \end{cases} \quad (8.11)$$

As mentioned in Section 8.2.2.2, there is also the possibility of introducing special nodes to the first slice or last slice of the DBN when needed (Figure 8.18). This can be done by introducing the nodes A (anchor) and T (terminal). In this case, Eq. (8.10) must be adjusted accordingly to include the additional variables.

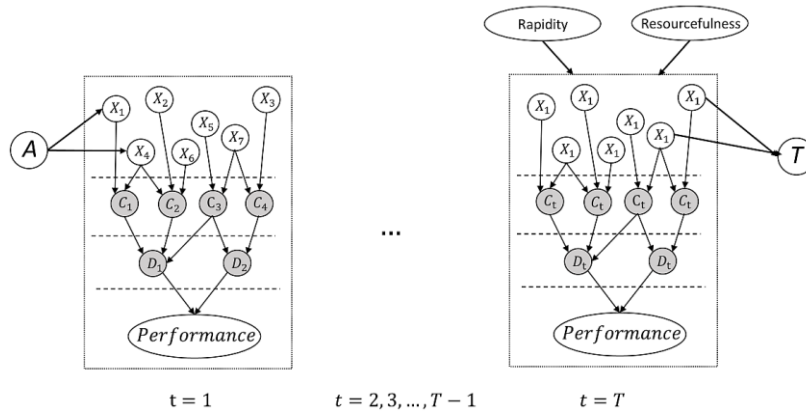


**Figure 8.18** Bayesian network with additional variables in the first and last slices

## 8.7 Concluding remarks

Unlike the static resilience analysis which assumes a constant state of a system and measures the resilience by a static quantity, the dynamic resilience analysis additionally models the evolvement of the system with time. This chapter introduced a probabilistic resilience assessment and prediction framework using the Bayesian and Dynamic Bayesian Networks (BN and DBNs). The framework employed resilience indicators for its implementation to make it more usable by decision makers in the industry. The methodology can handle both static and dynamic engineering systems using quantitative and/or qualitative data. The uncertainty in the inputs and in the variables' relationships is accounted for and propagated throughout the model; hence, the output is probabilistic in nature. Two case studies have been presented in the chapter. The first is a static system that uses the indicators of the Hyogo Framework for Action (HFA) to assess the resilience of a country, while the second is a transportation network modeled as a dynamic system. The case studies illustrate the applicability of the framework for both static and dynamic systems.

In the static analysis, the indicators are the main determinant of the resilience output. A highly uncertain state of the indicator (i.e., uniform probability distribution among the indicator's states) would result in a high standard deviation in the probability distribution of the resilience's states. For the dynamic analysis, results show a nonlinear behavior of resilience as a function of time. The recovery variables play a significant role in the resilience assessment, where the resilience

function shows an increasing trend whose slope depends on the recovery capacity of the system. The damage variables also contribute to the overall resilience output as they are the primary determinant of the system's functionality drop following the disaster event. A large functionality drop would result in a longer recovery time under the same recovery characteristics of a system. In both static and dynamic analyses, the uncertainty is introduced in the indicators' initial conditions. This is rather useful when deterministic numbers are not available to initiate the analysis.

The quantitative resilience analysis tools that can be readily available to system designers to model and quantify engineering resilience are still underdeveloped. This work aims at motivating the resilience community to agree on the universal resilience framework proposed here. The presented framework provides a tool for decision-makers to systematically learn about the state of their systems given a specific event. It allows them to improve the systems' performance using the backward analysis feature of BN. This is done by setting a desirable state of the resilience and getting the variables inputs that lead to the predefined resilience state.

Future work will be aimed at building detailed networks for the damage and recovery variables as this would allow expressing the system in more details. In addition, a procedure to evaluate the interdependency among the variables, as well as their weighting factors, will be further addressed.

# Chapter 9

## 9. Summary and conclusions

### 9.1 Summary of the dissertation

This dissertation presented a holistic disaster resilience study at different geographical levels. Chapter 3 introduced a method to assess resilience at the state level. The study is based on a previous study done by the United Nations. As a case study, the resilience of 37 countries has been quantified. Going from the global to the local level, Chapter 4 provided two methodologies to estimate the resilience of urban communities. The introduced methodologies differ in their nature; the first is deterministic and the other is fuzzy-based. The use of either one depends on data availability. That is, the first methodology requires a large amount of data for its implementation while the second can use the fuzzy characteristics to account for missing data. A case study of the city of San Francisco has been presented to illustrate the applicability of the methodologies.

Generally, a community is composed of infrastructure systems. Chapters 5 and 6 were dedicated to focus on individual infrastructure systems within a community, namely water and transportation networks. Simulation oriented approaches have been employed in both studies to achieve the objective of assessing resilience. While only the damage is assessed in these chapters, Chapter 7 provided restoration fragility curves that can be used to estimate the restoration time of different types of infrastructures following an earthquake of a certain magnitude. Chapter 7 is complimentary to the previous two chapters; that is, combining the results of Chapter 7 with those of Chapters 5 and 6 will lead to a full resilience analysis. The dissertation also presented a probabilistic method to tackle the resilience of any engineering system (Chapter 8). While this method can be a good substitute to the already introduced methodologies, the main reason it was proposed in the dissertation is to cover other systems that haven't been covered in previous chapters.

## 9.2 Concluding remarks

As seen in the results of this work and the applications provided in this thesis, the established resilience frameworks provide valuable insights into the decision-making process of community resilience. The proposed solutions are improvements to previous work carried out and can benefit decision-makers before, during and after a disaster. The objectives of this work, listed in Section 1.3, have been fully achieved. The dissertation provided new modeling techniques for complex and large-scale infrastructure systems within a community. New baselines for monitoring progress and success related to community resilience have been defined. This was accompanied by application examples of real case studies. In addition, by providing several resilience quantification methodologies at different scales, the costs and benefits of improving resilience have been highlighted. Knowing how resilient a community is would permit a better understanding of the efficiency of the resources that would be spent. The dissertation also introduced frameworks that help in assessing and prioritizing the needs and goals for communities. Decision-makers need to understand the weaknesses of their communities to be able to take proper actions that aim at efficiently enhancing the resilience level of their communities. For instance, if the weakness of a community was determined in the emergency sector, resources should be assigned for this sector. This can eventually help decision-makers take proper actions following a disaster event.

This work has also had a contribution in studying the interdependency among infrastructure systems. A new systematic interdependency method based on expert knowledge is introduced. The methodology is practical and can be applied by decision-makers in their day-to-day life. The interdependency between infrastructure systems is important to determine the functionality of one infrastructure system given the functionality of other infrastructure systems. For example, the functionality of the water network would be low if the power service is interrupted.

Going in more detail, at the country level, a framework to calculate the resilience and the resilience-based risk has been introduced. Results of the study showed that the risk of being below a certain resilience threshold depends mostly on the exposure level of that country. At the community level, two methodologies have been introduced. Choosing between the two methods depends on the availability of data and on the level of complexity sought. Results show the resilience of communities incorporates the hardness and adaptive capacity of a community and not only to the recovery capacity. Finally, at the infrastructure level, methodologies to identify the vulnerable components of infrastructure systems are introduced. Since the most vulnerable components in an infrastructure system are the main cause of resilience loss when a disaster event occurs, these components need to be prioritized when improving the overall resilience of the system.

### 9.3 Future work

In the context of the studies provided in the dissertation, there are potential opportunities to continue the effort made here and build upon it in the future. For example, at the country level, the proposed methodology is generic, and it can be applied to new data when available. The Sendai framework is a successor of the Hyogo framework, and they are now in the phase of data collection. Once the data is available, it can be used in the proposed methodology to generate updated results for the resilience of the countries. At the community level, the introduced fuzzy-based methodology can still be further developed, and case studies can be generated to illustrate the applicability of the methodology. At the infrastructure level, for the water and transportation networks analyzed, future work can focus on performing a parametric study to understand the effect of each parameter on the resilience evaluation. The methodology can be generalized to include the possibility of changing the seismic input and the geometry of the network. As for the restoration fragility curves of infrastructure, special attention can be given to the infrastructure interdependency, which can enhance the accuracy of the restoration curves. Other lifelines such as the transportation system can be included in the analysis when data is available. Finally, for the general resilience quantification methodology introduced in Chapter 8, detailed networks for the damage and recovery variables can be built as this would help in expressing the analyzed system in more details. In addition, interdependency analysis to the study the interactions between the variables as well as their weighting factors can be a topic for future research.

# References

- Abeling, T., Huq, N., Wolfertz, J., and Birkmann, J. (2014). "Interim Update of the Literature. Deliverable 1.3, emBRACE project."
- Afshar, A., and Kazemi, H. (2012). "Multi objective calibration of large scaled water quality model using a hybrid particle swarm optimization and neural network algorithm." *KSCE Journal of Civil Engineering*, 16(6), 913-918.
- Ahmadizadeh, M., and Shakib, H. (2004). "On the December 26, 2003, southeastern Iran earthquake in Bam region." *Engineering structures*, 26(8), 1055-1070.
- Allenby, B., and Fink, J. (2005). "Toward Inherently Secure and Resilient Societies." *Science*, 309(5737), 1034-1036. 10.1126/science.1111534.
- Almufti, I., and Willford, M. (2013). "REDi™ Rating System: Resilience-based Earthquake Design Initiative for the Next Generation of Buildings, Version 1.0." *October, ARUP, San Francisco, CA.*
- ANG H-S, A., and TANG, H. W. (1975). *PROBABILITY CONCEPTS IN ENGINEERING PLANNING AND DESIGN. Vol. 1, Basic Principles.*
- Ayyub, B. M. (2015). "Practical resilience metrics for planning, design, and decision making." *ASCE-ASME Journal of Risk and Uncertainty in Engineering Systems, Part A: Civil Engineering*, 1(3). 04015008.
- Baker, J. W. (2013). "An introduction to probabilistic seismic hazard analysis." *White paper version*, 2(1), 79.
- Balbi, S., Villa, F., Mojtahed, V., and Giupponi, C. (2014). "Estimating the benefits of early warning systems in reducing urban flood risk to people: a spatially explicit Bayesian model."
- Basöz, N., and Mander, J. (1999). "Enhancement of the highway transportation lifeline module in HAZUS." *National Institute of Building Sciences*, 16(1), 31-40.
- BayesFusion, L. "Smile engine and Genie modeler."
- BayesFusion, L. (2016). "GeNIE Modeler." *User Manual, Version*, 2(1).
- Beatley, T., and Newman, P. (2013). "Biophilic Cities Are Sustainable, Resilient Cities." *Sustainability*, 5(8), 3328.
- Beck, J., Kiremidjian, A., Wilkie, S., King, S., Achkire, Y., Olson, R., Goltz, J., Porter, K., Irfanoglu, A., and Casari, M. (1999). Decision support tools for earthquake recovery of businesses. *Interim report for CUREe-Kajima phase III project.*
- Berardi, G., Paci-Green, R., and Hammond, B. (2011). "Stability, sustainability, and catastrophe: applying resilience thinking to US agriculture." *Research in Human Ecology*, 18(2), 115.
- Birkmann, J. (2006). *Measuring vulnerability to natural hazards: towards disaster resilient societies*, United Nations University New York.
- Bonstrom, H., and Corotis, R. B. (2014). "First-order reliability approach to quantify and improve building portfolio resilience." *Journal of Structural Engineering*, 142(8), C4014001.

- Bowman, A. O. M., and Parsons, B. M. (2009). "Vulnerability and resilience in local government: assessing the strength of performance regimes." *State & Local Government Review*, 13-24.
- Bozorgnia, Y., and Bertero, V. V. (2004). *Earthquake engineering: from engineering seismology to performance-based engineering*, CRC press.
- Bradley, D., and Grainger, A. (2004). "Social resilience as a controlling influence on desertification in Senegal." *Land Degradation & Development*, 15(5), 451-470.
- Brocher, T. M., Baltay, A. S., Hardebeck, J. L., Pollitz, F. F., Murray, J. R., Llenos, A. L., Schwartz, D. P., Blair, J. L., Ponti, D. J., and Lienkaemper, J. J. (2015). "The Mw 6.0 24 August 2014 South Napa Earthquake." *Seismological Research Letters*, 86(2A), 309-326.
- Brody, S. D., Peacock, W. G., and Gunn, J. (2012). "Ecological indicators of flood risk along the Gulf of Mexico." *Ecological Indicators*, 18, 493-500.
- Bruneau, M., Chang, S. E., Eguchi, R. T., Lee, G. C., O'Rourke, T. D., Reinhorn, A. M., Shinozuka, M., Tierney, K., Wallace, W. A., and von Winterfeldt, D. (2003). "A framework to quantitatively assess and enhance the seismic resilience of communities." *Earthquake spectra*, 19(4), 733-752.
- Bruneau, M., and Reinhorn, A. (2007). "Exploring the concept of seismic resilience for acute care facilities." *Earthquake Spectra*, 23(1), 41-62.
- Burton, C. G. (2015). "A Validation of Metrics for Community Resilience to Natural Hazards and Disasters Using the Recovery from Hurricane Katrina as a Case Study." *Annals of the Association of American Geographers*, 105(1), 67-86. 10.1080/00045608.2014.960039.
- C.N.E. (2012). Sismo 7.6 Mw (Magnitud de Momento) samara, region de guanacaste, sector peninsula de Nicoya. Comisin Nacional de Prevencin de Riesgos y Atencin de Emergencias Gobierno de Costa Rica.
- Cai, B., Xie, M., Liu, Y., Liu, Y., Ji, R., and Feng, Q. "A novel critical infrastructure resilience assessment approach using dynamic Bayesian networks." *Proc., AIP Conference Proceedings*, AIP Publishing, 040043.
- Cardon, O.-D., Maarten, v. A., Joern, B., Maureen, F., Glenn, M., and R, M. (2012). *Determinants of Risk: Exposure and Vulnerability Managing the Risks of Extreme Events and Disasters to Advance Climate Change Adaptation*, Cambridge University Press.
- CCSF Lifelines Council (2014). Lifelines Interdependency Study. Report. San Francisco, CA: City and County of San Francisco Lifelines Council.
- Chakravarti, I. M., Laha, R. G., and Roy, J. (1967). *Handbook of Methods of Applied Statistics: Techniques of Computation, Descriptive Methods and Statistical Inference/by IM Chakravarti, RG Laha, J. Roy*, Wiley.
- Chandra, A., Acosta, J., Stern, S., Uscher-Pines, L., and Williams, M. V. (2011). *Building community resilience to disasters: A way forward to enhance national health security*, Rand Corporation.
- Chang, S., and Li, L. "Reliability analysis of highway and transportation network with paths failure." *Proc., Advanced Research and Technology in Industry Applications (WARTIA), 2014 IEEE Workshop on*, IEEE, 50-53.
- Chang, S. E., McDaniels, T., Fox, J., Dhariwal, R., and Longstaff, H. (2014). "Toward Disaster-Resilient Cities: Characterizing Resilience of Infrastructure Systems with Expert Judgments." *Risk Analysis*, 34(3), 416-434. 10.1111/risa.12133.
- Chang, S. E., and Shinozuka, M. (2004). "Measuring improvements in the disaster resilience of communities." *Earthquake spectra*, 20(3), 739-755.

- Chen, A., Kasikitwiwat, P., and Yang, C. (2013). "Alternate capacity reliability measures for transportation networks." *Journal of Advanced Transportation*, 47(1), 79-104. 10.1002/atr.216.
- Chootinan, P., Wong, S. C., and Chen, A. (2005). "A reliability-based network design problem." *Journal of Advanced Transportation*, 39(3), 247-270.
- Cimellaro, G. P. (2016). *Urban Resilience for Emergency Response and Recovery*, Springer.
- Cimellaro, G. P., Reinhorn, A. M., and Bruneau, M. (2010). "Framework for analytical quantification of disaster resilience." *Engineering Structures*, 32(11), 3639-3649. <http://dx.doi.org/10.1016/j.engstruct.2010.08.008>.
- Cimellaro, G. P., Renschler, C., Reinhorn, A. M., and Arendt, L. (2016a). "PEOPLES: a framework for evaluating resilience." *Journal of Structural Engineering, ASCE*. [http://dx.doi.org/10.1061/\(ASCE\)ST.1943-541X.0001514](http://dx.doi.org/10.1061/(ASCE)ST.1943-541X.0001514).
- Cimellaro, G. P., Renschler, C., Reinhorn, A. M., and Arendt, L. (2016b). "PEOPLES: A Framework for Evaluating Resilience." *Journal of Structural Engineering*, 04016063.
- Cimellaro, G. P., Tinebra, A., Renschler, C., and Fragiadakis, M. (2016c). "New Resilience Index for Urban Water Distribution Networks." *Journal of Structural Engineering*, 142(8), C4015014. doi:10.1061/(ASCE)ST.1943-541X.0001433.
- Cimellaro, G. P., Zamani-Noori, A., Kammouh, O., Terzic, V., and Mahin, S. A. (2016d). Resilience of Critical Structures, Infrastructure, and Communities. Pacific Earthquake Engineering Research Center (PEER), Berkeley, California, pp. 318.
- Cockburn, G., and Tesfamariam, S. (2012). "Earthquake disaster risk index for Canadian cities using Bayesian belief networks." *Georisk: Assessment and Management of Risk for Engineered Systems and Geohazards*, 6(2), 128-140.
- Cohen, O., Leykin, D., Lahad, M., Goldberg, A., and Aharonson-Daniel, L. (2013). "The conjoint community resiliency assessment measure as a baseline for profiling and predicting community resilience for emergencies." *Technological Forecasting and Social Change*, 80(9), 1732-1741. <https://doi.org/10.1016/j.techfore.2012.12.009>.
- Comerio, M. (2005). "Downtime modeling for risk management." *Proceedings of the ninth international conference on structural safety and reliability (icosar)*, G. Augusti, G. I. Schuëller, and M. Ciampoli, eds., MILLPRESS ROTTERDAM NETHERLANDS, Rome, Italy.
- Comerio, M. C. (2006). "Estimating downtime in loss modeling." *Earthquake Spectra*, 22(2), 349-365.
- Cox, A., Prager, F., and Rose, A. (2011). "Transportation security and the role of resilience: A foundation for operational metrics." *Transport policy*, 18(2), 307-317.
- Crowder, J. A., Carbone, J. N., and Demijohn, R. (2015). *Multidisciplinary systems engineering: Architecting the design process*, Springer.
- Cumming, G. S., Barnes, G., Perz, S., Schmink, M., Sieving, K. E., Southworth, J., Binford, M., Holt, R. D., Stickler, C., and Van Holt, T. (2005). "An exploratory framework for the empirical measurement of resilience." *Ecosystems*, 8(8), 975-987.
- Cutter, S. L. (2016a). "The landscape of disaster resilience indicators in the USA." *Natural Hazards*, 80(2), 741-758. 10.1007/s11069-015-1993-2.

- Cutter, S. L. (2016b). "Resilience to What? Resilience for Whom?" *The Geographical Journal*, 182(2), 110-113. 10.1111/geoj.12174.
- Cutter, S. L., Ash, K. D., and Emrich, C. T. (2014). "The geographies of community disaster resilience." *Global Environmental Change*, 29, 65-77.
- Cutter, S. L., Barnes, L., Berry, M., Burton, C., Evans, E., Tate, E., and Webb, J. (2008a). "Community and regional resilience: Perspectives from hazards, disasters, and emergency management." *Community and Regional Resilience Initiative (CARRI) Research Report*, 1.
- Cutter, S. L., Barnes, L., Berry, M., Burton, C., Evans, E., Tate, E., and Webb, J. (2008b). "A place-based model for understanding community resilience to natural disasters." *Global environmental change*, 18(4), 598-606.
- Cutter, S. L., Burton, C. G., and Emrich, C. T. (2010). "Disaster resilience indicators for benchmarking baseline conditions." *Journal of Homeland Security and Emergency Management*, 7(1).
- Davis, E., and Phillips, B. (2009). *Effective Emergency Management: Making Improvements for Communities and People with Disabilities*. National Council on Disability, Washington, DC.
- De Iuliis, M., Kammouh, O., Cimellaro, G. P., and Tesfamariam, S. (2018). "Downtime estimation of building structures using fuzzy logic." *International Journal of Disaster Risk Reduction*.  
https://doi.org/10.1016/j.ijdr.2018.11.017.
- Dorbritz, R. "Assessing the resilience of transportation systems in case of large-scale disastrous events." *Proc., Proceedings of the 8th International Conference on Environmental Engineering, Vilnius, Lithuania*, 1070-1076.
- Dynes, R. R., Haas, J. E., and Quarantelli, E. L. (1964). *Some Preliminary Observation on Organizational Responses in the Emergency Period After The Niigata, Japan, Earthquake of June 16, 1964*. DTIC Document, Ohio state univ columbus disaster research center.
- Eckel, E. B. (1967). *Effects of the earthquake of March 27, 1964, on air and water transport, communications, and utilities systems in south-central Alaska: Chapter B in The Alaska earthquake, March 27, 1964: effects on transportation, communications, and utilities*, US Government Printing Office, Washington, D.C.
- Edrissi, A., Nourinejad, M., and Roorda, M. J. (2015). "Transportation network reliability in emergency response." *Transportation Research Part E-Logistics and Transportation Review*, 80, 56-73.  
10.1016/j.tre.2015.05.005.
- Edwards, C., Eidinger, J., and Schiff, A. (2003). "Lifelines." *Earthquake Spectra*, 19(S1), 73-96.
- EERI (2003). "Preliminary Observations on the November 3, 2002 Denali Fault, Alaska, Earthquake." *EERI Newsletter*.
- Eidinger, J. (2001). "Seismic fragility formulations for water systems." *sponsored by the American Lifelines Alliance, G&E Engineering Systems Inc., web site*. < <http://homepage.mac.com/eidinger>.
- Eliades, D. "OpenWaterAnalytics/EPANET-Matlab-Toolkit." <https://it.mathworks.com/matlabcentral/fileexchange/25100-openwateranalytics-epanet-matlab-toolkit>.
- ESRI (2011). "ArcGIS Desktop: Release 10. Redlands, CA: Environmental Systems Research Institute."
- Evans, N., and McGhie, C. (2011). "The Performance of Lifeline Utilities following the 27th February 2010 Maule Earthquake Chile." *Proc.*,

- Proceedings of the Ninth Pacific Conference on Earthquake Engineering Building an Earthquake-Resilient Society*, 14-16.
- Félix, D., Branco, J. M., and Feio, A. (2013). "Temporary housing after disasters: A state of the art survey." *Habitat International*, 40, 136-141. <http://dx.doi.org/10.1016/j.habitatint.2013.03.006>.
- Fragiadakis, M., Vamvatsikos, D., and Christodoulou, S. E. "Reliability assessment of urban water networks." *Proc., 15th world conference on earthquake engineering, Lisbon, Portugal*.
- Gallopín, G. C. (2006). "Linkages between vulnerability, resilience, and adaptive capacity." *Global Environmental Change*, 16(3), 293-303. <http://dx.doi.org/10.1016/j.gloenvcha.2006.02.004>.
- Gertsbakh, I., and Shpungin, Y. (2008). "Network reliability importance measures: combinatorics and monte carlo based computations." *WSEAS Transactions on Computers*, 7(4), 216-227.
- Gertsbakh, I. B., and Shpungin, Y. (2009). *Models of network reliability: analysis, combinatorics, and Monte Carlo*, CRC Press, Inc.
- Gertsbakh, I. B., and Shpungin, Y. (2012). "Using D-spectra in network Monte Carlo: estimation of system reliability and component importance." *Recent Advances in System Reliability*, Springer, 23-31.
- Gilbert, S., and Ayyub, B. M. (2016). "Models for the Economics of Resilience." *ASCE-ASME Journal of Risk and Uncertainty in Engineering Systems, Part A: Civil Engineering*, 2(4). 04016003.
- Gillies, A. G., Anderson, D. L., Mitchell, D., Tinawi, R., Saatcioglu, M., Gardner, N. J., and Ghoborah, A. (2001). "The August 17, 1999, Kocaeli (Turkey) earthquake lifelines and preparedness." *Canadian Journal of Civil Engineering*, 28(6), 881-890.
- Giovinazzi, S., Wilson, T., Davis, C., Bristow, D., Gallagher, M., Schofield, A., Villemure, M., Eidinger, J., and Tang, A. (2011). Lifelines performance and management following the 22 February 2011 Christchurch earthquake, New Zealand: highlights of resilience. University of Canterbury. Civil and Natural Resources Engineering University of Canterbury. Geological Sciences, 2011.
- Godschalk, D. R. (2003). "Urban hazard mitigation: creating resilient cities." *Natural hazards review*, 4(3), 136-143.
- Google "Google Maps Elevation API. <https://developers.google.com/maps/documentation/elevation/intro>."
- Grover, J. (2013). "Bayesian Belief Networks (BBN) Experimental Protocol." *Strategic Economic Decision-Making*, Springer, 43-48.
- Guide, M. U. s. (1998). "The mathworks." *Inc., Natick, MA*, 5, 333.
- Guidotti, R., Gardoni, P., and Chen, Y. (2017). "Network reliability analysis with link and nodal weights and auxiliary nodes." *Structural Safety*, 65, 12-26.
- Hamburger, R., Rojahn, C., Heintz, J., and Mahoney, M. "FEMA P58: Next-generation building seismic performance assessment methodology." *Proc., 15th World Conf. on Earthquake Engineering*.
- Henry, D., and Ramirez-Marquez, J. E. (2012). "Generic metrics and quantitative approaches for system resilience as a function of time." *Reliability Engineering & System Safety*, 99, 114-122.
- Hilfinger Messias, D. K., Barrington, C., and Lacy, E. (2012). "Latino social network dynamics and the Hurricane Katrina disaster." *Disasters*, 36(1), 101-121. 10.1111/j.1467-7717.2011.01243.x.

- Hollnagel, E., Woods, D. D., and Leveson, N. (2007). *Resilience engineering: Concepts and precepts*, Ashgate Publishing, Ltd.
- Hosseini, S., and Barker, K. (2016). "Modeling infrastructure resilience using Bayesian networks: A case study of inland waterway ports." *Computers & Industrial Engineering*, 93, 252-266.
- Hosseini, S., Barker, K., and Ramirez-Marquez, J. E. (2016). "A review of definitions and measures of system resilience." *Reliability Engineering & System Safety*, 145, 47-61.
- Hulst, J. (2006). "Modeling physiological processes with dynamic Bayesian networks." *Faculty of Electrical Engineering, Mathematics, and Computer Science, University of Pittsburgh*.
- Immers, B., Yperman, I., Stada, J., and Bleukx, A. (2002). "Reliability and robustness of transportation networks." *Problem survey and examples*.
- Ip, W. H., and Wang, D. (2011). "Resilience and friability of transportation networks: evaluation, analysis and optimization." *IEEE Systems Journal*, 5(2), 189-198.
- ISDR, U. "Hyogo framework for action 2005-2015: building the resilience of nations and communities to disasters." *Proc., Extract from the final report of the World Conference on Disaster Reduction (A/CONF. 206/6)*, The United Nations International Strategy for Disaster Reduction Geneva.
- Ismail, M. A., Sadiq, R., Soleymani, H. R., and Tesfamariam, S. (2011). "Developing a road performance index using a Bayesian belief network model." *Journal of the Franklin Institute*, 348(9), 2539-2555.
- Jenelius, E. (2009). "Network structure and travel patterns: explaining the geographical disparities of road network vulnerability." *Journal of Transport Geography*, 17(3), 234-244.
- Jennings, P. C. (1971). "Engineering features of the San Fernando earthquake of February 9, 1971." *California Institute of Technology; 1st Edition edition*.
- Johansen, C., and Tien, I. (2018). "Probabilistic multi-scale modeling of interdependencies between critical infrastructure systems for resilience." *Sustainable and Resilient Infrastructure*, 3(1), 1-15.
- Jones, L. M., Bernknopf, R., Cox, D., Goltz, J., Hudnut, K., Mileti, D., Perry, S., Ponti, D., Porter, K., and Reichle, M. (2008). "The shakeout scenario." *US Geological Survey Open-File Report*, 1150, 308.
- Jovanović, A., Klimek, P., Choudhary, A., Schmid, N., Linkov, K., Øien, V. M., Sanne, J., Andersson, S., Székely, Z., and Molarius, R. (2016). "Analysis of existing assessment for resilience approaches, indicators and data sources." *Usability and limitations of existing indicators for assessing, predicting and monitoring critical infrastructure resilience. Research project: SmartResilience*, 40-41.
- Kabir, G., Sadiq, R., and Tesfamariam, S. (2016). "A fuzzy Bayesian belief network for safety assessment of oil and gas pipelines." *Structure and Infrastructure Engineering*, 12(8), 874-889.
- Kabir, G., Tesfamariam, S., Francisque, A., and Sadiq, R. (2015). "Evaluating risk of water mains failure using a Bayesian belief network model." *European Journal of Operational Research*, 240(1), 220-234.
- Kammouh, O., and Cimellaro, G. P. (2017). "Restoration Time of Infrastructures Following Earthquakes." *Proc., 12th International Conference on Structural Safety & Reliability (ICOSSAR 2017)*, IASSAR, Vienna, Austria.

- Kammouh, O., Cimellaro, G. P., and Mahin, S. A. (2018a). "Downtime estimation and analysis of lifelines after an earthquake." *Engineering Structures*, 173, 393-403. <https://doi.org/10.1016/j.engstruct.2018.06.093>.
- Kammouh, O., Dervishaj, G., and Cimellaro, G. P. (2016). "Resilience assessment at the state level." *1st International Conference on Natural Hazards & Infrastructure (ICONHIC2016)* Chania, Greece.
- Kammouh, O., Dervishaj, G., and Cimellaro, G. P. (2017). "A New Resilience Rating System for Countries and States." *Procedia Engineering*, 198(Supplement C), 985-998. <https://doi.org/10.1016/j.proeng.2017.07.144>.
- Kammouh, O., Dervishaj, G., and Cimellaro, G. P. (2018b). "Quantitative Framework to Assess Resilience and Risk at the Country Level." *ASCE-ASME Journal of Risk and Uncertainty in Engineering Systems, Part A: Civil Engineering*, 4(1), 04017033. doi:10.1061/AJRUA6.0000940.
- Kammouh, O., Gardoni, P., and Cimellaro, G. P. (2019a). "Resilience assessment of dynamic engineering systems." *MATEC Web Conf.*, 281, 01008.
- Kammouh, O., Noori, A. Z., Taurino, V., Mahin, S. A., and Cimellaro, G. P. (2018c). "Deterministic and fuzzy-based methods to evaluate community resilience." *Earthquake Engineering and Engineering Vibration*, 17(2), 261-275. 10.1007/s11803-018-0440-2.
- Kammouh, O., Zamani-Noori, A., Cimellaro, G. P., and Mahin, S. A. (2019b). "Resilience Assessment of Urban Communities." *ASCE-ASME Journal of Risk and Uncertainty in Engineering Systems, Part A: Civil Engineering*, 5(1), 04019002. doi:10.1061/AJRUA6.0001004.
- Katayama, T. (1980). "Seismic behaviors of lifeline utility systems: Lessons from a recent Japanese experience." *Natural disaster science*, 2(2), 1-25.
- Katayama, T., Kubo, K., and Sato, N. (1977). "Quantitative analysis of seismic damage to buried utility pipelines." *Proc., Proceedings Sixth World Conference Earthquake Engineering. Institute Association Earthquake Engineering, New Delhi*, 3369-3375.
- Kircher, C. A., Whitman, R. V., and Holmes, W. T. (2006). "HAZUS earthquake loss estimation methods." *Natural Hazards Review*, 7(2), 45-59.
- Klein, R. J. T., Nicholls, R. J., and Thomalla, F. (2003). "Resilience to natural hazards: How useful is this concept?" *Global Environmental Change Part B: Environmental Hazards*, 5(1-2), 35-45. <http://dx.doi.org/10.1016/j.hazards.2004.02.001>.
- Knight, S., Giovinazzi, S., and Liu, M. (2012). "Impact and Recovery of the Kaiapoi Water Supply Network following the September 4th 2010 Darfield Earthquake." *Dept. of Civil and Natural Resources Engineering. University of Canterbury. Final Year Projects*.
- Kuraoka, S., and Rainer, J. (1996). "Damage to water distribution system caused by the 1995 Hyogo-ken Nanbu earthquake." *Canadian Journal of Civil Engineering*, 23(3), 665-677.
- Kwasinski, A., Trainor, J., Wolshon, B., and Lavelle, F. M. (2016). "A Conceptual Framework for Assessing Resilience at the Community Scale." *NIST GCR*, 16-001.
- Laskey, K. B. (1995). "Sensitivity analysis for probability assessments in Bayesian networks." *IEEE Transactions on Systems, Man, and Cybernetics*, 25(6), 901-909.
- Leu, G., Abbass, H., and Curtis, N. (2010). "Resilience of ground transportation networks: a case study on Melbourne."

- Lewis, T. G. (2011). *Network science: Theory and applications*, John Wiley & Sons.
- Litman, T. (2006). "Lessons from Katrina and Rita: What major disasters can teach transportation planners." *Journal of Transportation Engineering*, 132(1), 11-18.
- Liu, X., Ferrario, E., and Zio, E. (2017). "Resilience Analysis Framework for Interconnected Critical Infrastructures." *ASCE-ASME Journal of Risk and Uncertainty in Engineering Systems, Part B: Mechanical Engineering*, 3(2), 021001-021001-021010. 10.1115/1.4035728.
- Manyena, S. B. (2006). "The concept of resilience revisited." *Disasters*, 30(4), 434-450.
- MathWorks "MATLAB. [www.mathworks.com/products/matlab.htm](http://www.mathworks.com/products/matlab.htm)".
- Mendel, J. (1995). "Fuzzy logic systems for engineering: a tutorial." *Proc., Proceedings of the IEEE*, 345-377.
- Miles, S. B., and Chang, S. E. (2011). "ResilUS: A Community Based Disaster Resilience Model." *Cartography and Geographic Information Science*, 38(1), 36-51. 10.1559/1523040638136.
- Mishra, S., Welch, T. F., and Jha, M. K. (2012). "Performance indicators for public transit connectivity in multi-modal transportation networks." *Transportation Research Part A: Policy and Practice*, 46(7), 1066-1085.
- Morrow B. (2008). Community Resilience: A Social Justice Perspective. CARRI Research Report 4 Community and Regional Resilience Institute, Oak Ridge, TN.
- Mucke, P. (2015). WorldRiskReport. United Nations University for Environment and Human Security (UNU-EHS).
- Murphy, B. L. (2007). "Locating social capital in resilient community-level emergency management." *Natural Hazards*, 41(2), 297-315.
- Murphy, K. P., and Russell, S. (2002). "Dynamic bayesian networks: representation, inference and learning."
- Nakamura, S., Aoshima, N., and Kawamura, M. (1983). "A review of earthquake disaster preventive measures for lifelines." *Proc., Proceedings of japan earthquake engineering symposium*.
- Nastev, M., and Todorov, N. (2013). "Hazus: A standardized methodology for flood risk assessment in Canada." *Canadian Water Resources Journal / Revue canadienne des ressources hydriques*, 38(3), 223-231. 10.1080/07011784.2013.801599.
- NIST (2015). Disaster Resilience Framework, . National Institute of Standards and Technology, 75% Draft for San Diego, CA Workshop
- Niu, Y.-F., Gao, Z.-Y., and Lam, W. H. (2017). "Evaluating the reliability of a stochastic distribution network in terms of minimal cuts." *Transportation Research Part E: Logistics and Transportation Review*, 100, 75-97.
- Nojima, N. (2012). "Restoration processes of utility lifelines in the great east Japan earthquake Disaster, 2011." *Proc., 15th World Conference on Earthquake Engineering (15WCEE)*, 24-28.
- Norris, F. H., Stevens, S. P., Pfefferbaum, B., Wyche, K. F., and Pfefferbaum, R. L. (2008). "Community Resilience as a Metaphor." *Theory, Set of Capacities*.
- O'Rourke, T. (1996). "Lessons learned for lifeline engineering from major urban earthquakes." *Proc., Proceedings, Eleventh World Conference on Earthquake Engineering*.

- ONEMI (2015). Anlisis Multisectorial Eventos 2015: Evento Hidrometeorolgico Marzo-Terremoto/Tsunami Septiembre. Report by the government of Chile, Chile.
- Ormsbee, L. E., and Lingireddy, S. (1997). "Calibrating hydraulic network models." *Journal-American Water Works Association*, 89(2), 42-50.
- Ouyang, M., Dueñas-Osorio, L., and Min, X. (2012). "A three-stage resilience analysis framework for urban infrastructure systems." *Structural safety*, 36, 23-31.
- Papadopoulos, G. (2016). "Chapter 6 - Hazard, Vulnerability, and Risk Assessment." *Tsunamis in the European-Mediterranean Region*, Elsevier, Boston, 137-178.
- Parehkar, A., Mousavi, S. J., Bayazidi, S., Karami, V., Shahidi, L., Azaranfar, A., Moridi, A., Shabakhti, M., Ariyan, T., and Tofigh, M. (2015). "Auto-Calibration and Optimization of Large-Scale Water Resources Systems." *World Academy of Science, Engineering and Technology, International Journal of Environmental, Chemical, Ecological, Geological and Geophysical Engineering*, 8(3), 233-239.
- Park, J., Seager, T. P., Rao, P. S. C., Convertino, M., and Linkov, I. (2013). "Integrating risk and resilience approaches to catastrophe management in engineering systems." *Risk Analysis*, 33(3), 356-367.
- Peacock, W. G., Brody, S., Seitz, W., Merrell, W., Vedlitz, A., Zahran, S., Harriss, R., and Stickney, R. (2010). "Advancing Resilience of Coastal Localities: Developing, Implementing, and Sustaining the Use of Coastal Resilience Indicators: A Final Report. Hazard Reduction and Recovery Center."
- Peeta, S., Salman, F. S., Gunneç, D., and Viswanath, K. (2010). "Pre-disaster investment decisions for strengthening a highway network." *Computers & Operations Research*, 37(10), 1708-1719.
- Peng, X., Roueche, D. B., Prevatt, D. O., and Gurley, K. R. (2016). "An Engineering-Based Approach to Predict Tornado-Induced Damage." *Multi-hazard Approaches to Civil Infrastructure Engineering*, Springer, 311-335.
- Pfefferbaum, R., Pfefferbaum, B., and Van Horn, R. (2011). Communities Advancing Resilience Toolkit (CART): The CART Integrated System. Terrorism and Disaster Center at the University of Oklahoma Health Sciences Center, Oklahoma City.
- Piemonte, R. "Indagini e studi finalizzati alla predisposizione del Piano di Tutela delle Acque. **Error! Hyperlink reference not valid.**
- Pietrzak, R. H., Tracy, M., Galea, S., Kilpatrick, D. G., Ruggiero, K. J., Hamblen, J. L., Southwick, S. M., and Norris, F. H. (2012). "Resilience in the Face of Disaster: Prevalence and Longitudinal Course of Mental Disorders following Hurricane Ike." *PLoS ONE*, 7(6), e38964. 10.1371/journal.pone.0038964.
- Pingali, P., Alinovi, L., and Sutton, J. (2005). "Food security in complex emergencies: enhancing food system resilience." *Disasters*, 29(s1), S5-S24.
- Porter, K., and Ramer, K. (2012). "Estimating earthquake-induced failure probability and downtime of critical facilities." *Journal of business continuity & emergency planning*, 5(4), 352-364.
- Pourret, O., Naïm, P., and Marcot, B. (2008). *Bayesian networks: a practical guide to applications*, John Wiley & Sons.

- Protezionecivile "Hazard maps. <http://www.protezionecivile.gov.it/>, <http://esse1-gis.mi.ingv.it/>."
- Recovery, I. (2013). "The Oregon Resilience Plan."
- Reduction, U. N. O. f. D. R. (2012). *How to Make Cities More Resilient: A Handbook for Local Government Leaders: a Contribution to the Global Campaign 2010-2015: Making Cities Resilient-My City is Getting Ready!*, UNISDR.
- Reed, D. A., and Park, J. "Lifeline performance evaluation." *Proc., 13th world conference on earthquake engineering*.
- Renschler, C. S., Frazier, A., Arendt, L., Cimellaro, G.-P., Reinhorn, A. M., and Bruneau, M. (2010). "A framework for defining and measuring resilience at the community scale: the PEOPLES resilience framework." *MCEER, Buffalo*.
- Richard, J. T. K., Smit, M. J., Goosen, H., and Hulsbergen, C. H. (1998). "Resilience and Vulnerability: Coastal Dynamics or Dutch Dikes?" *The Geographical Journal*, 164(3), 259-268. 10.2307/3060615.
- Rose, A. (2007). "Economic resilience to natural and man-made disasters: Multidisciplinary origins and contextual dimensions." *Environmental Hazards*, 7(4), 383-398. 10.1016/j.envhaz.2007.10.001.
- Rose, A., and Krausmann, E. (2013). "An economic framework for the development of a resilience index for business recovery." *International Journal of Disaster Risk Reduction*, 5, 73-83.
- Ross, T. J. (2009). *Fuzzy logic with engineering applications*, John Wiley & Sons.
- Rubinoff, P., and Courtney, C. (2008). "How resilient is your coastal community." *A guide for evaluating coastal community resilience to tsunamis and other hazards. Basins Coasts*, 1(1), 24-28.
- Sabetta, F., and Pugliese, A. (1996). "Estimation of response spectra and simulation of nonstationary earthquake ground motions." *Bulletin of the Seismological Society of America*, 86(2), 337-352.
- Scawthorn, C., Blais, N., Seligson, H., Tate, E., Mifflin, E., Thomas, W., Murphy, J., and Jones, C. (2006a). "HAZUS-MH flood loss estimation methodology. I: Overview and flood hazard characterization." *Natural Hazards Review*, 7(2), 60-71.
- Scawthorn, C., Flores, P., Blais, N., Seligson, H., Tate, E., Chang, S., Mifflin, E., Thomas, W., Murphy, J., and Jones, C. (2006b). "HAZUS-MH flood loss estimation methodology. II. Damage and loss assessment." *Natural Hazards Review*, 7(2), 72-81.
- Scawthorn, C., Miyajima, M., Ono, Y., Kiyono, J., and Hamada, M. (2006c). "Lifeline aspects of the 2004 Niigata ken Chuetsu, Japan, earthquake." *Earthquake Spectra*, 22(S1), 89-110.
- Schiff, A. J. (1995). "Northridge earthquake: lifeline performance and post-earthquake response." *New York: American Society of Civil Engineers*.
- Schiff, A. J. (1998). Loma prieta, california, earthquake of october 17, 1989: Lifelines. Professional paper, U.S. Geological Survey, US.
- Schultz, M. T., and Smith, E. R. (2016). "Assessing the resilience of coastal systems: A probabilistic approach." *Journal of Coastal Research*, 32(5), 1032-1050.
- Sematech/NIST "e-Handbook of Statistical Methods, <http://www.itl.nist.gov/div898/handbook/>, April, 2018." (April, 2018).
- Shahriar, A., Sadiq, R., and Tesfamariam, S. (2012). "Risk analysis for oil & gas pipelines: A sustainability assessment approach using fuzzy based bow-tie

- analysis." *Journal of Loss Prevention in the Process Industries*, 25(3), 505-523.
- Sharma, N., Tabandeh, A., and Gardoni, P. (2018). "Resilience analysis: A mathematical formulation to model resilience of engineering systems." *Sustainable and Resilient Infrastructure*, 3(2), 49-67.
- Sharpe, R. L. (1994). "July 16, 1990 Luzon (Philippines) earthquake. Cupertino, Calif., USA."
- Sherrieb, K., Norris, F. H., and Galea, S. (2010). "Measuring capacities for community resilience." *Social Indicators Research*, 99(2), 227-247.
- Shinozuka, M., Feng, M. Q., Lee, J., and Naganuma, T. (2000). "Statistical analysis of fragility curves." *Journal of engineering mechanics*, 126(12), 1224-1231.
- Siraj, T., Tesfamariam, S., and Duenas-Osorio, L. (2015). "Seismic risk assessment of high-voltage transformers using Bayesian belief networks." *Structure and Infrastructure Engineering*, 11(7), 929-943.
- Soltani-Sobh, A., Heaslip, K., Stevanovic, A., El Khoury, J., and Song, Z. (2016). "Evaluation of transportation network reliability during unexpected events with multiple uncertainties." *International journal of disaster risk reduction*, 17, 128-136.
- Soong, T. T., Yao, G. C., and Lin, C. (2000). "Damage to Critical Facilities Following the 921 Chi-Chi, Taiwan Earthquake." *MCEER/NCREE Reconnaissance Report*, 33-43.
- SPUR San Francisco Planning and Urban Research Association (2009). "Defining what San Francisco needs from its seismic mitigation policies." [http://mitigation.eeri.org/files/SPUR\\_Seismic\\_Mitigation\\_Policies.pdf](http://mitigation.eeri.org/files/SPUR_Seismic_Mitigation_Policies.pdf). (Accessed 25 July, 2015).
- Tabandeh, A., Gardoni, P., Murphy, C., and Myers, N. (2018). "Societal Risk and Resilience Analysis: Dynamic Bayesian Network Formulation of a Capability Approach." *ASCE-ASME Journal of Risk and Uncertainty in Engineering Systems, Part A: Civil Engineering*, 5(1), 04018046.
- Tamvakis, P., and Xenidis, Y. (2012). "Resilience in transportation systems." *Procedia-Social and Behavioral Sciences*, 48, 3441-3450.
- Tang, W. H., and Ang, A. (2007). *Probability concepts in engineering: Emphasis on applications to civil & environmental engineering*, Wiley Hoboken, NJ.
- Terzic, V., Mahin, S., and Comerio, M. "Comparative life-cycle cost and performance analysis of structural systems." *Proc., Proceedings of the 10th National Conference in Earthquake Engineering, Earthquake Engineering Research Institute, Anchorage, AK*.
- Tesfamariam, S., and Saatcioglu, M. (2008a). "Risk-based seismic evaluation of reinforced concrete buildings." *Earthquake Spectra*, 24(3), 795-821.
- Tesfamariam, S., and Saatcioglu, M. (2008b). "Seismic risk assessment of RC buildings using fuzzy synthetic evaluation." *Journal of Earthquake Engineering*, 12(7), 1157-1184.
- Tesfamariam, S., and Saatcioglu, M. (2010). "Seismic vulnerability assessment of reinforced concrete buildings using hierarchical fuzzy rule base modeling." *Earthquake Spectra*, 26(1), 235-256.
- Tesfamariam, S., and Wang, Y. (2011). "Risk-based seismic retrofit prioritization of reinforced concrete civic infrastructure: Case study for state of Oregon schools and emergency facilities." *Natural Hazards Review*, 13(3), 188-195.

- Tierney, K. (2009). *Disaster Response: Research Findings and Their Implications for Resilience Measurement*. CARRI Research Report 6 Community and Regional Resilience Institute, Oak Ridge, TN.
- Tierney, K., and Bruneau, M. (2007). "Conceptualizing and measuring resilience: A key to disaster loss reduction." *TR news*, (250).
- Tobin, G. A. (1999). "Sustainability and community resilience: the holy grail of hazards planning?" *Global Environmental Change Part B: Environmental Hazards*, 1(1), 13-25.
- Twigg, J. (2009). "Characteristics of a disaster-resilient community: a guidance note (version 2)."
- UNDE (2007). *Indicators of sustainable development: Guidelines and methodologies*, United Nations Publications.
- UNISDR (2005). "Hyogo framework for action 2005-2015: building the resilience of nations and communities to disasters-Extract from the final report of the World Conference on Disaster Reduction (A/CONF. 206/6)." *Extract from the final report of the World Conference on Disaster Reduction (A/CONF. 206/6)*, <<http://www.unisdr.org/2005/wcdr/intergover/official-doc/L-docs/Hyogo-framework-for-action-english.pdf>>.
- UNISDR (2008). "Indicators of progress: guidance on measuring the reduction of disaster risks and the implementation of the Hyogo Framework for Action." <[http://www.unisdr.org/files/2259\\_IndicatorsofProgressHFAannexes.pdf](http://www.unisdr.org/files/2259_IndicatorsofProgressHFAannexes.pdf)>
- UNISDR (2011). "Hyogo Framework for Action 2005-2015 mid-term review." <[http://www.preventionweb.net/files/18197\\_midterm.pdf](http://www.preventionweb.net/files/18197_midterm.pdf)>.
- UNISDR (2012). *How to Make Cities More Resilient: A Handbook for Local Government Leaders : a Contribution to the Global Campaign 2010-2015 : Making Cities Resilient - My City is Getting Ready!*, United Nations Office for Disaster Risk Reduction.
- UNISDR (2015). "Reading the Sendai Framework for Disaster Risk Reduction 2015 - 2030."
- USEPA "United States Environmental Protection Agency (USEPA, C., Ohio), EPANET. 2008: <https://www.epa.gov/water-research/epanet>."
- Vickery, P., Skerlj, P., and Twisdale, L. (2000a). "Simulation of hurricane risk in the US using empirical track model." *Journal of structural engineering*, 126(10), 1222-1237.
- Vickery, P. J., Lin, J., Skerlj, P. F., Twisdale Jr, L. A., and Huang, K. (2006a). "HAZUS-MH hurricane model methodology. I: Hurricane hazard, terrain, and wind load modeling." *Natural Hazards Review*, 7(2), 82-93.
- Vickery, P. J., Skerlj, P., Steckley, A., and Twisdale, L. (2000b). "Hurricane wind field model for use in hurricane simulations." *Journal of Structural Engineering*, 126(10), 1203-1221.
- Vickery, P. J., Skerlj, P. F., Lin, J., Twisdale Jr, L. A., Young, M. A., and Lavelle, F. M. (2006b). "HAZUS-MH hurricane model methodology. II: Damage and loss estimation." *Natural Hazards Review*, 7(2), 94-103.
- Wagner, I., and Breil, P. (2013). "The role of ecohydrology in creating more resilient cities." *Ecohydrology & Hydrobiology*, 13(2), 113-134. <<http://dx.doi.org/10.1016/j.ecohyd.2013.06.002>>.
- White, R. K., Edwards, W. C., Farrar, A., and Plodinec, M. J. (2015). "A Practical Approach to Building Resilience in America's Communities." *American Behavioral Scientist*, 59(2), 200-219. doi:10.1177/0002764214550296.

- Whitman, R. V., Anagnos, T., Kircher, C. A., Lagorio, H. J., Lawson, R. S., and Schneider, P. (1997). "Development of a national earthquake loss estimation methodology." *Earthquake Spectra*, 13(4), 643-661.
- Yamazaki, F., Meguro, K., and Tong, H. (1995). "General review of recent five damaging earthquakes in japan." *Bulletin of Earthquake Resistant Structure Research Center*, (28), 7.
- Yasuda, S., and Tohno, I. (1988). "Sites of reliquefaction caused by the 1983 Nihonkai-Chubu earthquake." *Soils and Foundations*, 28(2), 61-72.
- Yodo, N., and Wang, P. (2016). "Resilience modeling and quantification for engineered systems using Bayesian networks." *Journal of Mechanical Design*, 138(3), 031404.
- Yodo, N., Wang, P., and Zhou, Z. (2017). "Predictive resilience analysis of complex systems using dynamic Bayesian networks." *IEEE Transactions on Reliability*, 66(3), 761-770.
- Zadeh, L. A. (1965). "Fuzzy sets." *Information and control*, 8(3), 338-353.
- Zhang, J., Xu, X., Hong, L., Wang, S., and Fei, Q. (2011). "Networked analysis of the Shanghai subway network, in China." *Physica A: Statistical Mechanics and its Applications*, 390(23), 4562-4570.

# Appendix A

PEOPLES' dimensions, components, indicators, and measures with corresponding indicators' nature (Nat.)

Dimension/ component/indicator	The measure (0 ≤value ≤1)	Ref.	Nat.
<b>1- Population and demographics</b>			
1-1- Distribution\ Density			
-Population density	1-(Average number of people per area ÷ TV)		D
-Population distribution	% population living in urban area		D
1-2- Composition			
-Age	% population whose age is between 18 and 65		S
-Place attachment-not recent immigrants	1- (% population, not foreign-born persons who came within the previous five years)	( <a href="#">Sherrieb et al. 2010</a> )	S
-Population stability	1-% population change over the previous five-year period	( <a href="#">Sherrieb et al. 2010</a> )	S
-Equity	% nonminority population – % minority population		S
-Race/Ethnicity	1-Absolute value of (% white – % nonwhite)		S
-Family stability	% of two parent families	( <a href="#">Sherrieb et al. 2010</a> )	S
-Gender	1-Absolute value of (%female-%male)		S
1-3- Socio-Economic Status			
-Educational attainment equality	% population with college education – % population with less than high school education		S
-Homeownership	% owner-occupied housing units	( <a href="#">Cutter et al. 2014</a> )	D
-Race/ethnicity income equality	1-Gini coefficient	( <a href="#">Sherrieb et al. 2010</a> )	S
-Gender income equality	1-Absolute value of (% male median income – % female median income)		S
-Income	Capita household income ÷ TV	( <a href="#">Tobin 1999</a> )	D
-Poverty	1-% population whose income is below minimum wage		D
-Occupation	Employment rate %		D
<b>2- Environmental and ecosystem</b>			
2-1- Water			
-Water quality/quantity	Number of river miles whose water is usable ÷ TV		D
2-2- Air			
-Air pollution	1- (Air quality index (AQI) ÷ TV)		D
2-3- Soil			
-Natural flood buffers	% of land in wetlands ÷ TV	( <a href="#">Beatley and Newman 2013</a> )	S
-Pervious surfaces	Average percent perviousness	( <a href="#">Brody et al. 2012</a> )	S
-Soil quality	% of land area that does not contain erodible soils	( <a href="#">Bradley and Grainger 2004</a> )	S
2-4- Biodiversity			
-Living species	1-% species susceptible to extinction		S
2-5- Biomass (Vegetation)			
-The total mass of organisms	Harvest index (HI) the ratio between root weight and total biomass		S
-The density of green vegetation across an area	Normalized difference vegetation index (NDVI)	( <a href="#">Cimellaro et al. 2016b</a> )	D

2-6- Sustainability			
-Undeveloped forest	% of land area that is undeveloped forest ÷ TV	(Cutter et al. 2008a)	S
-Wetland variation	% of land area with no wetland decline	((Cutter et al. 2008a)	S
-Land use stability	% of land area with no land-use change ÷ TV	(UNDE 2007)	S
-Protected land	% of land area under protected status ÷ TV	(Rubinoff and Courtney 2008)	S
-Arable cultivated land	% of land area that is arable cultivated land ÷ TV	(UNDE 2007)	S
<b>3- Organized governmental services</b>			
3-1-Executive/ Administrative			
-Health insurance	% population under age 65 with health insurance	(Chandra et al. 2011)	S
-Disaster aid experience	Presidential disaster declarations divided by number of loss-causing hazard events ÷ TV	(Tierney and Bruneau 2007)	S
-Local disaster training	% population in communities with Citizen Corps program	(Godschalk 2003)	S
-Emergency response services	% workforce employed in emergency services (fire-fighting, law enforcement, protection) ÷ TV	(Cutter et al. 2008b)	S
-Schools	Number of schools per 1000 students ÷ TV		S
3-2- Judicial			
-Jurisdictional coordination	Governments and special districts per 10,000 persons ÷ TV	(Murphy 2007)	S
3-3- Legal/ Security			
-Performance regimes-state capital	The proximity of county seat to state capital ÷ TV	(Bowman and Parsons 2009)	S
-Performance regimes-nearest metro area	The proximity of county seat to nearest county seat within a Metropolitan Statistical Area ÷ TV	(Bowman and Parsons 2009)	S
3-4- Mitigation/ Preparedness			
-Mitigation spending	Ten-year average per capita spending for mitigation projects ÷ TV	(Rose 2007)	S
-Nuclear plant accident planning	1-% population within 10 miles of a nuclear power plant	(Cutter et al. 2014)	S
-Effective mitigation plans	% population covered by a recent hazard mitigation plan	(Cutter et al. 2010)	S
-Exposure to hazards	% building infrastructure not in high hazard zones		S
-Protective resources	% of land area that consists of windbreaks and environmental plantings	(Cutter et al. 2008a)	S
-Financed activities for risk reduction	% governmental financial resources to carry out risk reduction activities ÷ TV	(UNISDR 2012)	S
-Essential infrastructure robustness	% of local schools, hospitals and health facilities that remained operational during emergencies in past events	(UNISDR 2012)	S
-Essential infrastructure assessment	% essential infrastructures that are under regular assessment programs		S
-The accuracy of building codes	% designed structural damage – % actual structural damage (from past events)		S
-Training programs for officials	% of officials and leaders who are under regular training programs		S
-Availability of early warning centers	Average number of early warning centers per each independent zone ÷ TV		S
-Citizen disaster preparedness and response skills	Red cross training workshop participants per 10,000 persons ÷ TV	(Cutter et al. 2014)	S
3-5- Recovery/ Response			
-Money dedicated to supporting the restoration	Microfinancing, cash aid, soft loans, loan guarantees available to affected households after disasters to restart livelihoods ÷ TV	(UNISDR 2012)	S
-Ecosystem support plans	A local government plan to support the restoration, protection and sustainable management of ecosystems services (0 or 1)	(UNISDR 2012)	S

-Local institutions access to financial reserves to support effective disaster response and early recovery	1 (there is access), 0 (no access)		S
-Local government access to resources and expertise to assist victims of psychosocial impacts of disasters	1 (there is access), 0 (no access)		S
-Disaster risk reduction measures integrated into post-disaster recovery and rehabilitation activities	1 (if there is), 0 (otherwise)		S
-Contingency plan degree including an outline strategy for post-disaster recovery and reconstruction	1 (if there is), 0 (otherwise)		S
<b>4- Physical infrastructure</b>			
4-1- Facilities			
-Sturdier housing types	% of housing units not manufactured homes	<a href="#">(Tierney 2009)</a>	D
-Temporary housing availability	% vacant units that are for rent	<a href="#">(Félix et al. 2013)</a>	D
-Housing stock construction quality	100-% housing units built prior to 1970	<a href="#">(Cutter et al. 2014)</a>	D
-Community services	%Area of community services (recreational facilities, parks, historic sites, libraries, museums) total area ÷ TV	<a href="#">(Burton 2015)</a>	D
-Economic infrastructure exposure	% of commercial establishments outside of high hazard zones ÷ total commercial establishment	<a href="#">(Rubinoff and Courtney 2008)</a>	S
-Distribution commercial facilities	%Commercial infrastructure area per area ÷ TV		D
-Hotels and accommodations	Number of hotels per total area ÷ TV	<a href="#">(Cutter et al. 2010)</a>	D
-Schools	Schools area (primary and secondary education) per population ÷ TV		D
4-2- Lifelines			
-Telecommunication	Average number of Internet, television, radio, telephone, and telecommunications broadcasters per household ÷ TV	<a href="#">(Pietrzak et al. 2012)</a>	D
-Mental health support	number of beds per 100 000 population ÷ TV	<a href="#">(Chandra et al. 2011)</a>	D
-Physician access	Number of physicians per population ÷ TV	<a href="#">(Cutter et al. 2014)</a>	S
-Medical care capacity	Number of available hospital beds per 100000 population ÷ TV	<a href="#">(Cutter et al. 2014)</a>	D
-Evacuation routes	Major road egress points per building ÷ TV	<a href="#">(Cutter et al. 2014)</a>	S
-Industrial re-supply potential	Rail miles per total area ÷ TV	<a href="#">(Cutter et al. 2014)</a>	D
-High-speed internet infrastructure	% population with access to broadband internet service	<a href="#">(Cutter et al. 2014)</a>	D
-Efficient energy use	The ratio of Megawatt power production to demand		D
-Efficient Water Use	The ratio of water available to water demand	<a href="#">(Cimellaro et al. 2016b)</a>	D
-Gas	The ratio of gas production to gas demand		D
-Access and evacuation	Principal arterial miles per total area ÷ TV	<a href="#">(Cutter et al. 2010)</a>	D
-Transportation	Number of rail miles per area ÷ TV	<a href="#">(Cutter et al. 2008b)</a>	D
-Wastewater treatment	Number of WWT units per population ÷ TV		S
<b>5- Lifestyle and community competence</b>			
5-1- Collective Action and Decision Making			
-Authorities interdependency	Less than 3 parties are involved in the decision-making process (1), otherwise (0)		S
5-2- Collective Efficacy and Empowerment			

-Creative class	% workforce employed in professional occupations ÷ TV	( <a href="#">Cumming et al. 2005</a> )	S
-Scientific services	Professional, scientific, and technical hour services per population ÷ TV	( <a href="#">Cumming et al. 2005</a> )	S
<hr/>			
5-3- Quality of Life			
-Means of transport	% of households with at least one vehicle	( <a href="#">Peacock et al. 2010</a> )	S
-Safety	1-Crime rate	( <a href="#">Sherrieb et al. 2010</a> )	D
-Quality of homes	Sustainability rating systems (LEED, BREEAM) ÷ maximum index number		S
-Quality of neighborhood	Sustainability rating systems (LEED, BREEAM) ÷ maximum index number		S
<hr/>			
<b>6- Economic development</b>			
6-1- Financial Services			
-Hazard insurance coverage	% of housing units covered by National Insurance Program	( <a href="#">Cutter et al. 2014</a> )	S
-Crop insurance coverage	Lands areas which are covered by Crop insurance program ÷ total area of cultivated lands	( <a href="#">Cutter et al. 2014</a> )	S
-Financial resource equity	Number of lending institutions per population ÷ TV	( <a href="#">Birkmann 2006</a> )	S
-Tax revenues	Corporate tax revenues per 1,000 population ÷ TV	( <a href="#">Sherrieb et al. 2010</a> )	S
<hr/>			
6-2- Industry- Employment Services			
-Employment rate	% labor force employed ÷ TV	( <a href="#">Sherrieb et al. 2010</a> )	S
-Business size	% large businesses	( <a href="#">Rose and Krausmann 2013</a> )	S
-Professional and business services	1-% population that is not institutionalized or infirmed	( <a href="#">Rubinoff and Courtney 2008</a> )	D
-Economic stability	% employment rate	( <a href="#">Burton 2015</a> )	D
-Economic diversity	% population not employed in primary industries ÷ total employed population	( <a href="#">Cutter et al. 2010</a> )	S
-Households insurance	% of households covered by National Insurance Program policies		S
-Research and development firms	Number of research and development firms ÷ TV	( <a href="#">Cumming et al. 2005</a> )	S
-Business development rate	Business gain /total business	( <a href="#">Sherrieb et al. 2010</a> )	S
<hr/>			
6-3- Industry- Production			
-Food provisioning capacity	Food security rate	( <a href="#">Pingali et al. 2005</a> )	D
-Large retail-regional/national geographic distribution	Large retail stores ÷ total number of stores	( <a href="#">Rose and Krausmann 2013</a> )	S
-Local food suppliers	Farms marketing products through Community supported Agriculture per 10,000 persons ÷ TV	( <a href="#">Berardi et al. 2011</a> )	S
-Manufacturing	Mean sales volume of businesses ÷ TV	( <a href="#">Rose 2007</a> )	S
<hr/>			
<b>7- Social-cultural capital</b>			
7-1- Child and Elderly Services			
-Child and elderly care programs	1 (if there is a program), 0 (if no)		S
<hr/>			
7-2- Commercial Centers			
-Social capital-civic organizations	Number of civic organizations per population ÷ TV	( <a href="#">Sherrieb et al. 2010</a> )	S
-Commercial establishments	Area of commercial establishments per population ÷ TV	( <a href="#">Rubinoff and Courtney 2008</a> )	S
<hr/>			
7-3- Community Participation			
-Pre-retirement age	% population below 65 years of age	( <a href="#">Morrow B. 2008</a> )	S
-Non-special needs	% population without a sensory, physical, or mental disability	( <a href="#">Davis and Phillips 2009</a> )	D
-Political engagement	% voting age population participating in the presidential election	( <a href="#">Sherrieb et al. 2010</a> )	S

-Female labor force participation	% female labor force participation	( <a href="#">Cutter et al. 2010</a> )	S
-Population participating in community Rating System	% population participating in the Community Rating System (CRS)	( <a href="#">Cutter et al. 2010</a> )	D
-Emergency community participation	% community participation in case of warning systems	( <a href="#">UNISDR 2012</a> )	D
<hr/>			
7-4- Cultural and Heritage Services			
-Cultural resources	National Historic Registry sites area per population ÷ TV	( <a href="#">Rubinoff and Courtney 2008</a> )	S
<hr/>			
7-5- Education Services/ Disaster Awareness			
1-English language competency	% population proficient English Speakers	( <a href="#">Hilfinger Messias et al. 2012</a> )	S
2-Adult education and training programs	Number of yearly adult education and training programs per population ÷ TV	( <a href="#">Burton 2015</a> )	S
3-Education programs on DRR and disaster preparedness for local communities	Number of education programs on DRR and disaster preparedness per each local community by local government per year ÷ TV	( <a href="#">UNISDR 2012</a> )	S
4-Integration of disaster risk reduction in educational curriculum	Number of courses in disaster risk reduction as part of the educational curriculum per schools and colleges ÷ TV	( <a href="#">UNISDR 2012</a> )	S
5-Citizens awareness of evacuation plans or drills for evacuations	Average number of maneuver per institution ÷ TV		S
<hr/>			
7-6- Non-Profit Organization			
1-Social capital-disaster volunteerism	Red cross volunteers per 10,000 persons ÷ TV	( <a href="#">Cutter et al. 2014</a> )	D
<hr/>			
7-7- Place Attachment			
-Social capital-religious organizations	Persons affiliated with a religious organization per 10,000 persons ÷ TV	( <a href="#">Sherrieb et al. 2010</a> )	S